Technische Universität München
TUM School of Life Sciences
Lehrstuhl für Systembiologie der Pflanzen

# Gibberellin signaling interactions with strigolactone and cold stress

Ourania Lantzouni

Vollständiger Abdruck der von der TUM School of Life Sciences der Technischen Universität München zur Erlangung des akademischen Grades eines Doktors der Naturwissenschaften genehmigten Dissertation.

Vorsitzende: Prof. Dr. Aphrodite Kapurniotu
Prüfer der Dissertation: 1. Prof. Dr. Claus Schwechheimer, 2. Prof. Dr. Caroline Gutjahr

Die Dissertation wurde am 12.05.2021 bei der Technischen Universität München eingereicht und durch die TUM School of Life Sciences am 09.07.21 angenommen.

## Table of Contents

# Abstract

The phytohormone gibberellin (GA) participates in the regulation of plant growth as well as responses to environmental stimuli. GA signaling is mediated via the degradation of DELLA proteins, which act mainly as transcription regulators by interacting with transcription factors. Here, GA signaling was studied in relation to the hormone strigolactone (SL) and low temperature (4 °C) stress in *Arabidopsis thaliana*.

Both GA and SL control plant growth and have similarities in their signal perception mechanisms. Furthermore, an interaction was reported between the rice DELLA protein and the SL receptor. Although, crosstalk between the two hormone pathways was suggested, it remained largely unclear how they interact at the physiological and molecular level. For the investigation of such interactions, GA and SL biosynthesis single and double mutants were phenotypically and biochemically analyzed in the response to the two hormones. Additive effects on phenotypical traits were observed while treatments with the synthetic SL, *rac*-GR24, did not affect DELLA stability. Furthermore, a transcriptomics analysis of GA- and SL-deficient *ga1 max1-4* mutants was performed in response to GA and *rac*-GR24 and largely additive changes in the mRNA abundance of a substantial number of genes were observed in response to the two hormones. The findings suggest that signaling interaction of the two hormones occurs at the level of gene transcription regulation of common target genes.

Upon low temperature exposure, DELLA proteins are stabilized in plants and control growth and gene expression changes, but the signaling events downstream of DELLAs in this condition remained unknown. Therefore, the role of GA in the regulation of growth and transcription in cold temperature stress was investigated. First, the gene expression changes in response to GA in ambient temperature and in combination with cold stress of the wild type were analyzed and found to be largely different. In addition, more than 200 new DELLA-transcription factor interactions were identified with the yeast two-hybrid system and, by combining the

two data sets, putative targets of the pathway were identified. Evidence that *GROWTH REGULATORY FACTORs* (*GRFs*) interact with DELLA proteins and affect growth and transcription changes in response to cold stress was obtained.

## Zusammenfassung

Das Phytohormon Gibberellin (GA) ist an der Regulation des Pflanzenwachstums sowie an den Reaktionen auf Umweltreize beteiligt. Die GA-Signalübertragung wird über den Abbau von DELLA-Proteinen vermittelt, die hauptsächlich als Transkriptionsregulatoren durch Wechselwirkung mit Transkriptionsfaktoren wirken. Hier wurde die GA-Signalübertragung in Bezug auf das Hormon Strigolakton (SL) und den Stress bei niedriger Temperatur (4 ° C) bei *Arabidopsis thaliana* untersucht.

Sowohl GA als auch SL steuern das Pflanzenwachstum und weisen Ähnlichkeiten in ihren Signalwahrnehmungsmechanismen auf. Darüber hinaus wurde eine Wechselwirkung zwischen dem Reis-DELLA-Protein und dem SL-Rezeptor berichtet. Obwohl eine Wechselwirkung zwischen den beiden Hormonwegen vorgeschlagen worden war, blieb weitgehend unklar, wie diese auf physiologischer und molekularer Ebene interagieren. Zur Untersuchung solcher Wechselwirkungen wurden Einzel- und Doppelmutanten der GA- und SL-Biosynthese in Reaktion auf die beiden Hormone phänotypisch und biochemisch analysiert. Additive Effekte auf phänotypische Merkmale wurden beobachtet, während Behandlungen mit dem synthetischen SL *rac*-GR24 die DELLA-Stabilität nicht beeinflussten. Darüber hinaus wurde eine Transkriptomanalyse von GA1- und SL-defizienten *ga1 max1-4* Mutanten als Reaktion auf GA und *rac*-GR24 durchgeführt, und es wurden weitgehend additive Änderungen in der mRNA-Häufigkeit einer beträchtlichen Anzahl von Genen als Reaktion auf die zwei Hormone beobachtet. Die Ergebnisse legen nahe, dass die Signalinteraktion der beiden Hormone auf der Ebene der Gentranskriptionsregulation gemeinsamer Zielgene stattfindet.

Bei Exposition mit niedriger Temperatur werden DELLA-Proteine in Pflanzen stabilisiert und kontrollieren Wachstums- und Genexpressionsänderungen, aber die

den DELLAs nachgeschaltete Signalereignisse in dieser Reaktion blieben unbekannt. Daher wurde die Rolle von GA bei der Regulation von Wachstum und Transkription bei Kältestress untersucht. Zunächst wurden die Genexpressionsänderungen beim Wildtyp als Reaktion auf GA bei Umgebungstemperatur und in Kombination mit Kältestress analysiert und als weitgehend unterschiedlich befunden. Darüber hinaus wurden mehr als 200 neue DELLA-Transkriptionsfaktor-Wechselwirkungen mit dem Hefe-Zwei-Hybrid-System identifiziert und durch Kombination der beiden Datensätze wurden vermeintliche Ziele des Signalwegs identifiziert. Es wurde der Nachweis erbracht, dass GROWTH REGULATORY FACTORs (GRFs) mit DELLA-Proteinen interagieren und Wachstums- und Transkriptionsänderungen als Reaktion auf Kältestress beeinflussen.

# 1. Introduction

Plants have evolved numerous molecular signaling mechanisms in order to coordinate their developmental program and responses to changes in the environment. They have to decide when and where to germinate, grow, develop organs, and reproduce according to temperature, soil composition, water availability, light conditions and other environmental factors. Plant hormones are utilised for transferring external and internal information to achieve survival and reproductive success.

Gibberellins (GAs), a group of tetracyclic diterpenoid hormone molecules, have been extensively studied because of their importance for agricultural production. GA insensitive gene variants were first introduced into commercial wheat varieties in the 1950's by the Nobel prize laureate Norman Borlaug. These high yielding varieties have shorter and stronger stems and thus can support more grain without lodging. Yield is additionally increased due to nutrient allocation in grain filling instead of shoot growth. These mutations are currently present in more than 70 % of the total cultivated wheat and, in combination with fertilizer use and pest control, have contributed to significant increases in yield production in the second half of the last century (Hedden, 2003).

GAs are growth stimulants and, in the last two decades, have also emerged as central regulators of defence versus growth responses. GAs promote germination, shoot and leaf growth and flowering, whereas reduced GA levels and signaling inhibit growth and promote stress resistance (Colebrook et al., 2014; Schwechheimer, 2014). GAs are involved in the regulation of plant responses to multiple environmental cues such as abiotic stress (temperature, shade avoidance, phosphate starvation, salt stress, drought stress) and biotic interactions (arbuscular mycorrhiza, insects) (Achard et al., 2006; Jiang et al., 2007; Achard et al., 2008; Colebrook et al., 2014; Li et al., 2015; Fonouni-Farde et al., 2016; Du et al., 2018). Furthermore, GA signaling interconnects with other hormone signaling pathways including those of auxin, jasmomic acid as well as the more recently identified SLs

(Daviere and Achard, 2016). GA responses are determined by specific interactions at the molecular level, which vary depending on the environment, plant organ and developmental stage (Cao et al., 2006; Wild et al., 2016; Serrano-Mislata et al., 2017; Rizza and Jones, 2018). A detailed examination and identification of GA signaling components and interactions will increase our understanding of the pathway and facilitate the creation of new varieties with better stress tolerance and improved yield, through breeding or genetic engineering.

## 1.1. Gibberellin (GA)

GA research sparked in Japan in the beginning of the 20$^{th}$ century because of the plant disease “bakanae”, which is caused by the GA-producing fungus *Gibberellla fujugikuroi.* Symptoms of the disease include slender seedling growth and infertility, today known effects of GA signaling saturation (Hedden and Sponsel, 2015). In 1958, the plant endogenous gibberellin $A_1$ ($GA_1$) was first isolated and since then more than 130 GAs have been found in diverse species including bacteria, fungi, and vascular plants (MacMillan and Suter, 1958; Hedden and Sponsel, 2015). However, only a few, structurally distinct GAs are bioactive in angiosperms, namely $GA_1$, $GA_3$, $GA_4$ and $GA_7$ (Sun, 2011).

### 1.1.1. GA acts to suppress the DELLA transcription factors

GA-dependent phenotypes in plants are the result of changes in gene transcription rates and protein trafficking. These are influenced by a variety of factors including intracellular GA levels, developmental stage, cell/organ type, environmental conditions and other hormones (Daviere and Achard, 2016). Genetic and biochemical evidence suggests that the primary target of GA signaling are the nuclear-localized DELLA-domain transcription regulators (Silverstone et al., 2001; Daviere and Achard, 2016). Although, DELLA-independent GA-promoted changes in gene expression have been reported, 95% of gene expression changes depend

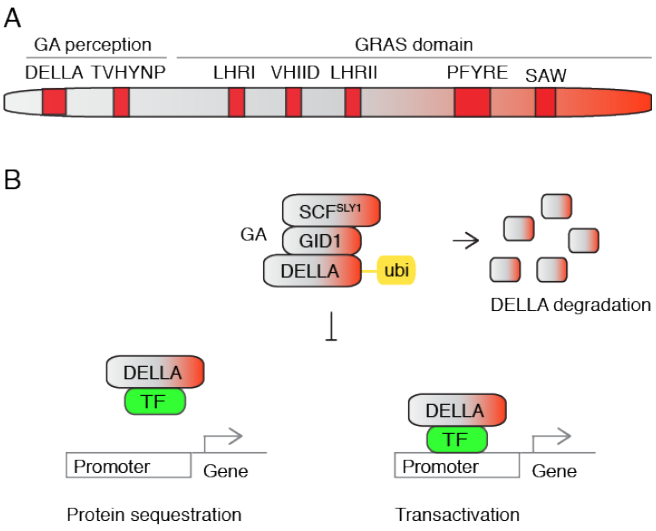


**Figure 1. Schematic representation of DELLA protein domain composition and GA signal perception.**

(A) DELLA proteins are composed by the N-terminal GA-sensing domain and the C-terminal GRAS domain, which is shared with other GRAS proteins. (B) In the presence of GA, DELLA proteins are ubiquitylated and targeted for proteasomal degradation. Changes in DELLA abundance affect gene transcription rates by either transcription factor (TF) sequestration or gene expression transactivation.

on DELLA abundance and their interactions with other transcription factors (Willige et al., 2007; Livne et al., 2015).

DELLAs proteins belong to the GRAS (*GAI, RGA, SCR*) family of transcription factors with 32 members in *Arabidopsis* and 54 in rice. GRAS proteins share the conserved C-terminal GRAS domain, which includes the LHRI, VHIID, LHRII, PFYRE and SAW motifs (Pysh et al., 1999; Tian et al., 2004). DELLA proteins have additionally the DELLA and TVHVNP domains in their N-terminus that are necessary for their interaction with the GA receptor (Fig. 1A) (Tian et al., 2004; Griffiths et al., 2006; Ueguchi-Tanaka et al., 2007; Willige et al., 2007). Non-DELLA GRAS proteins are not direct targets of GA signaling, although the GA-regulated SCARECROW-LIKE3 (SCL3) has been implicated in the control of GA homeostasis (Yoshida and Ueguchi-Tanaka, 2014).The suggested mechanism involves protein-protein interactions between the DELLAs, SCL3 and INDETERMINATE DOMAIN (IDD) transcription factors to control downstream responses (Zhang et al., 2011; Yoshida et al., 2014). Thus, other GRAS factors might be involved in GA responses by interfering with the DELLA function or by antagonizing DELLA interactions.

Inside the cell, bioactive GAs bind to the nuclear GA receptor GIBBERELLIN INSENSITIVE DWARF1 (GID1) that was first characterised in rice (Ueguchi-Tanaka et al., 2005; Griffiths et al., 2006; Ueguchi-Tanaka et al., 2007). GA-binding causes structural changes in GID1 that promote the interaction between GID1 and the

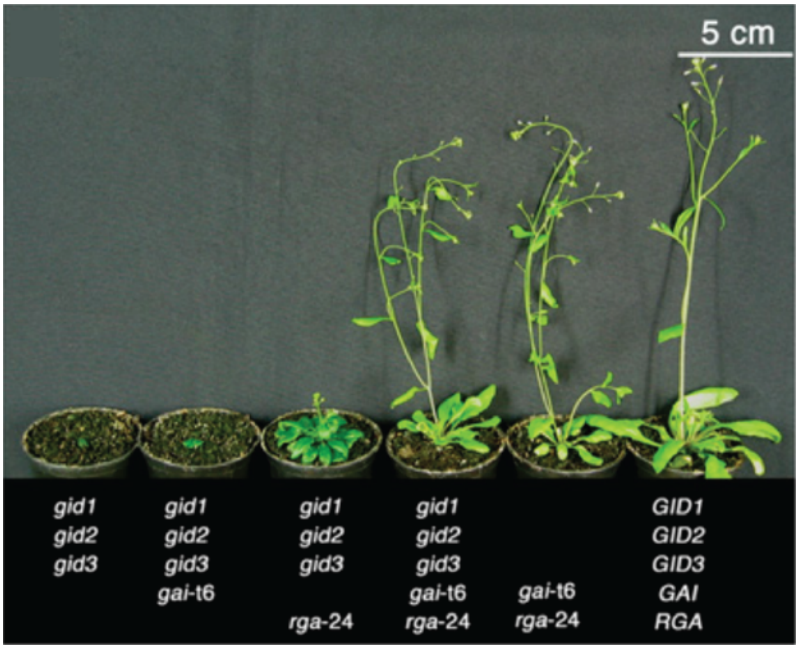


**Figure 2. The dwarf phenotype of the GA-insensitive gid1 receptor triple mutant is suppressed by loss-of-function of DELLA mutations.**

The DELLA proteins RGA and GAI in Arabidopsis repress growth downstream of the GA receptor. 6-week-old *Arabidopsis thaliana* plants of the specified genotypes. Figure from Willige et al., 2007.

DELLA transcription regulators (Murase et al., 2008). The GID1-DELLA complex subsequently associates to the SKP1-CULLIN1-F-box protein-type ($SCF^{F\text{-}box}$) E3 ubiquitin ligase complex. This requires the presence of the F-box protein GID2 in rice and SLEEPY 1 (SLY1) or SNEEZY (SNZ) in *Arabidopsis* (Dill et al., 2004; Fu et al., 2004; Ariizumi et al., 2011). Ubiquitinylated DELLA proteins are subjected to degradation via the 26S proteasome (Fig. 1B) (Silverstone et al., 2001; Fu et al., 2002; Willige et al., 2007). Exogenous application of GA can rescue the growth restrain of GA-deficient mutants such as *ga1* but not that of GA-insensitive mutants (Fig. 2) (Griffiths et al., 2006; Willige et al., 2007).

A functional GA-GID1-DELLA signaling module is present in vascular plants but not in the moss *Physcomitrella patens* (Hirano et al., 2007). The number of gene copies of the GA receptor and the DELLA-domain proteins varies between different plant species. For example, *Arabidopsis thaliana* has three receptor (*GID1A*, *GID1B* and *GID1C*) and five DELLA genes (*REPRESSOR OF GA1-3 1*, *RGA*; *GIBBERELLIC ACID INSENSITIVE*, *GAI*; *RGA-LIKE 1*, *RGL1*; *RGA-LIKE 2*, *RGL2* and *RGA-LIKE 3*, *RGL3*) whereas rice has only one receptor (*GID1*) and one DELLA (*SLENDER RICE 1*, *SLR1*). The GID1 receptors are structurally similar to *a/b* hydrolases. An amino acid substitution in the loop region of the GID1B allele of *Arabidopsis* allows

it to interact with the DELLA proteins in the absence of GA. It was suggested that GID1B responds differently than other GID1 proteins to various stimuli and that *GID1B* may show a developmental stage- or organ-specific expression (Nakajima et al., 2006; Yamamoto et al., 2010). *RGA* and *RGL2,* two different *DELLA* genes of *Arabidopsis*, on the other hand, where shown to have the same biochemical function but different mRNA expression patterns based on promoter exchange experiments (Gallego-Bartolome et al., 2010). Thus, the main GA perception complex is conserved and functional diversification occurs mainly form differences in the spatio-temporal regulation of gene expression of individual components.

Cellular DELLA protein levels are controlled by the amount of bioactive GAs and are therefore influenced by the rates of GA biosynthesis, catabolism and transport. GAs are synthesised from geranylgeranyl diphosphate (GGDP) through a series of enzymatic reactions. In the initial steps, GGDP is converted to $GA_{12}$ by the enzymes ent-copalyl diphosphate synthase (CPS), ent-kaurene synthase (KS), ent-Kaurene oxidase (KO) and ent-kaurenoic acid oxidase (KAO). $GA_{12}$ is then converted to bioactive GAs by two classes of 2-oxoglutarate–dependent dioxygenases the GA 20-oxidases (GA20oxs) and the GA 3-oxidases (GA3oxs). The deactivation of bioactive GAs is catalyzed by GA 2-oxidases (GA2oxs) (Fig. 3) (Yamaguchi, 2008). Both, GA biosynthesis (GA20oxs and GA3oxs) and catabolism (GA2oxs), as well as GA signaling genes are subject to feedback regulation by GA. This includes the activation of GA biosynthesis and the suppression of GA catabolism genes by DELLA proteins (Yoshida and Ueguchi-Tanaka, 2014; Yoshida et al., 2014). Feedback regulation occurs after exogenous GA treatment or can be the result of intracellular changes in GA content due to hormone transport or environmental inputs. This homeostatic mechanism strongly influences intracellular GA and DELLA levels (Middleton et al., 2012). Furthermore, spatial separation of GA biosynthesis and catabolism in combination with the long and short distance transport of GAs have been suggested to control developmental processes and cell type-specific GA responses (Binenbaum et al., 2018). The intermediate non-bioactive $GA_{12}$ has been shown to move through the xylem and phloem to support

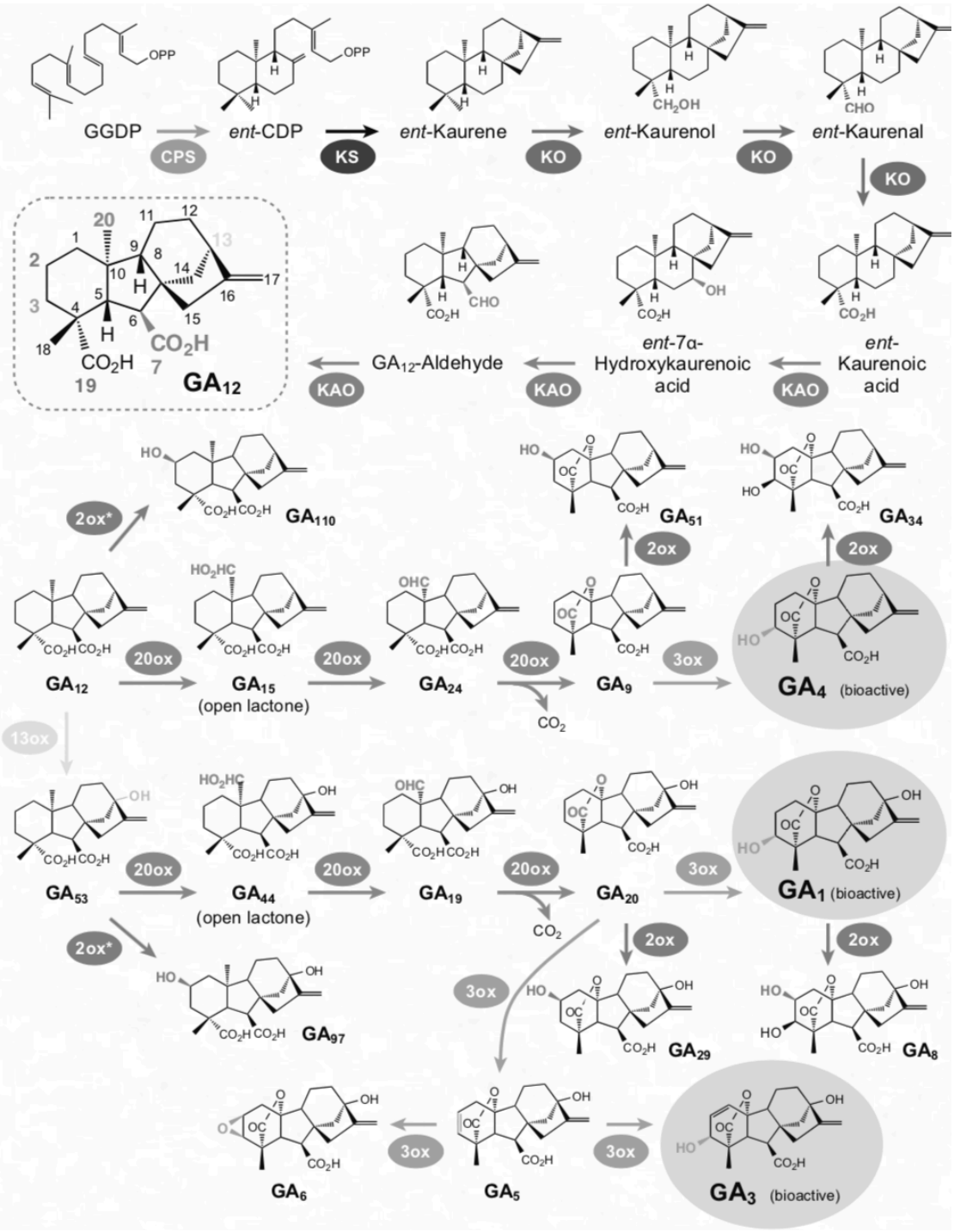


**Figure 3. Diagram of the enzymatic biosynthesis and catabolism steps of bioactive GAs in plants.**

GGDP, geranylgeranyl diphosphate; *ent*-CDP, *ent*-copalyl diphosphate; CPS, *ent*-copalyl diphosphate synthase; KS, *ent*-kaurene synthase; KO, *ent*-kaurene oxidase; KAO, *ent*-kaurenoic acid oxidase; 2ox, GA 2-oxidase; 3ox, GA 3-oxidase; 13ox, GA 13-oxidase; 20ox, GA 20-oxidase. Figure from Yamaguchi, 2008.

growth (Regnault et al., 2015). The transport of bioactive GAs by transporter proteins has been demonstrated to contribute to cell-type specific DELLA accumulation and to influence GA-dependent growth responses (Chiba et al., 2015; Saito et al., 2015; Kanno et al., 2016; Tal et al., 2016). The spatio-temporal regulation of GA metabolism and transport contribute to the control of DELLA accumulation and to promote developmental changes and responses to fluctuations in environmental conditions (Galvao et al., 2012; Shani et al., 2013; Wild et al., 2016; Rizza et al., 2017).

DELLAs control transcription changes in response to GA through protein-protein interactions with numerous structurally diverse transcription factors (Yoshida et al., 2014; Daviere and Achard, 2016). More than 150 such interactions have been reported to date and about 50 of them have been biologically validated and connected to specific plant phenotypes (Van De Velde et al., 2017). In the majority of cases, these interactions prevent the DELLA-targeted transcription factors from binding to gene promoters through protein sequestration. For example, the interaction of DELLAs with the PHYTOCHROME-INTERACTING FACTORs (PIFs) inhibits their binding to gene promoters and reduces cell elongation (de Lucas et al., 2008; Feng et al., 2008; Hou et al., 2010; Bai et al., 2012; Oh et al., 2012; Schwechheimer, 2014; Daviere and Achard, 2016; Van De Velde et al., 2017). Additionally, DELLAs can transactivate genes when being tethered to their promoters by interacting with members of the INDETERMINATE DOMAIN (IDDs), ABA-INSENSITIVE3 and type-B ARABIDOPSIS RESPONSE REGULATORS (ARRs) transcription factor families (Lim et al., 2013; Fukazawa et al., 2014; Yoshida et al., 2014; Marin-de la Rosa et al., 2015). DELLA interactions with the RING domain proteins BOTRYTIS SUSCEPTIBLE1 INTERACTOR (BOI), BOI-RELATED GENE1 (BRG1), BRG2, and BRG3 have been suggested to co-regulate gene expression but the factor that brings the complex to gene promoters remains unknown (Park et al., 2013). Although the ability to bind DNA has been described for rice GRAS proteins, there is no evidence of direct DNA-binding in the case of the DELLAs (Li et al., 2016).

Apart from GA-promoted DELLA ubiquitinylation, other post-translational modifications that affect DELLA abundance and interactions have been identified (Camut et al., 2017). *O*-fucosylation of DELLA proteins by SPINDLY (SPY) increases their binding affinity to PIFs and BRASSINAZOLE RESISTANT1 (BZR1) transcription factors (Zentella et al., 2017). Moreover, DELLA *O*-GlcNAcylation by SECRET AGENT (SEC) inhibits the same interactions as well as the DELLA interaction with JASMONATE-ZIM DOMAIN1 (JAZ1) (Zentella et al., 2016). Phosphorylation has also been reported to affect DELLA activity and proteasomal mediated degradation (Hussain et al., 2005; Dai and Xue, 2010). Finally, salt stress-promoted SUMOylation of DELLAs has been shown to mediate the GA-independent DELLA-GID1 binding and GID1 sequestration. This mechanism has been suggested to increase DELLA abundance and thus limits growth under stress conditions (Conti et al., 2014).

DELLAs have also emerged as regulators of intracellular protein trafficking through interactions that do not affect transcription but protein localization (Locascio et al., 2013; Shanmugabalaji et al., 2018). They control microtubule orientation to regulate cell expansion though interactions with subunits of the prefoldin complex (PFD) in *Arabidopsis*. DELLA stabilization mediates the relocation of the complex from the cytoplasm to the nucleus and negatively affects tubulin heterodimerization and microtubule orientation in a GA-dependent manner (Locascio et al., 2013). Furthermore, DELLAs interact with a member of a translocon complex at the outer envelope membrane of chloroplasts (TOC159), an essential component of an import machinery for proplastid to chloroplast differentiation (Bauer et al., 2000; Shanmugabalaji et al., 2018). This interaction promotes the proteasomal degradation of TOC159 and inhibits chloroplast biogenesis during germination whereas GA has the opposite effect (Shanmugabalaji et al., 2018).

Auxin transport is also regulated by GA and DELLAs in a post-transcriptional manner. GA deficiency results in reduced root gravitropic response, auxin transport and membrane content of the PIN-FORMED2 (PIN2) auxin transporter, which is targeted for vacuolar degradation (Willige et al., 2011; Lofke et al., 2013). GA-

dependent DELLA degradation increases PIN2 membrane levels and facilitates auxin transport by promoting protein recycling to the plasma membrane (Willige et al., 2011; Lofke et al., 2013; Salanenka et al., 2018). The regulation of protein trafficking by GA requires the retromer complex and an intact microtubule cytoskeleton. It has been suggested that the DELLA-PFD interactions promote protein targeting to the vacuoles by affecting the microtubule dynamics (Salanenka et al., 2018). Thus, DELLAs regulate intracellular protein trafficking and auxin transport in addition to gene expression through protein-protein interactions.

In conclusion, DELLA abundance and interactions with numerous transcription regulators and other proteins control gene expression and intracellular protein trafficking and depend on the presence of bioactive GA as well as DELLA protein modifications.

### 1.2. Strigolactone (SL) signaling interaction with GA

Strigolactones (SLs) are plant-produced carotenoid compounds that control plant root and shoot architecture and are secreted from the roots to trigger biotic interactions (Brewer et al., 2013). SLs were initially identified in the 1950s as germination-promoting agents of parasitic weeds belonging to the families of *Striga* and *Orobanche.* These weeds infect a wide range of grasses and flowering plants such as maize, rice and tomato causing big yield loses (Xie et al., 2010). SL production is triggered by low phosphate availability to inhibit shoot branching and promote biotic interactions between arbuscular mycorrhiza and plants (Akiyama et al., 2005; Gomez-Roldan et al., 2008; Umehara et al., 2008). While the increased branching is the most prominent phenotype of SL-deficient and -signaling mutants, effects on root architecture, plant stature, leaf senescence and secondary growth have been reported (Brewer et al., 2013). Thus, SLs signal both inside the plant and in the rhizosphere to coordinate plant response to low phosphate and increase their nutrient assimilation though beneficial symbiotic interactions (Waldie et al., 2014).

Both, GA and SL signaling pathways are involved in the regulation of shoot outgrowth and elongation, the response to low phosphate availability and the root colonization by arbuscular mycorrhiza (Jiang et al., 2007; Gomez-Roldan et al., 2008; Umehara et al., 2008; Kohlen et al., 2011; Mayzlish-Gati et al., 2012; Floss et al., 2013; Takeda et al., 2015; Fonouni-Farde et al., 2016; Wang et al., 2017). SL biosynthesis and signaling mutants have increased branch number and reduced plant height, phenotypes that have also been reported for semi-dwarf GA-deficient mutants (Silverstone et al., 1997; Booker et al., 2004; Shen et al., 2007; Lo et al., 2008; Rieu et al., 2008; Lin et al., 2009). Furthermore, low phosphate availability triggers SL production that modifies the *Arabidopsis* shoot and root architecture, although this species does not interact with beneficial fungi (Kohlen et al., 2011; Mayzlish-Gati et al., 2012). Phosphate starvation also promotes the reduction of GA levels and the stabilization of DELLA proteins to inhibit growth and regulate root architecture (Jiang et al., 2007). Thus, the two hormones might interact in the control of growth and responses to external stimuli (Marzec, 2017).

SLs are a diverse group of compounds comprised of a butenolide D-ring connected to an additional element with specific stereochemistry, important for signal transduction (Fig. 4A) (Al-Babili and Bouwmeester, 2015). Several SL biosynthesis mutants have been characterized in different plant species. As SLs are still detected in most of them, it has been suggested that additional uncharacterized biosynthesis pathways must exist (Waldie et al., 2014; Al-Babili and Bouwmeester, 2015). In *Arabidopsis*, the isomerase DWARF27 (D27) and the carotenoid cleavage dioxygenases MORE AXILLARY BRANCHES3 (MAX3; CAROTENOID CLEAVAGE DIOXYGENASE 7) and MORE AXILLARY BRANCHES4 (MAX4; CAROTENOID CLEAVAGE DIOXYGENASE 8) convert the all-*trans*-β-carotene to the SL intermediate carlactone (Waters et al., 2012; Al-Babili and Bouwmeester, 2015). The latter is subsequently changed to bioactive SLs by the enzymes MORE AXILLARY BRANCHES1 (MAX1; CYTOCHROME P450, FAMILY 711) and LATERAL BRANCHING OXIDOREDUCTASE (LBO) (Fig. 4B) (Booker et al., 2005; Brewer et al., 2016).

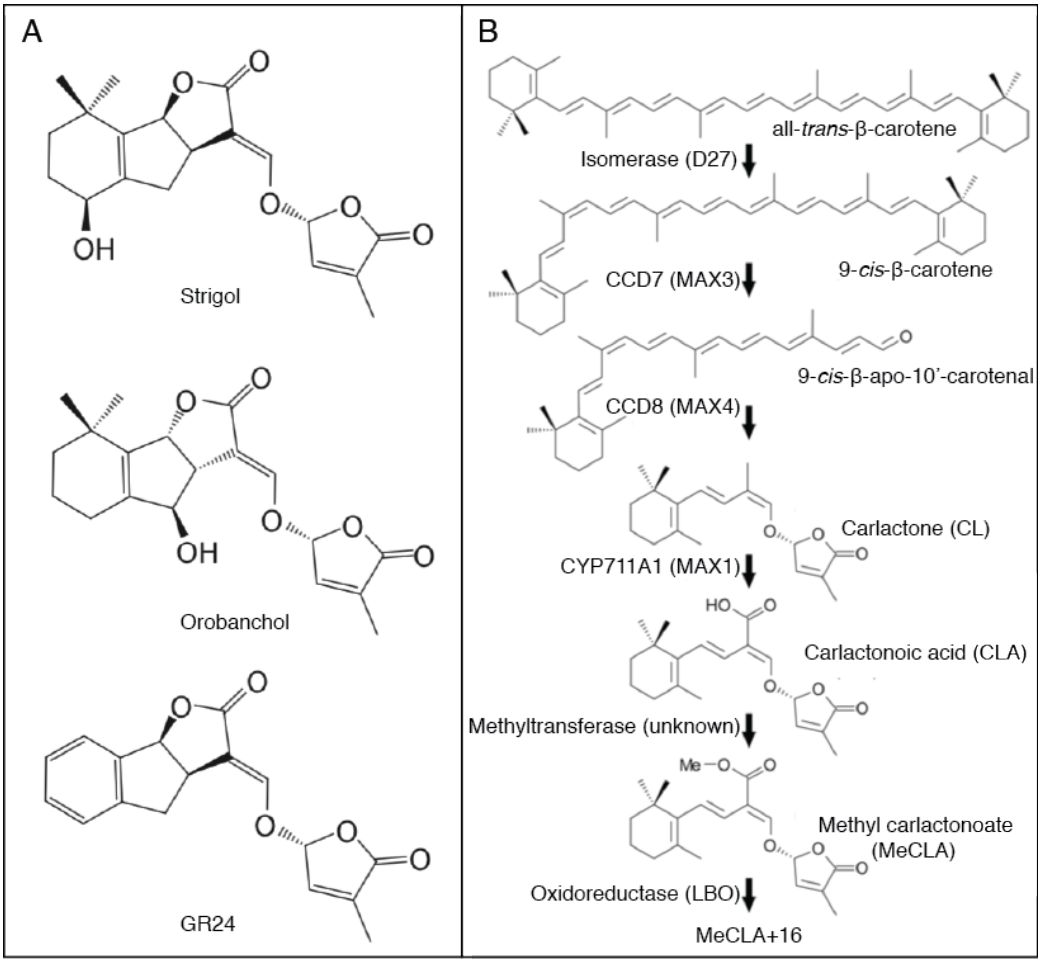


**Figure 4. SL structures and biosynthesis pathway.**

(A) Chemical structures of two of the naturally derived SLs with different stereochemistry strigol and orobanchol as well as that of the commonly used synthetic SL, GR24. (B) The identified steps and enzymes of SL production in Arabidopsis. Figure modified from Al-Babili and Bouwmeester, 2015 and Brewer et al., 2016.

The bioactivity of SLs depends on the regulation of SL biosynthesis and transport. They are transported inside the plant from root to shoot and from root to the rhizosphere (Al-Babili and Bouwmeester, 2015). Active transporters are most likely involved in this process as it has been shown with the characterization of a petunia PDR-type SL transporter (Kretzschmar et al., 2012; Sasse et al., 2015). Both the transporter and the biosynthesis genes *MAX3* and *MAX4* are subject to transcriptional regulation by SLs (Mashiguchi et al., 2009; Kretzschmar et al., 2012). Recently, the GA-promoted downregulation of SL production through changes in expression of SL biosynthesis genes has been reported for rice (Ito et al., 2017).

Whether this type of regulation and its contribution to SL and GA mutant phenotypes is conserved in other plant species remains to be investigated.

Similarly to GA signaling, SL signaling is perceived by the *a/b* hydrolase receptor DWARF14 (D14) to target specific proteins for ubiquitylation and proteasomal degradation through the $SCF^{F\text{-}box}$ E3 ubiquitin ligase complex (Arite et al., 2009; Waters et al., 2012; Jiang et al., 2013; Zhou et al., 2013; Marzec, 2016). Although GID1 and D14 belong to the same enzymatic group, only D14 hydrolyses the bound SLs, an activity that is required for SL perception (Ueguchi-Tanaka et al., 2005; Hamiaux et al., 2012; Nakamura et al., 2013; Zhao et al., 2015; de Saint Germain et al., 2016; Yao et al., 2016). The F-box proteins DWARF3 (D3) in rice and MORE AXILLARY BRANCHES2 (MAX2) in *Arabidopsis* interact with D14 and are necessary for SL signal transduction and ubiquitylation of the target proteins DWARF53 (D53) and SUPPRESSOR of *max2-1* LIKE7 (SMXL7), SMXL6 and SMXL8 in rice and *Arabidopsis*, respectively (Fig. 5A) (Jiang et al., 2013; Zhou et al., 2013; Soundappan et al., 2015; Wang et al., 2015).

The F-box proteins D3/MAX2 are also necessary for the response to the karrikins (KARs), a class of smoke-derived compounds (Nelson et al., 2011; Morffy et al., 2016). KARs promote seed germination after fire, affect seedling growth, and enhance stress tolerance (Morffy et al., 2016). The receptor of KARs is the D14 homologous protein, KARRIKIN INSENSITIVE2 (KAI2) (Waters et al., 2012). KAI2 recognizes KARs and non-naturally derived SL enantiomers such as $GR24^{ent\text{-}5DS}$. In contrast, D14 binds naturally-derived SLs such as strigol and the synthetic $GR24^{5DS}$. Thus, the commonly used synthetic SL, *rac*-GR24 ($GR24^{5DS}$ and $GR24^{ent5DS}$) confers responses to SL as well as KAR as each of the two enantiomers binds to one of the two receptor proteins (Scaffidi et al., 2014; Umehara et al., 2015). It has been hypothesized that plant-endogenous karrikin-like compounds are produced but these remain unidentified to date (Waldie et al., 2014; Conn and Nelson, 2015). The KAI2-MAX2 hormone-bound complex mediates the ubiquitylation and proteasomal degradation of the target proteins SUPPRESSOR of *max2-1* (SMAX1) and SUPPRESSOR of *max2-1* LIKE2 (SMXL2) (Fig. 5B) (Soundappan et al., 2015;

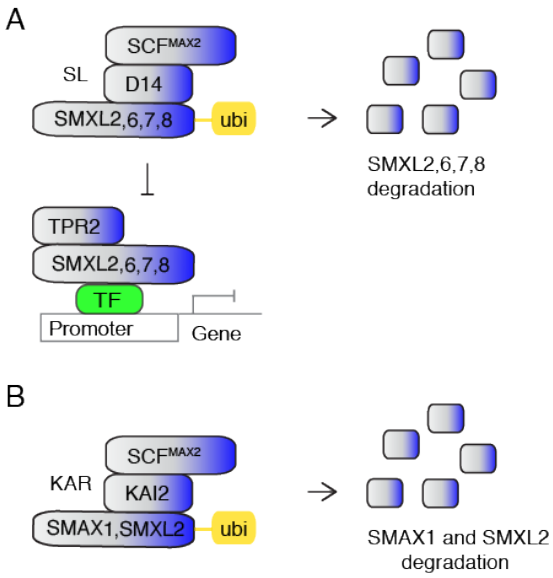


**Figure 5. Schematic representation of SL and KAR signal perception.**

(A) In the presence of SLs, the D14 receptor forms complexes with the SMXL2, SMXL6, SMXL7 and SMXL8 proteins, which are ubiquitylated and targeted for proteasomal degradation. This leads to the relieve of suppression of gene expression which is achieved through interactions of the SMXL transcription factors with TOPLESS-RELATED PROTEIN2 (TPR2) in Arabidopsis. (B) Similarly, SMAX1 and SMAXL2 are targeted for proteasomal degradation in the presence of KAR and the receptor KAI2, to regulate KAR-related responses. The F-box protein MAX2 is a common denominator of both SL and KAR signaling pathways.

Villaecija-Aguilar et al., 2019; Wang et al., 2020). Recently, SMAXL2 has also been suggested to be a target of the SL-D14-MAX2 complex and thus being targeted by both D14- and KAI2-dependent regulation of hypocotyl growth (Fig. 5) (Wang et al., 2020) .

Multiple evidences suggest that the control of gene expression is one mode of SL action. Transcript profiling after GR24 treatments results in altered transcript levels of about 100 and 500 genes in Arabidopsis and tomato, respectively (Mashiguchi et al., 2009; Mayzlish-Gati et al., 2010). The SL target proteins D53/SMXL6, SMXL7, SMXL8 suppress the gene expression of the branch-inhibiting transcription factors *FINE CULM1* (*FC1*) and *BRANCHED1* (*BRC1*) in rice and *Arabidopsis*, respectively (Zhou et al., 2013; Soundappan et al., 2015; Wang et al., 2015). Based on protoplast assays, it has been suggested that the repressor activity of D53/SMXL6, SMXL7, SMXL8 depends on the presence of the EAR motif (Wang et al., 2015). The latter is found in several transcription factors that interact with the transcription regulator TOPLESS (TPL) in Arabidopsis and other plant species (Causier et al., 2012). Interactions between D53/SMXL6, SMXL7, SMXL8 and TPL proteins have been shown in rice and Arabidopsis, and it has been hypothesized that TPL is required for the SL-mediated transcription responses (Jiang et al., 2013; Soundappan et al., 2015; Wang et al., 2015). Although not all the SL-related phenotypes are influenced

by the presence of the EAR motif indicating the involvement of additional signaling targets downstream of SMXLs (Liang et al., 2016). Recent work has shown that the three SL targeted SMXLs can suppress their own transcription thought promoter binding but for the regulation of other genes, such as *BRC1*, additional transcription factors are needed. This study confirmed their role as transcription factors, a function that has not been know when the work presented in this thesis was conducted (Wang et al., 2020).

Interestingly, the DELLA proteins have been suggested to be targets of SLs as the rice SLR1 interacts with D14 in yeast and protoplast cells. This interaction depends on a functional D14 and the presence of SLs, while it is inhibited by the GA-bound GID1 (Nakamura et al., 2013). Thus, the D14-DELLA complex formation might be interfering with the DELLA function by either reducing the free DELLA levels or promoting their degradation. In this scenario, SLs would be promoting GA responses and transcription changes. Furthermore, GA could be promoting SL responses if the DELLA proteins antagonize the D14-SMXL binding or reduce the D14 receptor abundance. Also, two independent studies demonstrate that the abundance of the fusion protein GFP-RGA is unaffected by GR24 treatments, while branching and internode elongation have been suggested to be independently controlled by the two hormones in pea (de Saint Germain et al., 2013; Bennett et al., 2016). The relevance of the DELLA-D14 interaction remains unclear and additional research is needed to understand how the two hormone signaling pathways are connected (Daviere and Achard, 2016).

Finally, auxin transport is regulated by SLs, but in a negative manner as opposed to the effect observed after GA application. SLs inhibit auxin transport and promote the removal of PIN1 transporters from the plasma membrane in *Arabidopsis* shoots and SL-deficient mutants have better auxin transport capabilities and higher PIN1 levels compared to the wild type (Bennett et al., 2006; Crawford et al., 2010; Agusti et al., 2012; Shinohara et al., 2013). In addition, SLs lead to a reduction in the plasma membrane-associated PIN2 transporter in Arabidopsis roots under low phosphate conditions in a MAX2-dependent manner (Kumar et al., 2015). The effect

of SLs on auxin transport and PIN1 levels depends on the SL-targeted SMXLs (Soundappan et al., 2015; Liang et al., 2016). The importance of the SL regulation of auxin transport for the inhibition of branch outgrowth has been debated (Bennett et al., 2006; Waldie et al., 2014; Brewer et al., 2015). A recent report suggests that both the control of auxin transport and transcriptional regulation of target genes such as *BRC1* from SL, contribute to the increased branch number phenotype of the SL-deficient and insensitive mutants (Bennett et al., 2016; Seale et al., 2017). Thus, the control of auxin transport could be another convergent point of GA and SL signaling.

### 1.3. GA in cold stress responses

Sub-optimal temperatures negatively impact plant growth and can cause cell damage and death with devastating results for agricultural yield production (Baxter, 2014; Jha et al., 2017). Thus, identification of the molecular signaling mechanisms that control plant cold stress responses is important for the development of high-yielding stress-resistant crops.

Plants have evolved various adaptive strategies to adjust their growth and development to temperature fluctuations and cold environments (Baxter, 2014). For example, monocot and dicot species from temperate climates including *Arabidopsis*, have the ability to increase their freezing tolerance after a temperature drop. This is achieved through transcription reprogramming and adjustments of cellular metabolism and composition that take place when the plants grow in above-zero cold temperatures (Miura and Furumoto, 2013). Important conserved regulators of the cold acclimation response are the C-REPEAT BINDING FACTORs (CBFs) transcription factors, which are rapidly upregulated when temperature decreases. *Arabidopsis* has three *CBF* genes, *CBF1*, *CBF2* and *CBF3* (Thomashow, 2010). *CBF* overexpression confers constitutive freezing tolerance while loss of functions *cbf* mutants are defect in cold acclimation and freezing sensitive (Miura and Furumoto, 2013; Jia et al., 2016; Zhao et al., 2016).

DELLA proteins are also involved in the response to low temperature to inhibit growth and promote stress resistance (Achard et al., 2008; Penfield, 2008; Colebrook et al., 2014). GA treatments promote the stem elongation of lettuce and wheat plants grown in low temperatures (Stoddart et al., 1978; Pinthus et al., 1989). In *Arabidopsis*, the root elongation of double and quadruple *DELLA* loss-of-function mutants is less inhibited compared to the wild type after exposure to 4 °C for several hours per day (Achard et al., 2008). Similarly, quintuple (global) *DELLA* mutant plants are not as strongly inhibited as the wild type in terms of leaf and stem growth and flowering time at 12 °C, compared to ambient temperature grown plants (Kumar et al., 2012; Zhou et al., 2017). The plant survival after freezing stress of the GA-insensitive *gai* mutant is enhanced compared to the wild type (Peng et al., 1997; Achard et al., 2008). In contrast, *gai* and *rga* double loss-of-function mutants are more vulnerable to freezing damage and death (Achard et al., 2008).

At the molecular level, cold stress supresses GA responses and promotes the stabilization of DELLA proteins. The $GA_1$ content of tall and semi-dwarf GA-insensitive *Rht* wheat varieties is lower when they grow at 10 °C as opposed to 25 °C (Pinthus et al., 1989). In Arabidopsis, a reduction in bioactive GA levels and stabilization of the fusion protein GFP-RGA are observed after short exposure to cold temperatures. It has been suggested that this is the result of noted changes in transcription of specific GA metabolism and *DELLA* genes (Achard et al., 2008; Zhou et al., 2017).

Genetic and biochemical evidence suggests that CBFs promote DELLA stabilization in cold stress. *CBF* overexpression affects the transcript levels of GA catabolism *GA2ox* genes and of *RGL3,* while the cold induction of those is compromised in a *cbf3* mutant (Achard et al., 2008; Li et al., 2017; Zhou et al., 2017). In addition, CBF3 has been suggested to control the cold-induced upregulation of *GA2ox7* by direct promoter binding (Zhou et al., 2017). Strikingly, ambient temperature-grown *CBF* overexpressing lines have reduced GA, and higher GFP-RGA content, are late flowering and dwarf. These phenotypes are rescued by exogenous GA treatments or the genetic introduction of double *GAI* and *RGA* or *quintuple DELLA* loss-of-

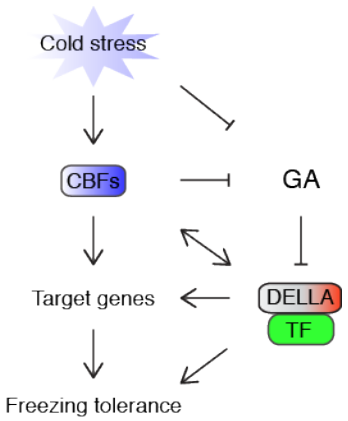


**Figure 6. Schematic representation of GA signaling in cold stress.**

Cold stress promotes DELLA protein stabilization in a CBF-dependent and -independent manner. DELLAs, in turn, together with unidentified transcription factors control gene expression and contribute to freezing tolerance.

function alleles (Achard et al., 2008; Zhou et al., 2017). Vice versa, DELLAs contribute to the cold stress-promoted upregulation of the *CBF* genes. *CBF* gene expression is not as strongly induced in quintuple *DELLA* gene mutants compared to the wild type after cold stress. It has been suggested that this might be the result of DELLA-JAZ interactions as this effect can be rescued by methyl jasmonate treatment (Hu et al., 2013; Zhou et al., 2017).

Another result of DELLA stabilization in cold stress is the increase of PFD protein nuclear localization (Perea-Resa et al., 2017). DELLA-PFD interactions have been suggested to regulate the daily fluctuations in cell expansion through the control of microtubule dynamics (Locascio et al., 2013). In addition, GA treatments stabilize the cold-sensitive microtubule cytoskeleton of maize protoplast cells (Huang and Lloyd, 1999). Interestingly, a fast rearrangement of the cytoskeleton after cold exposure is corelated with increased growth recovery and freezing tolerance in winter wheat varieties (Abdrakhamanova et al., 2003). It is thus tempting to hypothesize that the DELLA-PDF interactions could be involved in the rapid cold-promoted microtubule rearrangement to inhibit cell growth and promote cold acclimation. Notably, it has been suggested that PFDs negatively affect the ability to cold acclimate in Arabidopsis, since cold pre-treated *pfd* mutants are able to withstand lower freezing temperatures compared to the wild type. However, *pfd4* mutants are not freezing-resistant in the absence of cold pre-treatment (Perea-Resa et al., 2017). In contrast, DELLA proteins strongly enhance the survival of non-cold acclimated plants (Achard et al., 2008). Thus, the PFD-DELLA interaction might be

involved in the regulation of the cold acclimation response but one would expect that DELLAs have additional targets to inhibit growth and improve survival in response to reducing temperatures.

The role of GA and DELLA proteins in the control of cold-promoted gene expression changes remains to be elucidated. Functional interactions between DELLA proteins and other transcription factors could be expected to mediate these responses (Fig. 6). Analysis and identification of the GA signaling components in cold-stress can facilitate future biotechnological applications and germplasm selection.

### 1.4. Objectives of this study

The current work aims to unravel the contribution and targets of the growth- and defence-regulating hormone GA in the plant's response to SLs and cold stress.

Although an interplay between GA and SL at the molecular level has been suggested, it has been largely unclear whether molecular and developmental changes in response two hormones have mutual effects. To investigate the putative interaction between GA and SL signaling, *Arabidopsis thaliana ga1 max1-4* biosynthesis mutants of both hormones, were generated and examined in detail. Phenotypic and biochemical analyses, as well as a detailed investigation of the transcription responses of *ga1 max1-4* after single and combined GA and SL treatments, were performed. Furthermore, the use of next-generation sequencing of mRNA allowed an in-depth transcriptome profiling and the identification of additive changes in mRNA expression of specific gene clusters.

The effect and targets of GA in the control of early cold stress-promoted transcription changes were investigated in *Arabidopsis thaliana* seedlings. First, changes in transcript abundance in response to cold stress (4 °C) and GA were determined with mRNA sequencing. For the identification of candidate transcription factors that mediate this response downstream of GA, a yeast-two-hybrid screen of the two DELLA proteins, RGA and GAI, was performed against a transcription factor collection of almost 2000 transcription factors (Pruneda-Paz et al., 2014). By

combining the two datasets, the GROWTH-REGULATING FACTORS (GRFs) were identified and their role in cold stress growth regulation was elucidated.

# 2. Materials and methods

## 2.1. Biological material

**Biological material and growth conditions.** Wild type and mutants of the *Arabidopsis thaliana* ecotype Columbia were used for all experiments. The loss-of-function mutants *ga1* (SALK_109115), *max1-4* (Sail_25_A05), *max3-9* and *max2-1, grf1 line 1* (*grf1#1,* SALK_069339c)*, grf3 line 1* (*grf3#1,* SALK_026786)*, grf5-1* (SALK_086597) as well as the overexpression transgenic lines 35S:GRF5, 35S:miR396b, 35S:rGRF1 and 35S:rGRF3 were previously described (Stirnberg et al., 2002; Booker et al., 2004; Horiguchi et al., 2005; Willige et al., 2007; Rodriguez et al., 2010; Hewezi et al., 2012; Luo et al., 2012). Primer sequences used for genotyping of the single and double mutants are listed in Table 1.

The genomic construct pGRF3:GRF3 was cloned with the primers 5'-attB1-CCTCAGTCAGAACCGAATG-3' and 5'-attB2-ATGAAAGGCTTGTGTCGAGAC-3' and introduced into the entry vector pDNR201. The mutation that renders *GRF3* insensitive to the *miR396b* was introduced with mutation PCR with the primers 5'-GCACCGTGGCCGCAACAGGAGCCGTAAACCGGTCGAGACTCC-3' and 5'-GTTGCATTGACGGTGGTTGGAGTCTCGACCGGTTTACGGCTCCTGTTG-3'.
pGRF3:rGRF3 was then recombined with the destination vector pGWB459 to get the C-terminal RFP fusion (Tanaka et al., 2011). The pGRF3:rGRF3-RFP was cloned with the primers 5'-attB1-CCTCAGTCAGAACCGAATG-3' and 5'-attB2-GCTCAATTAAGTTTGTGCCCC-3' and inserted back to the pDNR201 to be finally introduced to the pFASTR07 vector (Shimada et al., 2010). The construct was used to transform the established pRGA:GFP-RGA (*Landsberg erecta* background) transgenic line and two T1 plant lines expressing pRGA:GFP-RGA/pGRF3:rGRF3-RFP were analysed (Silverstone et al., 2001).

**Table 1: List of primers used for genotyping in this study.**

| Primer | Sequence | Reference |
|---|---|---|
| 3step_max1_fw – 5/75 | TCC CCA TCT GAA ATC TGT TTG | |
| 3step_max1_rv – 5/76 | AAT TAA TAC GGA TTC CGT GCG | |
| LBb1.3 | ATT TTG CCG ATT TCG GAA C | |
| 3step_ga1_lp2 | CAG ACC CGA GAC AGT AAC TGC | |
| 3step_ga1_rp2 | TCT CTA CTC GAG GCA AGC TTG | |
| max2-1 dCAPS F | CCC AAA GCT CTC AAA GAT GC | (Stanga et al., 2013) |
| max2-1 dCAPS R | CAATAATCAAGCTCGCTCAAGC TCAAGCTTCCAATTCCGGTCAA GAAGAATCTTTCCCATAAACTCGAAT | (Stanga et al., 2013) |
| MAX3_fw_exon2 | TTTAAGATGCCACCGAAACG | (Booker et al., 2004) |
| MAX3_rv_exon2 | TTTACCACAAAATGTGAAGTTG | (Booker et al., 2004) |

## 2.2. Physiological experiments

Unless stated otherwise, plants were germinated on ½ MS 0.8% agar plates before seedlings were transferred to soil. Plants were grown in continuous white light (110-130 µmol $m^{-2}$ $s^{-1}$) in MobyLux GroBanks (CLF Plant Climatics, Wertingen, Germany) or MLR-351 SANYO growth chambers (Ewald, Bad Nenndorf, Germany). To overcome the germination defect imposed by the GA-deficiency of the *ga1* mutants, seeds were treated with $GA_3$ during imbibition. For the quantification of rosette diameters, seeds were surface-sterilized and incubated at 4 °C in water containing 100 µM $GA_3$ (Duchefa Biochemie, The Netherlands) for five days to induce germination. $GA_3$ was subsequently removed by repeated washes of the seeds before plating. For branch number and plant height measurements, stratified seeds were germinated for five days on ½ MS plates containing 100 µM $GA_3$ and subsequently transferred to soil. $GA_3$ treatments were performed by spraying four times with either 1 µM $GA_3$ or mock (n=10).

For assessing primary root elongation and RGA accumulation in the specified genotypes under low phosphate conditions, seeds were surface sterilized and then

stratified for five days in water supplemented with 100 µM $GA_3$ followed by washes to remove $GA_3$. Seeds were germinated on ½ MS 0.8% agar plates for 8 days and, subsequently, seedlings were transferred for seven days to ½ MS plates containing 1.5 mM $CaCl_2$, 9.4 mM $KNO_3$, 0.75 mM $MgSO_4$, 10.3 mM $NH_4NO_3$, 2.5 mM MES, 100 mL/L Murashige and Skoog basal salt micronutrient solution (Sigma-Aldrich, Taufkirchen, Germany), 0.5 mL 1000x Gamborg B5 Vitamin mixture (Duchefa Biochemie, The Netherlands), 0.8% agar supplemented with either 10 µM or 1.0 mM $KH_2PO_4$ for low and high phosphate conditions, respectively (n=36) (Jiang et al., 2007).

For the quantification of leaf, petiole and root growth, seeds were surface-sterilized, stratified and grown on ½ MS 0.8% agar plates in continuous white light (110 - 130 µmol $m^{-2}$ $s^{-1}$) in MLR-351 SANYO growth chambers (Ewald, Bad Nenndorf, Germany) for six days before they were transferred to plates containing mock or 10 µM $GA_3$ (Duchefa Biochemie, The Netherlands) or 0.1, 0.5 or 1 µM paclobutrazol (PAC; Duchefa Biochemie, The Netherlands). Plates and leaves were scanned after either seven days at 21 °C (7 days at 21 °C) or seven days at 4 °C and seven additional days at 21 °C (7 days recovery). At 4 °C, almost no growth was observed. The different parameters were quantified with the ImageJ software (NIH). The experiment was repeated three times with similar results. In the case of the first repeat, no ambient temperature condition was included. The cell size analysis was performed from ten images taken from ten different seedling true leaves in the mid-section of the respective leaves. For the quantification of the 3S:miR396b root phenotype on PAC, Col-0 and 3S:miR396b seeds were surface-sterilized, stratified and grown on ½ MS 0.8% agar plates for five days. Subsequently, they were transferred on plates containing either mock or 5 µM PAC or 5 µM PAC + 10 µM $GA_3$. Photos of the root tips were taken with an Olympus SZX16 stereoscope (Olympus, Hamburg, Germany) after eight days and the frequency of the disorganized meristem phenotype was counted. For the microscopic visualization of the phenotype, Col-0 and 35S:miR396b seeds were surface-sterilized and grown for five days before they were transferred to medium containing either mock or 1

µM PAC. The photos were taken after eight days using propidium iodide staining with an Olympus FV1000 (Olympus, Hamburg, Germany) confocal microscope.

### 2.2.1. Statistical tests

The effect of the genotype and treatment in the branching, plant height and primary root elongation, and leaf growth assays was assessed with two-way ANOVA and Tukey's honestly significant difference post-hoc test. Differences with p-value $< 0.05$ were accepted as significant. All statistical analyses were performed with the R statistical package.

## 2.3. Immunoblot analysis

Protein extracts for immunoblot analyses were prepared using an established anti-RGA antibody as previously described (Willige et al., 2007). For the hormonal treatments, *ga1 max1-4* seeds were surface sterilized and incubated at 4 °C in 100 µM $GA_3$ for five days to induce germination. Subsequently they were grown on ½ MS 0.8% agar plates and, 10 days after germination, were transferred to liquid ½ MS in 24-well plates for 5 hours to acclimate before the addition of 100 µM $GA_3$ or 5 µM GR24 (Chiralix, Nijmwegen, The Netherlands) or 100 µM $GA_3$ + 5 µM GR24 or a mock solution. Pooled samples were taken from three individual wells. For the investigation of RGA levels in ambient temperature and after exposure to cold stress, Columbia-0 seeds were surface-sterilized, stratified for two days, and grown on ½ MS agar for nine days at 21 °C under continuous light (110–150 µmol $m^{-2}$ $s^{-1}$) in a Sanyo growth chamber. Seedlings were then placed at 4 °C under the same light conditions and spray-treated with 100 µM $GA_3$ or a mock solution.

## 2.4. Transcriptomics

### 2.4.1. RNA-sequencing (RNA-seq) analysis of the *ga1 max1-4* mutant after GA and GR24 treatments

*ga1 max1-4* seeds were surface-sterilised and stratified for 6 days at 4 °C in 100 µM GA3. Following the removal of GA3 by extensive washes, seeds were grown on ½ MS agar plates for seven days at 21 ° C. Seedlings were then transferred to 24-well plates in liquid MS (mock) for 7 hrs before hormone treatments for 0, 30, 60 and 120 min with mock, 5 µM GR24, 100 µM GA3 and 5 µM GR24 + 100 µM GA3. Three independent biological replicates were collected for each treatment.

RNA was isolated as described above, quantified with a Qubit (2.0 Fluorometer; RNA-seq Fisher, Schwerte, Germany) using the QuantiFluor RNA high sensitivity kit (Promega, Mannheim, Germany) and its quality was further determined with a Bioanalyzer 2100 (Agilent Technologies, Waldbronn, Germany). cDNA libraries were prepared using the TruSeq Stranded mRNA Sample Preparation kit (Illumina, San Diego, CA) according to the manufacturer's instructions. Clusters were generated and sequenced on two-lane flow cells in four batches with the HiSeq 2500 platform (Illumina). The TruSeq Rapid SR Cluster kit (Illumina) and the TruSeq Rapid SBS kit (Illumina) were used generating 50 bp single stranded reads.

The analysis of the raw sequences and the differential expression analysis were performed on the CLC Genomics Workbench v. 7.0.4 (CLC bio, Aarhus, Denmark). Raw sequences were first quality trimmed (trim using quality scores: 0.05, maximum number of ambiguous nucleotides: 1) and then aligned and mapped to the *Arabidopsis thaliana* Columbia-0 (TAIR10) genome using the RNA-seq analysis tool with default settings (Maximum number of hits for a read, 10; Global alignment, No; Similarity fraction, 0.8; length fraction, 0.8; mismatch cost, 2; Insertion cost, 3; Deletion cost, 3). Differential expression analysis was performed using the Empirical Analysis of the DGE tool (Estimate tagwise dispersions, Yes; Total count filter cutoff, 5.0). Genes with a false discovery rate corrected p-value < 0.01 and fold change > 1.5 were classified as differentially expressed genes (DEGs). Raw sequence reads

from this study were submitted to NCBI under the Bioproject PRJNA266229 and are available from the Sequence Read Archive as SRP050945.

The FC values for the 261 DEGs of the combined treatment that would occur based on the read counts of the single treatments were calculated as $FC_{calculated}$ = ($ReadCounts_{GA}$ + $ReadCounts_{GR24}$ - $ReadCounts_{mock}$)/$ReadCounts_{mock}$, in response to GA, $FC_{GA}$ = $ReadCounts_{GA}$/$ReadCounts_{mock}$ and in response to GR24, $FC_{GR24}$ = $ReadCounts_{GR24}$/$ReadCounts_{mock}$. The output FC values of the Empirical Analysis of the CLC DGE tool cannot be calculated from the original counts as they are based on average counts per million for each group of biological replicates and derive internally in the Exact Test algorithm (CLC Genomics Workbench 7.0 manual). The later were used and $FC_{calculated}$ was estimated as $FC_{calculated}$ = $FC_{GA}$ + $FC_{GR24}$ – 1.

### 2.4.2. RNA-Seq analysis of the response to cold stress and GA

*Arabidopsis thaliana* Col-0 seeds were surface-sterilized, stratified for two days, and grown on ½ MS agar for nine days at 21 °C under continuous light (110 – 150 µmol m-2 s-1) in a Sanyo growth chamber. Seedlings were then spray-treated with 100 µM GA3 or a mock solution and placed at 21 °C or 4 °C under the same light conditions. Three biological replicates of seedling shoots were collected after 0, 1, 2 and 4 h for each treatment. Total RNA was isolated using the NucleoSpin RNA Plant kit (Machery-Nagel, Düren, Germany). DNA was removed by an on-column treatment with rDNase (Machery-Nagel, Düren, Germany). For library preparation and RNA sequencing, RNA was quantified with the KAPA library quantification kit (Illumina, San Diego, CA) and cDNA libraries were prepared using the TruSeq RNA Sample Preparation v2 kit (Illumina, San Diego, CA) following the manufacturer's instructions. Clusters were generated and sequenced on eight lane flow cells with a HiSeq 1000 platform (Illumina, San Diego, CA). The TruSeq Paired-End Cluster kit v3 (Illumina) and the TruSeq SBS kit v3 (Illumina) were used to generate 100 bp paired-end reads. The analysis of the raw sequences and the differential expression analysis were performed on the CLC Genomics Workbench v. 7.5.1 (Qiagen, Aarhus, Denmark). Raw sequences were first quality trimmed (trim using quality

scores: 0.05; maximum number of ambiguous nucleotides: 1) and then aligned and mapped to the *Arabidopsis thaliana* Columbia-0 (TAIR10) genome using the RNA-seq analysis tool with default settings (Maximum number of hits for a read, 10; Strand specific, both; Count paired reads as two, no; Expression value, total counts; Calculate RPKM for genes without transcripts, no; Global alignment, no; Auto-detect paired distances, yes; Similarity fraction, 0.8; length fraction, 0.8; mismatch cost, 2; Insertion cost, 3; Deletion cost, 3). Differential expression analysis was performed using the Empirical Analysis of DGE tool (Total count filter cutoff, 5.0; Estimate tagwise dispersions, yes; FDR corrected, yes). Genes with a false discovery rate corrected p-value < 0.01 and fold change > 1.5 were classified as differentially expressed genes (DEGs). Heat maps were generated using the Cluster 3.0 and Treeview tools (de Hoon et al., 2004; Saldanha, 2004). The raw data of this experiment can be found at NCBI SRA database under accession number SRP178244 and Bioproject PRJNA513856.

An independent RNA-seq experiment was performed in order to compare the responses to the 4 °C and GA treatment using nine days-old seedlings of the Col-0 wild type and *35S:GRF5* transgenic lines (Horiguchi et al., 2005). Growth conditions and RNA-preparation were as described above. Seedling shoot material was harvested from the three genotypes after four hours at 21 °C (mock), 4 °C (mock) and at 4 °C following 100 µM $GA_3$ treatment. Library preparation and sequencing using Illumina technology was performed by GATC Biotech (Constance, Germany). After selection of polyadenylated mRNAs, strand-specific cDNA libraries were generated and sequenced, producing more than 25 million stranded 50 bp-reads per sample. The raw sequence reads were quality trimmed (trim using quality scores: 0.05; maximum number of ambiguous nucleotides: 1) and aligned to TAIR10 using the RNA-seq analysis tool (Mismatch cost, 2; Insertion cost, 3; Deletion cost, 3; length fraction, 0.8; Similarity fraction, 0.8; Global alignment, no; Strand specific, reverse; Maximum number of hits for a read, 10; Count paired reads as two, no; Expression value, total counts; Calculate RPKM for genes without transcripts, no) of the CLC Genomics Workbench v. 10.1.1 (Qiagen, Aarhus, Denmark). Differential

expression analysis was performed using the Differential Expression for RNA-seq tool (CLC Genomics Workbench v. 10.1.1, Qiagen, Aarhus, Denmark). DEGs were classified as for the previous experiment (false discovery rate corrected p-value < 0.01, fold change > 1.5). Heat maps were generated using the Cluster 3.0 and Treeview tools (de Hoon et al., 2004; Saldanha, 2004). The raw data of this experiment can be found at NCBI SRA database under accession number SRP158655 and Bioproject PRJNA487166.

## 2.5. Quantitative real-time PCR

**Table 2: List of primers used for qRT-PCR analysis.**

| Primer | Sequence | Reference |
|---|---|---|
| D14_fw_2step | GCA GCT TGC TCA GTT TCT CC | |
| D14_rv_2step | CGA TAC GTG GAC CCC ACT AA | |
| MAX4_fw_2step | ACC CAC TTG GCT GAA TGG TA | |
| MAX4_rv_2step | GTG GAG TAG CCG TCG AAG AG | |
| MAX2_fw_2step | AGT TAG ATT GCG GGG ACA CA | |
| MAX2_rv_2step | GTG GTG GCC AAT AAT CAA GC | |
| D27_fw_2step | TGG ACA GAG CAT TAC CGA CA | |
| D27_rv_2step | CCT CAC CTC TGA AGG TCC AA | |
| MAX1_fw_2step | GGT TGC AAG GGA AAC TGC TA | |
| MAX1_rv_2step | TGC TAA CCA AAC CCA TGT CC | |
| QRTMAX3F | GAT TCG TTG GTG AGC CCA TG | (Hayward et al., 2009) |
| QRTMAX3R | CAC CGA AAC CGC ATA CTC GA | (Hayward et al., 2009) |
| BRC1_fw | AAC ACG ACC GAA ACA AGA GG | |
| BRC1_rv | GCT CTC TCC TCC TTG GAC AAC T | |

For qRT-PCR analyses, total RNA was isolated using the NucleoSpin RNA Plant kit (Machery-Nagel, Düren, Germany). DNA was removed by an on-column treatment with rDNase (Machery-Nagel, Düren, Germany). Subsequently, 2 $\mu$g of total RNA were reverse transcribed with an oligo(dT) primer and M-MuLV Reverse Transcriptase (Fermentas, St. Leon-Rot, Germany) and the cDNA equivalent of 60-

80 ng of total RNA was used in a 10 µl PCR reaction in a CFX96 Real-Time System Cycler with SsoAdvanced™ Universal SYBR® Green Supermix (Bio-Rad, München, Germany). A 40 cycle 2-step amplification protocol (10 s at 95 °C; 20 s at 60 °C) was used for all measurements. Relevant primers for qRT-PCR are listed in Table 2.

## 2.6. Protein-protein interaction assays

### 2.6.1. Molecular cloning

As the full-length DELLA proteins are not suitable as 'baits' for yeast two-hybrid experiments, N-terminally truncated M5 versions of RGA and GAI were used as previously described (de Lucas et al., 2008). DNA-binding domain (DB) yeast two-hybrid constructs of M5-truncated RGA (RGA204) and GAI (GAI141) were generated using Gateway-based cloning of PCR fragments obtained with the primers RGA-FW 5'-attB1-CGGAGTCAACTCGTTCTGTTATCCTGG-3' and RGA-RV 5'-attB2-GTCAGT ACGCCGCCGTCGA-3' as well as GAI-FW 5'-attB1-CGAACGGCGTCGTGG AAACC-3' and GAI-RV 5'-attB2-GCTAATTGGTGGAGAGTTTCCAAGCC-3', respectively (LifeTechnologies, Carlsbad, CA). AD yeast two-hybrid clones for *GRF4* were obtained in the same manner from Col-0 cDNA with the primers 5'-attB1-CGATGGACTTGCAACTGAAAC-3' and 5'-attB2-GTTAATGAAAAACTT GAGTAGAG-3' and for GRF6 with 5'-attB1-CGATGGCTACAAGGATTCC-3' and 5'-attB2-GTCAAATGAAGAGTGAAGTAG-3'. Yeast two-hybrid constructs for the remaining genes were retrieved from the transcription factor collection (Pruneda-Paz et al., 2014). *SCR* and *SCL3* yeast two-hybrid constructs were previously published (Consortium, 2011). For the bimolecular fluorescence complementation experiment, the coding sequence of *GRF5* was amplified with the primers 5'-attB1-CGATGATGAGTCTAAGTGGAAGTAG-3' and 5'-attB2-GTTAGCTACCA GTGTCGAGTC-3' and of *GRF3* with 5'-attB1-CGATGGATTTGCAACTGAAAC-3' and 5'-attB2-GTCAATGAAAGGCTTGTGTC-3' from the respective AD vectors. The

miRNA396-resistant version of *GRF3*, rGRF3 was obtained with mutation PCR with the primers 5'-GCACCGTGGCCGCAACAGGAGCCGTAAA CCGGTCGAGACTCC-3' and 5'-GTTGCATTGACGGTGGTTGGAGTCTCGAC CGGTTTACGGCTCCTGTTG-3' as described before (Hewezi et al., 2012). *GIF1* was cloned with 5'-attB1-CGATGCAACAGCACCTGATG-3' and 5'-attB2-GTCAATTCCCATCATCTGATG-3'. Entry vectors carrying the full-length sequences of *RGA* and *GAI* were previously published (Consortium, 2011). An entry vector with the *XERICO* coding sequence was provided by Andrea Holzer (Technische Universität München, Germany).

### 2.6.2. Yeast two-hybrid protein-protein interaction assays.

The N-terminally truncated M5 versions of RGA and GAI, *M5-RGA* and *M5-GAI*, as well as the full-length coding sequences of *SCR* and *SCL3* were cloned into pDEST-DB and screened by yeast mating against a previously published transcription factor collection fused to a GAL4 activation domain (AD) expressed via pDEST-AD (Pruneda-Paz et al., 2014). Yeast two-hybrid screening was done using previously described strains, plasmids, media and transformation protocols (Altmann et al., 2018). For detection of AD auto-activators, the AD-fused transcription factor collection in MATa Y8800 yeast strains was mated with the empty pDEST-DB expressing MAT$\alpha$ Y8930 and subsequently selected in the presence of 1 mM 3-amino-1,2,4-triazole (3-AT). The DELLA protein screens were performed twice, once with 1 mM 3-AT and a second time with 2 and 3 mM 3-AT for RGA and GAI, respectively. The SCR and SCL3 screens were performed once using 1 mM 3-AT. The molecular identities of all positive transcription factor clones were confirmed by sequencing of the respective inserts.

### 2.6.3. *In planta* protein-protein interaction analysis

Bimolecular fluorescence complementation (BiFC) assays were carried out using transient transformation of *Nicotiana benthamiana* leaves with transformed *Agrobacterium tumefaciens* grown to $OD_{600}$ = 0.4 as previously described (Bos et

al., 2010). Fluorescence complementation was observed after 2-3 days with an Olympus FV1000 (Olympus, Hamburg, Germany) confocal microscope. The specified open reading frames were cloned for this purpose into the vectors pCL112 and pCL113 (Bos et al., 2010).

### 2.7. Accession numbers

Sequence data from this article can be found in the Arabidopsis Genome Initiative database under the following accession numbers: GA1 (AT4G02780), MAX1 (AT2G26170), MAX3 (AT2G44990), SMXL8 (AT2G40130), BRC1 (AT3G18550), GA2OX2 (AT1G30040), DFL1 (AT5G54510), GA2 (AT1G79460), GA3 (AT5G25900), KAO1 (AT1G05160), KAO2 (AT2G32440), GA20OX1 (AT4G25420), GA20OX2 (GA20OX2), GA20OX3 (AT5G07200), GA3OX1 (AT1G15550), GA3OX2 (AT1G80340), GA2OX4 (AT1G47990), GA2OX6 (AT1G0240), GID1A (AT3G05120), GID1B (AT3G63010), GID1C (AT5G27320), GAI (AT1G14920), RGA (AT2G01570), RGL1 (AT1G66350), RGL2 (AT3G03450), RGL3 (AT5G17490), D27 (AT1G03055), MAX4 (AT4G32810), LBO1 (AT3G21420), D14 (AT3G03990), KAI2 (AT4G37470), MAX2 (AT2G42620), SMAX1(AT5G57710), SMXL2 (AT4G30350), SMXL3 (AT3G52490), SMXL4 (AT4G29920), SMXL5 (AT5G57130), SMXL6 (AT1G07200), SMXL7 (AT2G29970), AtNPF1.1 (AT3G16180), AtNPF2.5 (AT3G45710), AtNPF2.10 (AT3G47960), AtNPF2.13 (AT1G69870), AtNPF3.1 (AT1G68570), AtNPF5.2 (AT5G46050), AtNPF5.8 (AT5G14940), SWEET4 (AT3G28007), SWEET10 (AT5G50790), SWEET12 (AT5G23660), ABCA7 (AT3G47780), ABCB11 (AT1G02520), ABCB15 (AT3G28345), ABCC2 (AT2G34660), ABCC12 (AT1G30410), ABCG1 (AT2G39350), ABCG14 (AT1G31770), ABCG19 (AT3G55130), ABCG22 (AT5G06530), ABCG27 (AT3G52310), ABCG34 (AT2G36380), ABCG37 (AT3G53480), *GAI* (AT1G14920), *GIF1* (AT5G28640), *GRF1* (AT2G22840), *GRF2* (AT4G37740), *GRF3* (AT2G36400), *GRF4* (AT3G52910), *GRF5* (AT3G13960), *GRF6* (AT2G06200), *GRF7* (AT5G53660), *GRF9* (AT2G45480), *RGA* (AT2G01570), *SCR* (AT3G54220), *SCL3* (AT1G50420), *XERICO* (AT2G04240)

# 3. Results

## 3.1. GA and SL treatments affect gene expression and plant morphology in *Arabidopsis thaliana* in an additive manner

### 3.1.1. GA- and SL- deficient plant phenotypes are additive

Since a reduction in stem elongation and a high branch number are phenotypes observed in both SL- and GA-deficient mutants, it was hypothesised that the two hormones might control these traits in cooperation (Silverstone et al., 1997; Gomez-Roldan et al., 2008; Umehara et al., 2008).

To assess the interaction of GA and SL in the control of growth and axillary branch elongation, the phenotypic outcome a combined GA and SL deficiency was investigated. Homozygous *ga1 max1-4* and *ga1 max3-9* double mutants were generated and provided by Carina Klermund. The single mutations were previously described and the homozygosity of the double mutants was confirmed by genotyping PCR (Table1) (Booker et al., 2004; Willige et al., 2007; Luo et al., 2012). As the GA-deficiency of *ga1* prevents germination, all seeds used in these experiments were treated with 100 µM $GA_3$ for 5 days during the stratification at 4 °C, and were subsequently repeatedly washed with water to remove excess $GA_3$. Mutant lines of *ga1*, *ga1 max1-4* and *ga1 max3-9*, as well as the wild type, could then be germinated on ½ MS 0.8 % agar plates for 10 days before they were transferred to soil.

The double *ga1 max1-4* and *ga1 max3-9* mutants phenotypically resembled the single *ga1* mutant as suggested by the analysis of rosette growth (Fig. 7A). Thus, SL deficiency did not affect bud release and plant growth in the absence of GA biosynthesis in *ga1*. In order to examine the branching and plant height phenotypes, the GA biosynthesis defect of *ga1* was partially normalized by $GA_3$ treatments in a second experiment. Wild type and the aforementioned single and double mutants were germinated on ½ MS 0.8 % agar plates for four days and subsequently transferred to soil. The plants were treated with 1 µM $GA_3$ or mock solution and the

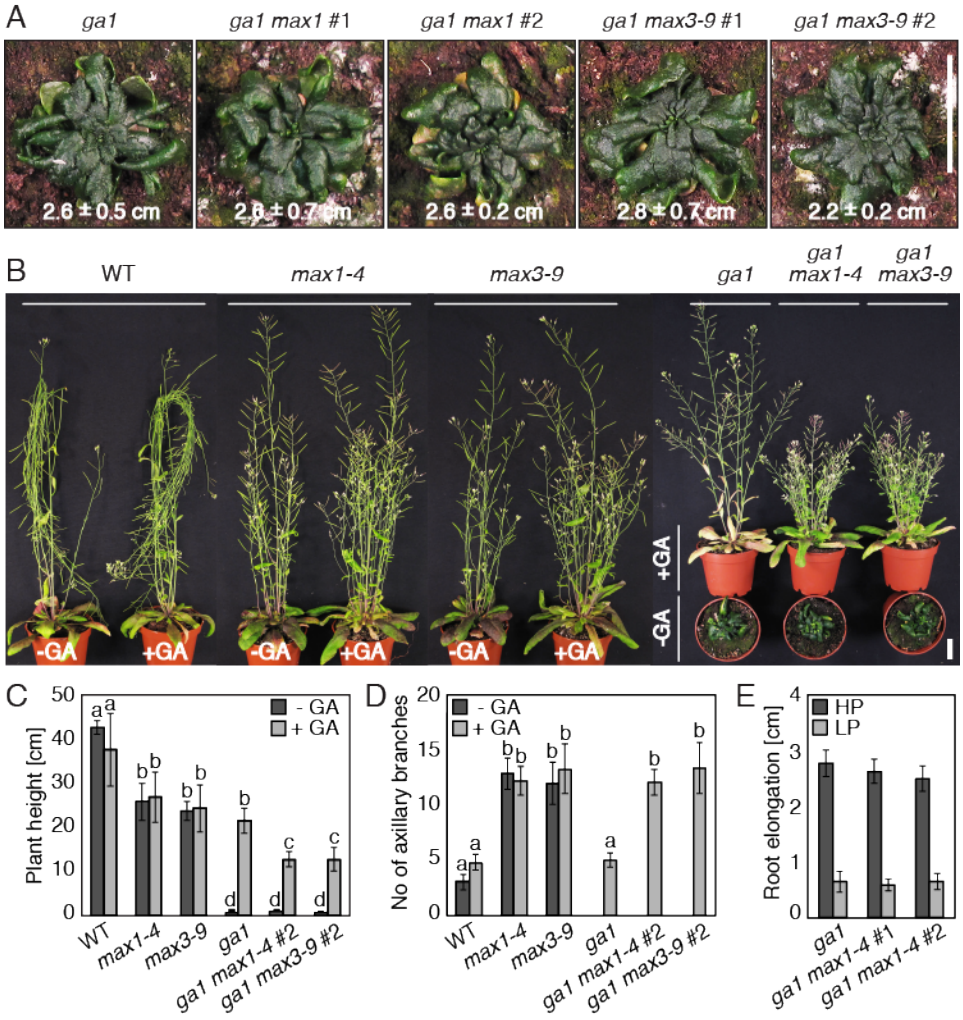


**Figure 7: Analysis of growth phenotypes of GA and SL deficient ga1 max1-4 and ga1 max3-9.**

(A) Six-week-old *ga1*, *ga1 max1* and *ga1 max3-9* plant-rosette photos. Mutant line numbers (#) and rosette diameters (mean; error bars SD; n = 10) are specified. Scale bar: 2 cm. (B) Photographs of 5-week-old plants with the genotypes as specified. WT, wild-type. Plants were treated four times at regular intervals with 1 µM $GA_3$ (+GA) or a mock solution (GA). Wild type plants were bent to fit the photograph. For actual plant heights, refer to (C). Scale bar: 2 cm. (C) and (D) Mean and SD of plant height (C) and number (No) of axillary branches (D) of 5-week-old plants with the genotypes as specified (n = 10). Axillary branches > 0.5 cm were counted. Same letters indicate no significant differences between genotypes or treatments (Tukey's HSD, $P < 0.05$). (E) Primary root elongation of 15-day-old seedlings (n = 36) grown on Murashige and Skoog (MS) for 8 days and transferred to high- (1.0 mM $KH_2PO_4$; HP) or low-phosphate (10 µM $KH_2PO_4$; LP) medium for an additional 7 days.

plant height and branch number were recorded after 5 weeks of growth (Fig. 7B, 7C and 7D). As expected, mock-treated *max1-4* and *max3-9* mutants were shorter

compared to wild-type whereas *ga1* and *ga1 max* mutants did not bolt (Fig. 1B, 1C and 1D). GA treatment partially rescued the stem elongation defect of the *ga1* mutant but had no effect on the single *max* mutants (Fig. 7B and 7C). Similarly, GA treatment promoted the stem elongation of the *ga1 max* mutants, but significantly less compared to *ga1* (Fig. 7C). Therefore, SL-dependent shoot elongation was unaffected by GA treatments. The number of axillary branches of the single *max* mutants was more than double compared to wild type, and not altered after GA treatment (Fig. 7D). GA-treated *ga1 max* mutants had the same branch number as the single *max* mutants, whereas the branch number did not differ in GA-treated *ga1* compared to the wild type (Fig. 7D). Hence, the increased branch number occurred only as a result of SL deficiency and required the presence of GA.

Lastly, since low phosphate-containing medium promotes SL biosynthesis as well as a reduction in root elongation, which in turn depends on GA and DELLA levels, the root growth of *ga1* and *ga1 max1* mutants was measured in two different phosphate regimes (Fig. 7E) (Jiang et al., 2007; Kohlen et al., 2011; Mayzlish-Gati et al., 2012). Seedlings were grown for eight days on ½ MS 0.8 % agar plates and subsequently for additional seven days on medium with either high phosphate (1.0 mM $KH_2PO_4$; HP) or low phosphate (10 µM $KH_2PO_4$; LP). However, the root elongation of *ga1* and *ga1 max1-4* was similarly inhibited in both HP and LP conditions and, therefore, the expected higher SL levels of *ga1* did not influence the LP-imposed root growth inhibition (Fig. 7E). In conclusion, GA- and SL-deficient plants expressed additive morphological phenotypes.

### 3.1.2. RGA levels in seedlings are not affected by SL

A previous report suggested the direct involvement of SL signaling in DELLA regulation through the binding of the rice SLR1 with the SL receptor D14 (Nakamura et al., 2013). To evaluate this observation in the novel genetic background described here, the amount of the DELLA protein RGA was surveyed (Stirnberg et al., 2002). Total protein was extracted from pools of eight-days-old plants grown in HP medium. Immunoblot analysis showed similar RGA levels between the wild type and single

*max1-4*, *max3-9* and *max2-1* mutants (Fig. 8A). In addition, *ga1* and *ga1 max1-4* had similarly increased RGA content (Fig. 8A). In addition, a time course experiment (30, 60, 120 and 240 minutes) of ten-days-old *ga1 max1-4* seedlings treated with 100 µM $GA_3$, 5 µM GR24, 100 µM $GA_3$ + 5 µM GR24 and mock solution revealed that GA, as expected, but not SL impacted RGA stability (Fig. 8B). Therefore, it was concluded that neither RGA levels nor RGA degradation are dependent on SL biosynthesis or signaling, at least not in seedlings.

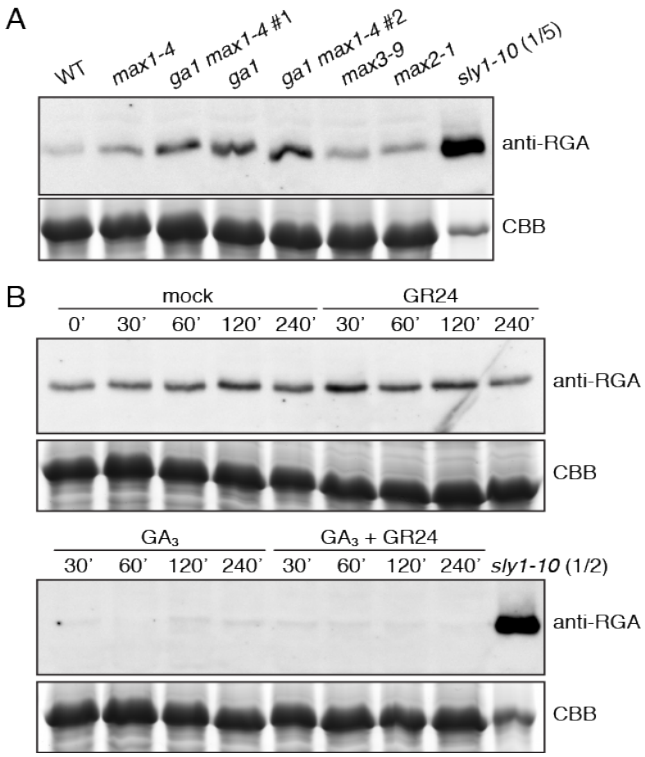


**Figure 8. Seedling DELLA protein content is not affected by SL.**

(A) Anti-RGA immunoblot and CBB (Coomassie Brilliant Blue) stained gel of protein extracted from 8-day-old seedlings grown on high-phosphate (HP) medium as specified in Figure 7E. (B) Anti-RGA immunoblot and CBB-stained gel of protein extracted from 10-day-old *ga1 max1-4 # 2* seedlings grown on 1/2 Murashige and Skoog (MS) and treated for the times indicated with a mock solution, 100 µM gibberellin ($GA_3$), 5 µM GR24 or 5 M GR24 plus 100 µM GA3 as specified. The samples were processed in parallel, incubated in two different blots as shown, and exposed for the same period of time.

### 3.1.3. GA and GR24 regulate gene transcription mostly in an additive manner

To understand how GA and SL induced transcription responses might be connected, an RNA-seq experiment was performed. The *ga1 max1-4* mutant line was used as it allows the study of both hormonal responses in one genetic background in the absence of the respective other pathway. Thus, the background activity of gene expression that would occur due to the developmental differences from the comparison of the respective single mutants was minimized.

Seven-days-old seedlings grown on ½ MS 0.8 % agar plates were transferred to liquid ½ MS for seven hours. Subsequently, the seedlings were transferred in liquid ½ MS medium that contained the hormone combinations of 100 µM $GA_3$, 5 µM GR24, 100 µM $GA_3$ + 5 µM GR24 as well as mock solution (Fig. 9A). The applied concentrations were previously used to rescue the increased number of axillary branches and the dwarf phenotype of the single *max3* and *ga1* mutants, respectively (Willige et al., 2007; Umehara et al., 2008). Three biological replicates for each treatment were sampled at 0 and after 30, 60 and 120 minutes (Fig. 9A). RNA was extracted from pooled whole seedlings and mRNA was sequenced as detailed in Materials and Methods. Three biological replicates were included in the analysis. The sequencing generated an average of $33 * 10^6$ reads (SD = ±4) per sample, which were mapped on the reference *Arabidopsis* genome TAIR10. The differentially expressed genes (DEGs) after $GA_3$, GR24 and $GA_3$+GR24 treatments were identified with the comparison of the respective samples to the mock samples for each time point. The filtering criteria fold-change (FC) > 1.5 and false discovery rate (FDR) corrected p-value < 0.01 were applied.

$GA_3$ treatment alone affected the expression of a total of 210 genes, 167 of which were suppressed over the course of two hours (Fig. 9B). These included 15 out of 20 genes that were previously identified to be differentially transcribed after GA treatment in multiple experiments (Claeys et al., 2014). In addition, gene ontology (GO) enrichment analysis of the 210 DEGs was performed, and the term “response to GA” (GO:0009739) was the most significantly enriched (p-value = 2.9E-14, Appendix I). Overall, the DEGs of *ga1 max1* after GA treatment included several previously known hormone targets (Claeys et al., 2014).

GR24 application caused a total of 73 DEGs, most of which were identified after two hours, whereas none were detected after 30 minutes. In contrast to the response to GA, a majority 64 DEGs were upregulated (Fig. 9B). The GO terms “response to chemical” (GO:0042221, p-value = 0.01) and “response to stimulus” (GO:0050896, p-value = 0.03) were significantly enriched (Appendix I). Seven of the 73 DEGs were also differentially expressed after $GA_3$ treatment. More specifically, a MATE

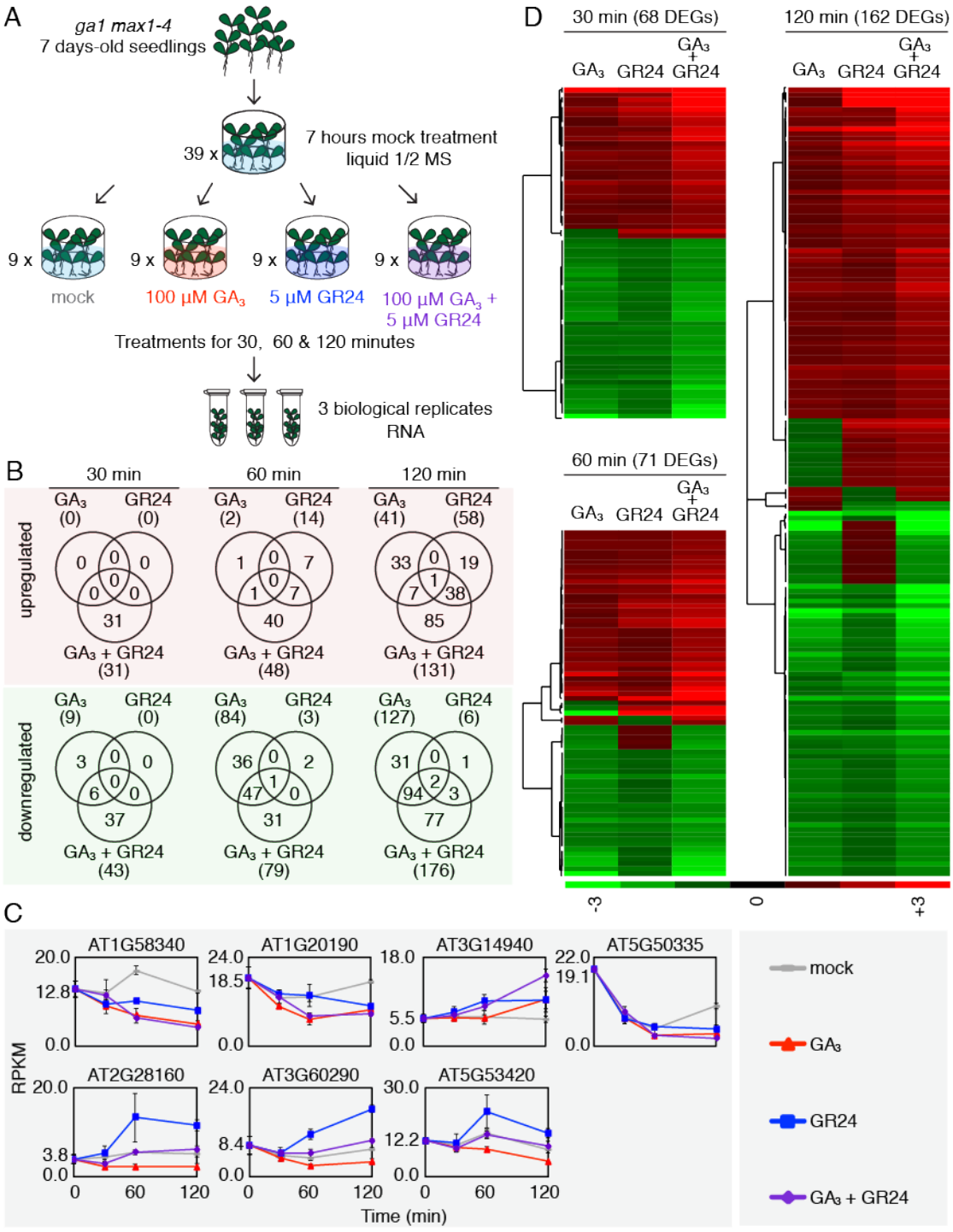


**Figure 9. GA and SL induced changes in gene expression in mutants.**

(A) Schematic representation of the experimental design of the RNA-seq experiment. (B) Venn diagrams of the differentially expressed genes (DEGs) after hormone treatments compared to the mock treatment at each of the three time points. Fold change (FC) >1.5; false discovery rate-corrected P-value <0.01. (C) RNA-seq results of genes regulated in both 100 µM $GA_3$ and 5 µM GR24 single treatments (D) Heat map of the 68, 71 and 162 DEGs that were identified only in response to the combined 100 µM $GA_3$ + 5 µM GR24 after 30, 60 and 120 min of treatment. log2-transformed FC values were used (cluster 3.0 algorithm, correlation uncentered, complete linkage).

transporter (AT1G58340), an EXPANSIN family gene (AT1G20190), a phosphoenolpyruvate carboxylase (AT3G14940) and an unknown protein (AT5G50335), were either activated or suppressed by both hormones (Fig. 9B and 9C). Three additional genes namely *FE-DEFICIENCY INDUCED TRANSCRIPTION FACTOR* 1 (AT2G28160), a 2-oxoglutarate and Fe (II)-dependent oxygenase (AT3G60290) and a CCT motif family protein (AT5G53420), were upregulated after GR24 and downregulated after $GA_3$ treatments whereas after the combined treatment gene expression was normalized to the mock levels (Fig. 9C). So, the vast majority of DEGs after single $GA_3$ and GR24 treatments were specifically controlled by one of the two hormones.

Surprisingly, $GA_3$ + GR24 treatments resulted in the differential expression of 386 genes in total, which included 261 unique DEGs for this condition. GO analysis revealed several enriched categories only for this group (261 DEGs), including “response to ethylene” (GO:0009723, p-value = 1.46E-04), “response to salicylic acid” (GO:0009751, p-value=1.30E-03) and “response to chitin” (GO:0010200, p-value = 1.08E-04) (Appendix I). Only 125 DEGs were also detected after either one or both the single hormone treatments (Fig. 9B and 9C).

The fact that the number of unique DEGs was increased when compared to the single treatments was consistent for each of the three time points (Fig. 9B). Notably, no DEGs were detected after 30 minutes of single GR24 treatment and only 9 DEGs after single $GA_3$ treatment as opposed to 68 DEGs after $GA_3$ + GR24 treatment. In addition, 71 and 162 DEGs were detected exclusively in the double $GA_3$ + GR24 treatment after 60 and 120 minutes, respectively (Fig. 9D). Hierarchical clustering and heatmap of the latter showed that the majority of upregulated DEGs had also positive FCs in the single hormone treatments. Similarly, the majority of downregulated genes had negative fold changes in the single hormone treatments (Fig. 9D). Although the 261 DEGs were detected only after the combined treatment, their expression pattern appeared to follow the same trend in the single hormone treatments.

This result could be explained by either additive or synergistic actions of GA and SL on the transcription activation or repression of the individual genes. In the case of additive gene regulation, analysis of the read-count results of the single hormone treatments, would be sufficient to closely estimate the experimental FC after double $GA_3$ + GR24 treatment as $FC_{Calculated} = FC_{GA} + FC_{GR24} - 1$. In contrast, changes in gene expression that cannot be predicted without the addition of other parameters would indicate synergistic action of the two hormones. The $FC_{Calculated}$ value for the 68, 71 and 162 unique $GA_3$ + GR24 identified DEGs was subtracted from the experimental FC after $GA_3$ + GR24 treatment ($FC_{Experimental}$). The resulted values for the three time points were plotted against the log2-transformed RPKM for each gene at the mock treatment (Fig. 10A). The majority of the differences was distributed around "zero", regardless of the expression level of the genes or up/downregulation by the treatment. In particular, 72 %, 77 % and 80 % of the $FC_{Calculated} - FC_{Experimental}$ values were between -0.5-FC and +0.5-FC for the 30, 60 and 120 minutes DEGs, respectively (Fig. 10B). A l0.5l-FC difference was set as an arbitrary threshold to account for technical variation between the single and combined treatments. This suggested that the majority of the transcription changes after the combined treatment occurred through the additive effects of the single hormone treatments (Fig. 10B). For the remaining 19 (30 min), 17 (60 min) and 31 (120 min) DEGs $|FC_{Calculated} - FC_{Experimental}| > 0.5$ implied synergistic regulation (Table 3).

In total, 22 upregulated genes were synergistically activated ($FC_{Calculated}$ - $FC_{Experimental} < -0.5$) while one upregulated gene was antagonistically regulated ($FC_{Calculated} - FC_{Experimental} > 0.5$). Similarly, nine downregulated genes were categorized as synergistically suppressed ($FC_{Calculated} - FC_{Experimental} > 0.5$) and 30 downregulated genes as antagonistically regulated ($FC_{Calculated} - FC_{Experimental} < -0.5$) (Table 3). The synergistically activated DEGs included the GA catabolism gene *GA2ox2* (AT1G30040), as well as the SL signaling target genes *SMXL8* (AT2G40130) and *BRANCHED1* (*BRC1*, AT3G18550). The later, and two additional genes, namely *DWARF IN LIGHT1* (*DFL1*, AT5G54510) and AT1G60060, were chosen for independent assessment of the RNA-seq results by quantitative reverse

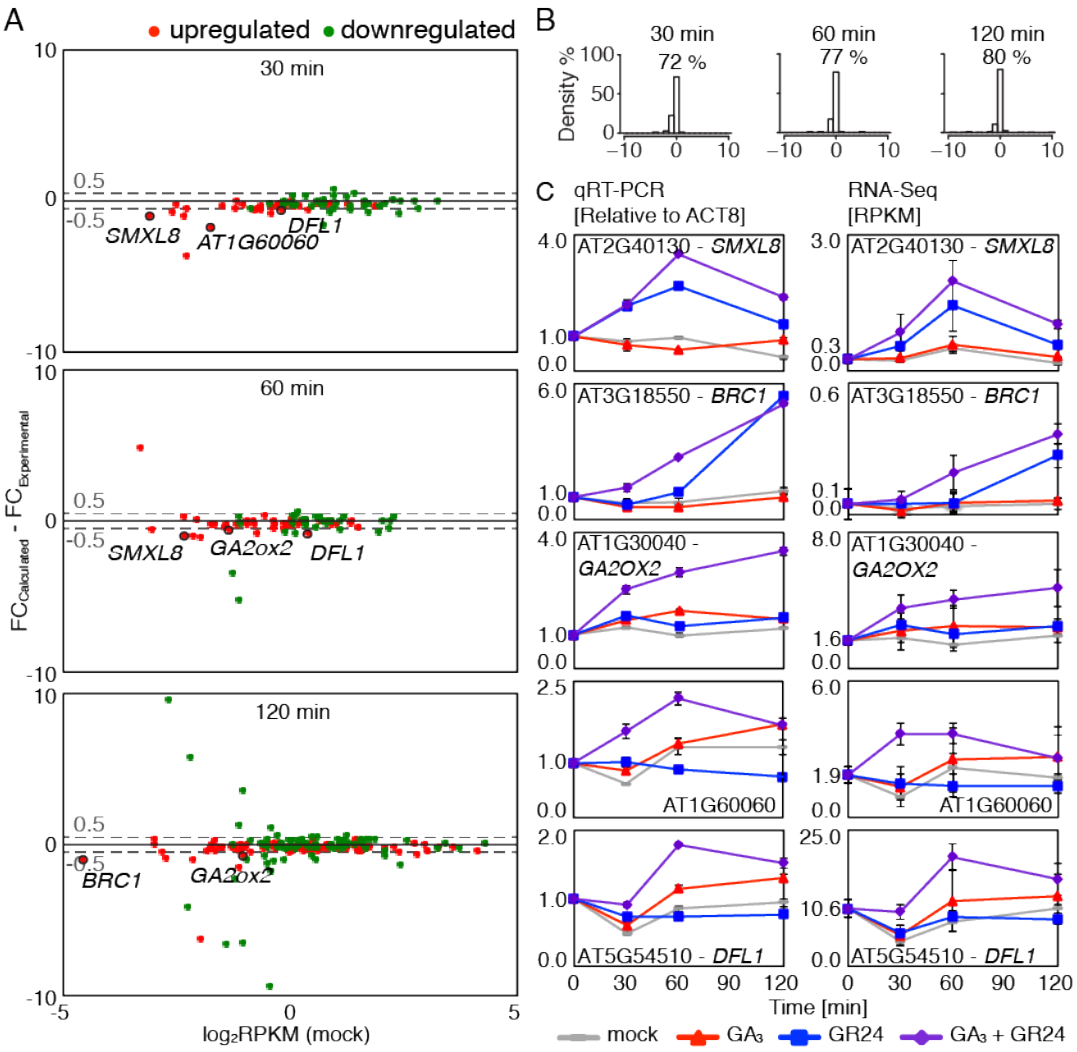


**Figure 10. DEGs detected only in response to the combined GA plus GR24 treatment show mostly additive changes in mRNA levels.**

(A) Scatterplots of the subtracted experimentally derived fold changes of the combined GA3 + GR24 treatment (FCexperimental) from the mathematically determined FC (FCcalculated) of DEGs detected in the combined treatment. (B) Density histograms of the distribution of the FCcalculated–FCexperimental for the DEGs presented in (A). (C) RNA-seq and quantitative reverse transcriptase-polymerase chain reaction (qRT- PCR) results of selected synergistically regulated genes in the RNA-seq.

transcriptase-polymerase reaction (qRT-PCR) (Fig.10C). The expression pattern of the selected genes was very similar in both analyses (Fig. 10C). The expression of *SMAXL8* was increased in the presence of GR24 (30 min, 2.34-FC, 60 min, 2.81-FC), not affected by the single $GA_3$ treatment (30 min, 1.2-FC, 60 min, 1.18-FC), and even more enhanced after the combined treatment compared to the mock treatment (30 min, 3.59-FC, 60 min, 3.93-FC). *BRC1* transcript levels followed a

similar pattern, but it was differentially expressed in a significant manner (DE) only after 120 minutes ($GA_3$, 1.3-FC; GR24, 4.91-FC; $GA_3$ + GR24, 6.2-FC) (Table 3). *GA2ox2* transcription was increased after 60 and 120 minutes of combined treatment, but remained almost unchanged after the single treatments. Furthermore, the protein kinase AT1G60060 was differentially expressed already after 30 minutes of combined treatment. Finally, *DFL1*, a gene that encodes an auxin amino-acid conjugation enzyme involved in auxin homeostasis was significantly upregulated after 30 and 60 minutes of combined treatment (Fig. 10C, Table 3). In conclusion, the transcription changes after $GA_3$ + GR24 treatments were mostly the result of additive effects of the two hormones, and only a small subset of genes was controlled in a synergistic manner.

**Table 3: List of 62 differentially expressed genes that undergo cooperative regulation by the two hormones. Genes that undergo positive synergism are annotated with bold.**

| Feature ID | Gene Symbol | 100 µM GA3 | 5 µM GR24 | 100 µM GA3 + 5 µM GR24 | FC calculated | FCcalculated-FCexperimental |
|---|---|---|---|---|---|---|
| | | | | 30 minutes | | |
| AT1G21910 | DREB26 | -1.76 | -1.27 | -2.12 | -2.81 | -0.69 |
| AT2G35640 | AT2G35640 | -1.39 | -1.48 | -2 | -2.53 | -0.53 |
| AT5G67300 | MYBR1 | -1.56 | -1.32 | -1.98 | -2.51 | -0.53 |
| **AT4G13395** | **RTFL12** | **-1.15** | **-1.03** | **-1.95** | **-1.19** | **0.76** |
| AT3G59940 | AT3G59940 | -1.75 | -1.27 | -1.89 | -2.79 | -0.90 |
| AT1G61660 | AT1G61660 | -1.36 | -1.45 | -1.74 | -2.35 | -0.61 |
| AT5G03230 | AT5G03230 | -1.82 | -1.34 | -1.73 | -3.38 | -1.65 |
| AT3G45260 | AT3G45260 | -1.54 | -1.25 | -1.71 | -2.23 | -0.52 |
| AT4G01720 | WRKY47 | -1.67 | -1.2 | -1.62 | -2.31 | -0.69 |
| **AT3G60220** | **ATL4** | **1** | **1.17** | **1.78** | **1.17** | **-0.61** |
| **AT5G54510** | **DFL1** | **1.2** | **1.28** | **2.11** | **1.48** | **-0.63** |
| **AT1G29160** | **AT1G29160** | **1.03** | **1.55** | **2.2** | **1.58** | **-0.62** |
| **AT2G34140** | **AT2G34140** | **1.05** | **1.66** | **2.28** | **1.71** | **-0.57** |
| **AT1G74890** | **ARR15** | **1.36** | **1.27** | **2.55** | **1.63** | **-0.92** |
| **AT5G03680** | **PTL** | **1.33** | **1.57** | **2.63** | **1.90** | **-0.73** |
| **AT3G61250** | **MYB17** | **1.26** | **1.95** | **3.15** | **2.21** | **-0.94** |
| **AT2G40130** | **SMXL8** | **1.2** | **2.34** | **3.59** | **2.54** | **-1.05** |
| **AT1G60060** | **AT1G60060** | **1.43** | **1.64** | **3.85** | **2.07** | **-1.78** |
| **AT2G47780** | **AT2G47780** | **3.94** | **2.78** | **9.39** | **5.72** | **-3.67** |
| | | | | 60 minutes | | |
| AT4G34419 | AT4G34419 | -5.21 | -1.22 | -7.86 | -86.13 | -78.27 |
| AT3G63110 | IPT3 | -1.77 | -1.36 | -2.65 | -3.33 | -0.68 |
| AT5G43890 | YUC5 | -1.89 | -1.65 | -2.17 | -7.40 | -5.23 |
| AT1G73805 | SARD1 | -1.94 | -1.51 | -2.15 | -5.63 | -3.48 |
| **AT1G62370** | **AT1G62370** | **-1.54** | **1.13** | **-1.85** | **-1.28** | **0.57** |
| AT1G61340 | FBS1 | -1.53 | -1.41 | -1.83 | -2.76 | -0.93 |
| AT1G61660 | AT1G61660 | -1.47 | -1.3 | -1.65 | -2.22 | -0.57 |
| AT1G21050 | AT1G21050 | -1.37 | -1.43 | -1.62 | -2.33 | -0.71 |

| | | | | | | |
|---|---|---|---|---|---|---|
| AT2G37180 | RD28 | -1.43 | -1.3 | -1.59 | -2.13 | -0.54 |
| **AT1G76620** | **AT1G76620** | **1.07** | **1.12** | **2.14** | **1.19** | **-0.95** |
| **AT1G18000** | **AT1G18000** | **1.63** | **-1.14** | **2.33** | **1.51** | **-0.82** |
| **AT5G54510** | **DFL1** | **1.47** | **1.09** | **2.42** | **1.56** | **-0.86** |
| **AT1G60750** | **AT1G60750** | **-1.36** | **2.08** | **2.89** | **1.82** | **-1.07** |
| **AT1G30040** | **GA2OX2** | **1.83** | **1.43** | **2.91** | **2.26** | **-0.65** |
| **AT5G59990** | **AT5G59990** | **2.36** | **1.62** | **3.57** | **2.98** | **-0.59** |
| **AT2G40130** | **SMXL8** | **1.18** | **2.81** | **3.93** | **2.99** | **-0.94** |
| AT4G28520 | CRU3 | -20.86 | 119.52 | 113.74 | 118.57 | 4.83 |
| | | | | 120 minutes | | |
| **AT4G00893** | **AT4G00893** | **-3.26** | **1.14** | **-11.78** | **-2.24** | **9.54** |
| **AT1G56650** | **PAP1** | **-5.2** | **1.14** | **-8.8** | **-3.01** | **5.79** |
| **AT5G49120** | **AT5G49120** | **-2.19** | **-1.08** | **-6.19** | **-2.61** | **3.58** |
| AT2G01200 | IAA32 | -2.32 | -1.45 | -4.21 | -8.29 | -4.08 |
| AT2G37390 | NAKR2 | -2.72 | -1.41 | -3.69 | -13.01 | -9.32 |
| AT4G01970 | STS | -2.09 | -1.61 | -3.38 | -10.04 | -6.66 |
| **AT1G62420** | **AT1G62420** | **-1.75** | **1.1** | **-2.7** | **-1.49** | **1.21** |
| AT1G29270 | AT1G29270 | -2.04 | -1.25 | -2.7 | -3.45 | -0.75 |
| AT4G32810 | MAX4 | -1.33 | -1.89 | -2.61 | -3.56 | -0.95 |
| **AT2G35270** | **GIK** | **-1.32** | **-1.06** | **-2.55** | **-1.43** | **1.12** |
| AT4G35720 | AT4G35720 | -2.27 | -1.49 | -2.49 | -8.95 | -6.46 |
| AT4G21310 | AT4G21310 | -2.04 | -1.28 | -2.47 | -3.68 | -1.21 |
| AT5G61610 | AT5G61610 | -2.05 | -1.26 | -2.47 | -3.55 | -1.08 |
| AT4G30290 | XTH19 | -1.4 | -1.74 | -2.46 | -3.46 | -1.00 |
| AT5G46050 | NPF5.2 | -1.85 | -1.33 | -2.37 | -3.42 | -1.05 |
| AT1G50280 | AT1G50280 | -1.89 | -1.42 | -2.02 | -4.29 | -2.27 |
| AT4G36670 | PMT6 | -1.45 | -1.48 | -1.98 | -2.74 | -0.76 |
| AT1G54010 | AT1G54010 | -1.63 | -1.44 | -1.94 | -3.25 | -1.31 |
| **AT4G28410** | **AT4G28410** | **-1.55** | **1.12** | **-1.91** | **-1.31** | **0.60** |
| AT1G72920 | AT1G72920 | -1.74 | -1.43 | -1.9 | -3.65 | -1.75 |
| **AT5G59080** | **AT5G59080** | **1.11** | **-1.36** | **-1.76** | **-1.18** | **0.58** |
| AT5G14360 | AT5G14360 | -1.4 | -1.43 | -1.71 | -2.42 | -0.71 |
| **AT4G21990** | **APR3** | **-1.15** | **1.22** | **1.76** | **1.09** | **-0.67** |
| **AT1G62975** | **AT1G62975** | **1.3** | **1.15** | **1.98** | **1.45** | **-0.53** |
| **AT1G35260** | **MLP165** | **1.19** | **1.57** | **2.29** | **1.76** | **-0.53** |
| **AT1G30040** | **GA2OX2** | **1.3** | **1.33** | **2.4** | **1.63** | **-0.77** |
| **AT2G37430** | **ZAT11** | **1.22** | **1.64** | **2.84** | **1.86** | **-0.98** |
| **AT1G76620** | **AT1G76620** | **1.73** | **1.46** | **3.05** | **2.19** | **-0.86** |
| **AT1G17180** | **GSTU25** | **1.05** | **4.01** | **5.52** | **4.06** | **-1.46** |
| **AT3G18550** | **BRC1** | **1.3** | **4.91** | **6.2** | **5.21** | **-0.99** |
| **AT4G33070** | **AT4G33070** | **1.81** | **3.75** | **10.84** | **4.56** | **-6.28** |

### 3.1.4. Gene transcript levels of GA and SL pathway genes after hormone treatments

An additional possibility for a hormone signaling interplay between GA and SL would be the mutual regulation of hormone levels or signaling proteins by the respective other pathway. Therefore, the gene expression results for metabolic and signaling genes of GA and SL from the RNA-seq experiment were investigated. In regard to GA biosynthesis, *GA3/KO*, *GA20ox1*, *GA20ox2*, *GA20ox3* and *GA3ox1* were

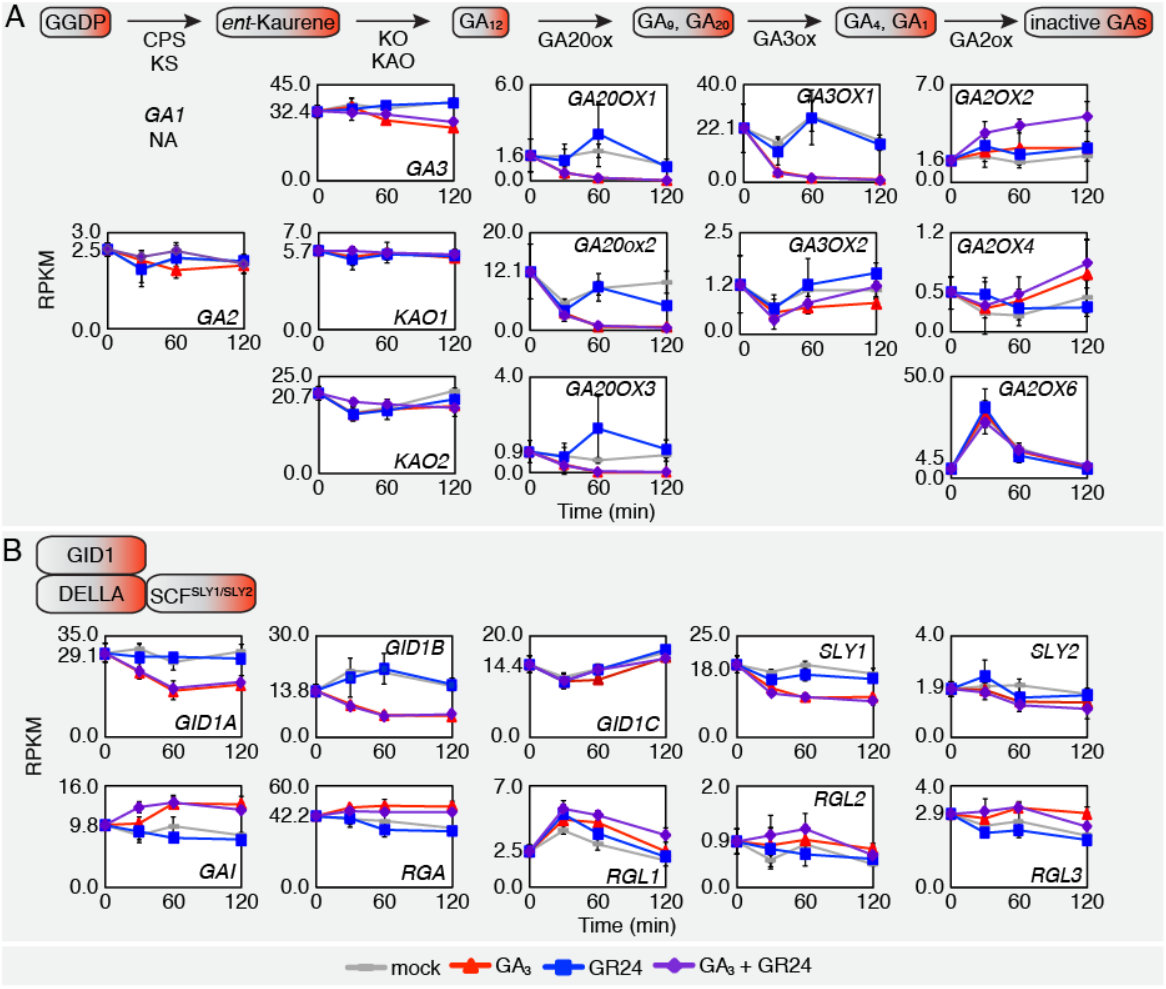


**Figure 11. mRNA level of GA pathway genes in the RNA-seq experiment.**

(A) and (B) Simplified diagrams of the GA biosynthesis and catabolism pathway (A) and the GA signaling pathway (B). Graphs displaying the RPKM normalized expression levels of the detected GA biosynthesis and catabolism genes (A) and GA signaling genes (B) in response to 100 µM GA3, 5 µM GR24 or 5 M GR24 plus 100 µM GA3 treatments in the RNA-seq experiment. GA1/CPS, GA REQUIRING2/ent-copalyl diphosphate synthase; GA2/KS, GA2/ent-kaurene synthase; GA3/KO, GA3/ent-kaurene oxidase; KAO, ent-kaurenoic acid oxidase; GA20OX, GA20 OXIDASE; GA3OX, GA3 OXIDASE; GA2OX, GA2 OXIDASE; GID1, GIBBERELLIC ACID INSENSITIVE DWARF1; SLY, SLEEPY; GAI, GIBBERELLIC ACID INSENSITIVE; RGA, REPRESSOR-OF -*ga1*; RGL, RGA-LIKE.

similarly downregulated after the treatments that included GA ($GA_3$ and $GA_3$ + GR24), whereas the GA catabolism gene *GA2ox4* was upregulated by $GA_3$ and $GA_3$ + GR24 treatment (Fig. 11A). This type of feedback regulation of GA biosynthesis and catabolism genes is a known effect of GA treatment (Yamaguchi, 2008; Hedden and Thomas, 2012; Claeys et al., 2014). Moreover, the GA receptor genes *GID1A* and *GID1B* as well as the F-box protein gene *SLY1* were suppressed, and DELLA

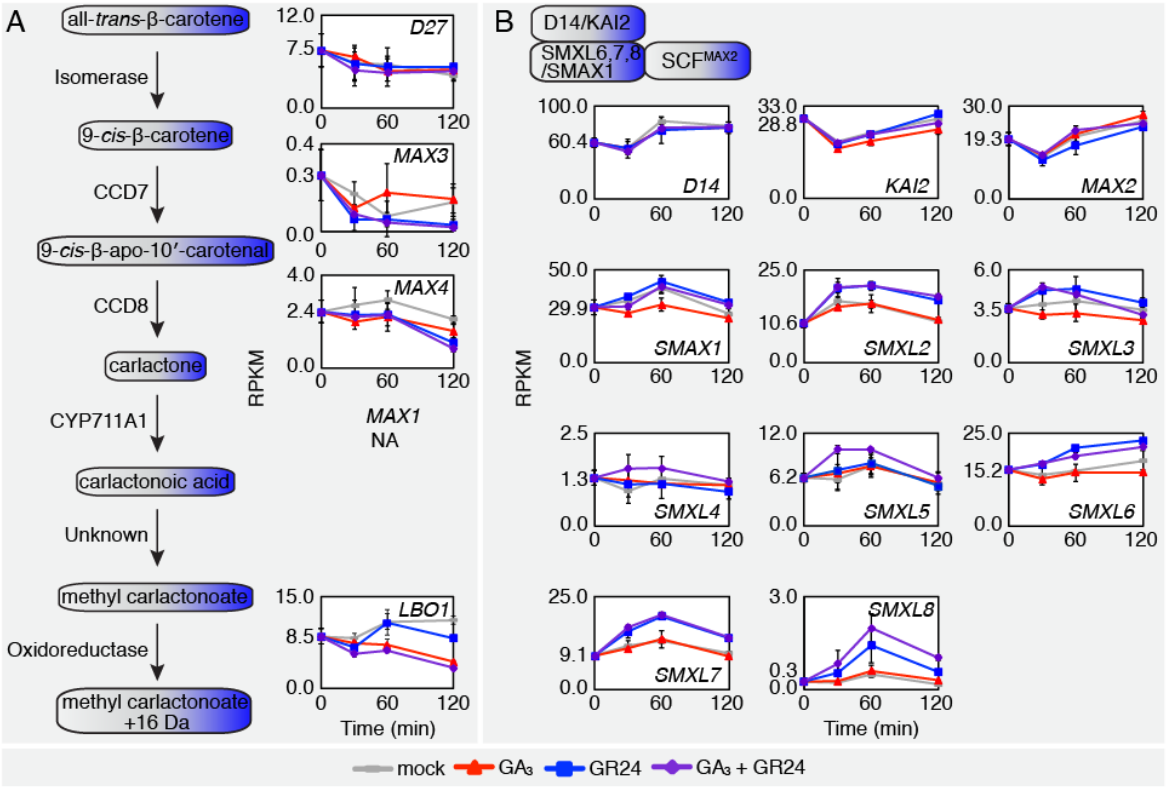


**Figure 12. mRNA level of SL pathway genes in the RNA-seq experiment.**

(A) and (B) Simplified diagrams of the SL biosynthesis (A) and signaling pathway (B). Graphs displaying the RPKM expression levels of the detected SL biosynthesis (A) and signaling genes (B) in response to 100 µM GA3, 5 µM GR24 or 5 M GR24 plus 100 µM GA3 treatments in the RNA-seq experiment. CCD7, CAROTENOID CLEAVAGE DIOXYGENASE7; CCD8, CAROTENOID CLEAVAGE DIOXYGENASE8; CYP711A1, CYTOCHROME P450 FAMILY 711 SUBFAMILY A POLYPEPTIDE 1; D27, DWARF27; KAI2, KARRIKIN INSENSITIVE2; MAX2, MORE AXILLARY BRANCHES2; MAX3, MORE AXILLARY BRANCHES3; MAX4, MORE AXILLARY BRANCHES4; LBO1, LATERAL BRANCHING OXIDOREDUCTASE1; D14, DWARF14; SMAX1, SUPPRESSOR OF *max2-1*; SMXL, SMAX1-LIKE.

encoding genes were upregulated after the treatments that contained GA (Fig. 11B). GR24 did not affect the expression of GA metabolic genes and pathway genes apart from the synergistically upregulated *GA2ox2* as discussed in the previous section (3.1.3).

The transcript abundance of the SL biosynthetic genes *MAX3* and *MAX4* was reduced after GR24 treatments, in line with a previous report (Fig. 12A) (Mashiguchi et al., 2009). *MAX4* downregulation was stronger after the combined ($GA_3$ + GR24) treatment and marginal after single $GA_3$ treatment. In addition, the oxidoreductase *LBO1*, which encodes an enzyme of a later SL biosynthesis step, was suppressed

after both the $GA_3$ and combined treatment, whereas GR24 alone did not affect its expression levels (Fig. 12A) (Brewer et al., 2016). Therefore, GA had a negative impact on SL biosynthesis gene expression. The latter has also been reported for GA-treated rice plants where SL hormone levels were decreased compared to untreated (Ito et al., 2017). On the other hand, the SL and KAR receptor genes *D14* and *KAI2*, as well as the F-box protein encoding *MAX2* were not differentially expressed by GR24 or GA treatments. However, *SMAXLs*, including the KAR-targeted *SMAXL2* and the SL targets *SMXL6*, *SMXL7*, *SMXL8*, were upregulated after GR24 treatments as reported previously (Fig. 12B) (Stanga et al., 2013). In addition, the double $GA_3$ + GR24 treatment led to the synergistic upregulation of *SMAXL8* (3.1.3). A similar transcript behavior was observed for *SMAXL4* and *SMAXL5* but the changes were not significant (p-value ≤ 0.5) (Fig. 12B). In conclusion, both $GA_3$ and GR24 single hormone treatments reduced the expression of SL biosynthesis genes, while SL/KAR signaling genes were upregulated only after GR24 treatments, or synergistically upregulated in the case of *SMAXL8* and *BRC1* after the combined treatment.

### 3.1.5. Gene transcript levels of hormone transporter genes

GA transporters belonging to the NITRATE TRANSPORTER1/PEPTIDE TRANSPORTER (NPF) and SWEET gene families as well as an ATP-binding cassette (ABC) transporter of SL in petunia, were previously described (Kretzschmar et al., 2012; Saito et al., 2015; Sasse et al., 2015; Kanno et al., 2016; Tal et al., 2016). Gene transcript levels of transporter genes were controlled by the respective hormones (Kretzschmar et al., 2012; Tal et al., 2016). Although, the later has not been investigated for all the proposed transporters, transcription changes after hormone treatments could be an indication for hormone transport activity. Therefore, the gene expression results for the reported transporters and proteins belonging to the same families were investigated (Fig. 13).

From the 53 *NFP* genes of *Arabidopsis*, six were differentially expressed in hormone-treated *ga1 max1-4* (RNA-seq). The characterized GA transporter *NPF3.1*

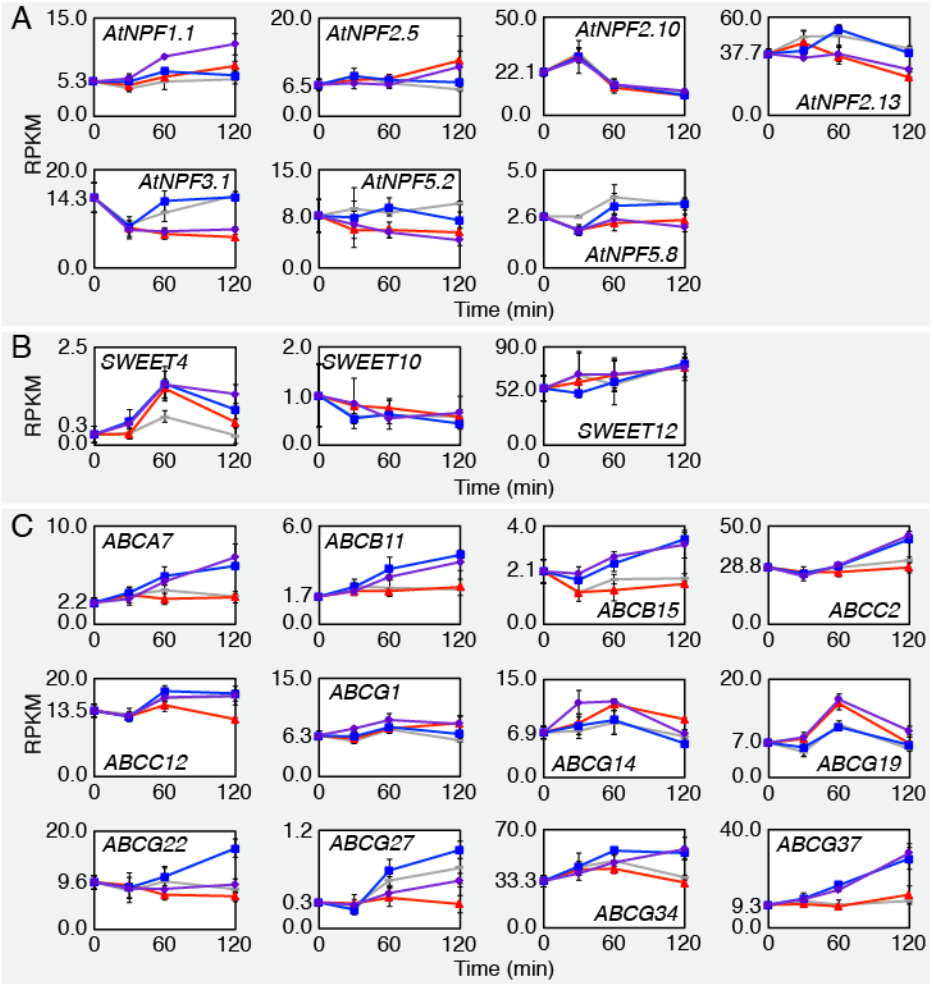


**Figure 13. mRNA levels of GA and SL transporter genes in the RNA-seq experiment.**

(A)–(C) RPKM normalized expression levels of chosen (a) NPF, (B) SWEET or (C) ABC transporter genes, in response to 100 µM GA3, 5 µM GR24 or 5 M GR24 plus 100 µM GA3 treatments in the RNA-seq experiment. Presented are genes that have been previously reported to transport either of the hormones or showed transcriptional regulation by $GA_3$ or GR24, and therefore qualify as candidate transporters.

(AT1G68570) was, as expected, suppressed following $GA_3$ treatments, but *NPF2.10/GTR1* (AT3G47960) was not differentially expressed (Fig.13A) (Saito et al., 2015; Tal et al., 2016). *NPF2.13* (AT1G69870) was also downregulated by $GA_3$, similarly to the known transporter *NPF3.1*. Although *NPF5.2* (AT5G46050) and *NPF5.8* (AT5G14940) appeared supressed after $GA_3$ treatment alone, they were only detected as DE in the combined treatment and thus categorized as additively and antagonistically regulated genes, respectively. Furthermore, *NPF2.5* (AT3G45710) was upregulated after $GA_3$ treatments and *NPF1.1* (AT3G16180) was

additively upregulated after the combined $GA_3$+GR24 treatments. Single GR24 treatments did not affect *NPF* gene expression (Fig.13A). The identified NPF DEGs in this experiment (*NPF1.1*, *NPF2.5*, *NPF2.13* and *NPF5.2*) showed GA transport activity in a previous yeast-based transporter screen, hence they could potentially represent functional GA transporters (Chiba et al., 2015).

The gene transcripts of the proposed SWEET GA transporters, *SWEET13* (AT5G50800) and *SWEET14* (AT4G25010), were not detected in this experiment. Furthermore, *SWEET10* (AT5G50790) and *SWEET12* (AT5G23660), which were shown to transport GA in a yeast assay, were not differentially expressed (Fig. 13B) (Kanno et al., 2016). In total, ten genes were expressed but only *SWEET4* (AT3G28007) was significantly upregulated in an additive manner after the combined treatment (Fig. 13B). For this reason, *SWEET4* may qualify as a transporter candidate for either GA or SL.

The gene expression data of the 130 members of the ABC-type transporter family in *Arabidopsis* were also analysed (Hwang et al., 2016). Among them, 12 genes were significantly regulated in this experiment (Fig. 13C). Interestingly, this family was the only enriched group in protein domain analysis of the 73 GR24 DEGs with six matches (Thalemine; p-value=0.007; InterPro, IPR003439). The transcript abundance of *ABCA7*, *ABCB11*, *ABCB15*, *ABCC2*, *ABCG34* and *ABCG37* was increased after GR24 treatments and was not affected by $GA_3$. Contrarily, *ABCG1*, *ABCG14* and *ABCG19* expression was upregulated after $GA_3$ treatments and did not change with GR24 (Fig. 13C). Three additional genes were identified as differentially expressed and their expression profiles suggested antagonistic regulation. More specifically, *ABCC12* was downregulated with $GA_3$, a response that was compromised in the $GA_3$+GR24 treatment. Similarly, *ABCG22* mRNA was increased after 120 minutes of GR24 treatment, but not in the combined treatment. Finally, *ABCG27* was downregulated after single GA treatment but not differentially expressed after the combined treatment (Fig. 13C). In conclusion, the differentially expressed transporters identified in this analysis could represent GA or SL hormone transporters.

### 3.1.6. Gene transcript levels of auxin pathway genes after hormone treatments

GA and SL are both involved in PIN-mediated auxin transport and the regulation of PIN abundance at the plasma membrane (Bennett et al., 2006; Crawford et al., 2010; Willige et al., 2011; Willige et al., 2012; Lofke et al., 2013; Shinohara et al., 2013; Salanenka et al., 2018). Hence, the possibility of transcription regulation of auxin transporters and auxin regulatory protein kinases was examined (Rademacher and Offringa, 2012). Amongst all the transporters and kinases, only *PIN2* (AT5G57090) was significantly upregulated after two hours in the treatments that contained GA according to the criteria FC > 1.5 and FDR corrected p-value < 0.0. Nevertheless, the resolution of the whole seedling analysis could have insufficient for the detection of expression changes of those genes as they have been previously shown in specific tissues such as root tip and apical hook.

## 3.2. GA transcription response and targets in low temperature stress.

### 3.2.1. GA cannot promote growth at 4 °C

DELLA protein stabilization occurs in *Arabidopsis* after short exposure to 4 °C temperature stress and it was suggested that it plays a growth inhibitory role (Achard et al., 2008). In order to investigate whether such an increase in DELLA abundance is causative for the limitation of growth in these conditions, wild type seedlings were grown in ½ MS 0.8 % agar plates for five days and then transferred to plates containing either $GA_3$ (1 or 10 μM), or the GA biosynthesis inhibitor PAC (1 or 5 μM), or mock solution for seven days at 4 °C. The root elongation was constrained, regardless of the treatment, while the growth of the PAC-treated seedlings was further limited (Fig. 14A and 14B). Hence, the degradation of DELLA proteins was not sufficient to relieve growth in these conditions.

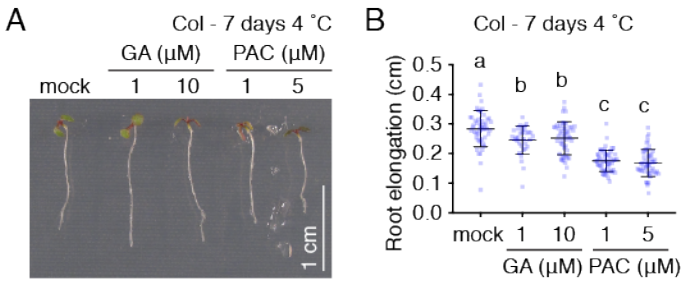


**Figure 14: GA cannot rescue 4 °C induced growth arrest.**

(A) Phenotypes and (B) root elongation of twelve-days-old Arabidopsis seedlings treated for 7 days with the specified concentrations of GA and PAC at 4 °C.

### 3.2.2. GA signaling is involved in cold stress-induced gene expression

Considering that there is no obvious phenotypic change related to the DELLA status when the plants grow in low temperature (4 °C), in order to examine the role of DELLA stabilization in this condition, a detailed gene expression and subsequently RNA-seq analysis were performed. Wild type seedlings were grown in ½ MS 0.8 % agar plates, at 21 °C for nine days before they were spray-treated with either 100 µM $GA_3$ or the corresponding mock (ethanol) control. Then, they were immediately placed in a 4 or a 21 ° C growth chamber with identical light conditions. Shoot tissue samples for protein and RNA analysis included one and three biological replicates, respectively (Fig. 15A). First, the RGA protein levels after exposure to 4 °C for 0, 1, 2, 4 and 6 hours were assessed. Total protein extract (45 µg) was analysed with anti-RGA immunoblot analysis where *sly1-10* (9 µg) served as a positive control. Increased protein content was observed as soon as 2 hours of cold stress treatment (Fig. 15B). In contrast, RGA was, as expected, not detected in GA-treated samples (Fig. 15C). In agreement with a previous report, cold-stress treatments increased the amount of RGA whereas GA treatments promoted RGA degradation in the same conditions (Fig. 15B and 15C) (Achard et al., 2008). Second, the gene expression levels of the cold-stress marker gene *CBF1* and the GA catabolism genes *GA2ox1*, *GA2ox3* and *GA2ox6* after 1, 2, 3, 4, 6 and 8 hours of treatments were analysed with qRT-PCR (Fig. 15A and 15D). *CBF1* was upregulated after 1 hour of cold stress treatment (4 °C mock), with a peak at 3 hours, compared to 21 °C samples where the transcript levels, relative to *ACT8*, were close to zero. Interestingly, after 1 hour of cold stress and 100 µM $GA_3$ treatment (4 °C GA) *CBF1* mRNA levels were the highest. *GA2ox1* expression was activated after 2, 3 and 8 hours of cold stress and

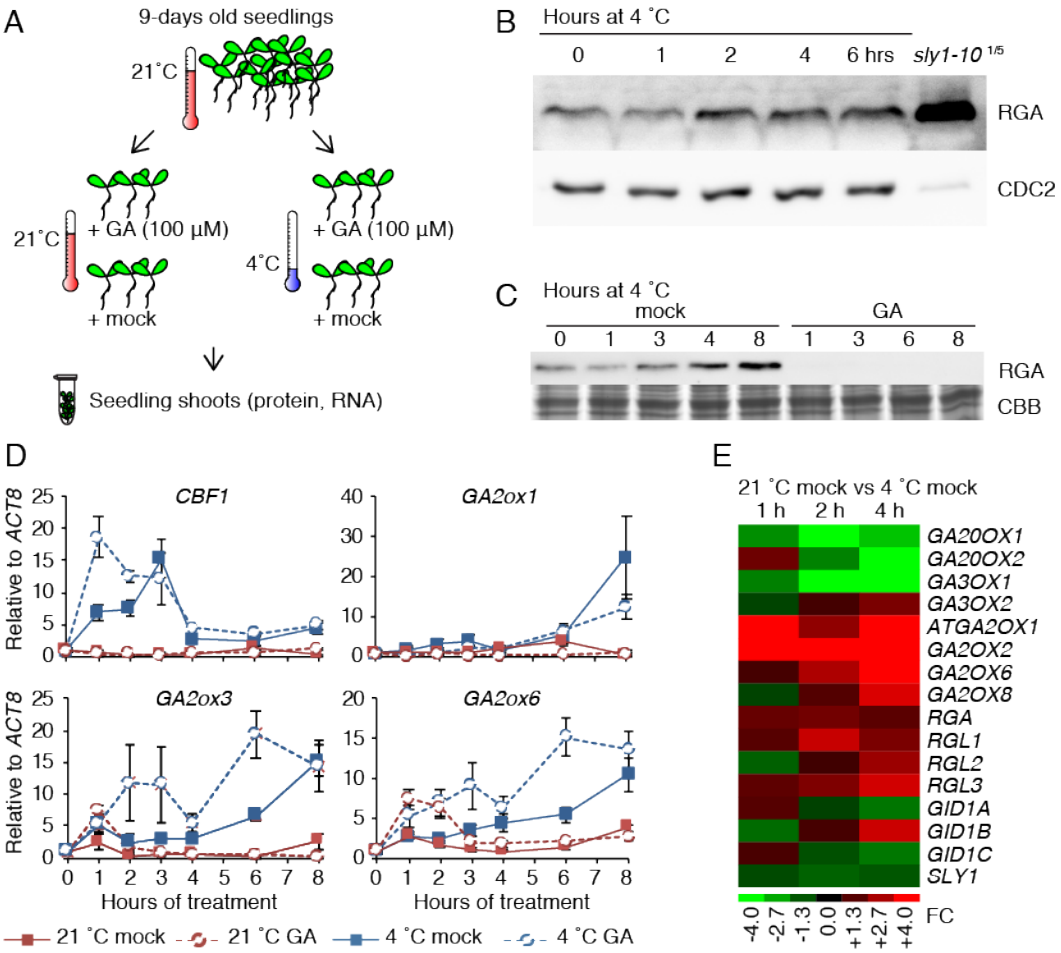


**Figure 15: Cold stress promotes DELLA protein increase, which in turn modifies transcription. Profound changes in transcript abundance of the GA pathway genes after GA3 and cold-stress transcription profiling.**

(A) Experimental design of the immunoblot and transcriptomics experiments. (B) Anti-RGA (DELLA) western-blot of shoot protein extract after seedling 4 °C treatments for the specified duration. (C) Anti-RGA (DELLA) western-blot of samples from the same experiment in response to 4 °C and 100 µM $GA_3$. (D) qRT-PCR gene expression analyses of the cold stress reporter gene *CBF1* and the GA catabolism genes *GA2ox1*, *GA2ox2* and *GA2ox6* of shoots in response to 4 °C and 100 µM $GA_3$ treatments. (E) Heat map of the fold changes in expression of GA pathway genes in response to cold stress treatment (21 °C mock vs 4 °C mock) in RNA-seq analysis. False discovery rate corrected p-value < 0.01 (Cluster 3.0, TreeView).

was not affected by GA. Finally, *GA2ox3* and *GA2ox6* were similarly upregulated after 100 µM $GA_3$ treatment at both 21 °C and 4 °C (21 °C GA; 4 °C GA) compared to the respective mock treatments. In addition, cold stress promoted the expression of the two genes already after 1 hour (Fig. 15D). Thus, while the increase in DELLA protein abundance at 4 °C was observed after two hours, its effect on transcriptional regulation was profound as early as one hour of cold exposure.

For the investigation of the effect of GA on gene expression in cold stress with RNA-seq, samples of the early time points (1, 2, and 4 hours) were selected in order to identify the direct DELLA targets. Total mRNA was sequenced with the Illumina technology and the resulting sequences were aligned to the reference genome TAIR10. Genes with FC > 1.5 and FDR corrected p-value < 0.01 were categorized as differentially expressed. The cold stress DEGs (21 °C vs 4 °C mock treated samples) included several components of GA metabolism and signaling (Fig. 15E). Cold stress supressed the transcription of the GA biosynthesis enzyme-encoding *GA20ox1*, *GA20ox2* and *GA3ox1* whereas the GA catabolism genes *GA2ox1*, *GA2ox2*, *GA2ox6* and *GA2ox8* were upregulated (Fig. 15E). Thus, transcription changes in hormone biosynthesis and catabolism could lead to the reduction of GA levels and consequently reduced DELLA degradation after cold stress exposure. Furthermore, cold-imposed upregulation of the DELLA-encoding genes *RGA*, *RGL1*, *RGL2* and *RGL3*, and suppression of the GA receptor gene *GID1A*, *GID1B* and the F-box *SLY1* were detected and these would further increase DELLA levels. Therefore, the cold stress effect on GA pathway gene expression could be causative for the observed DELLA stabilization.

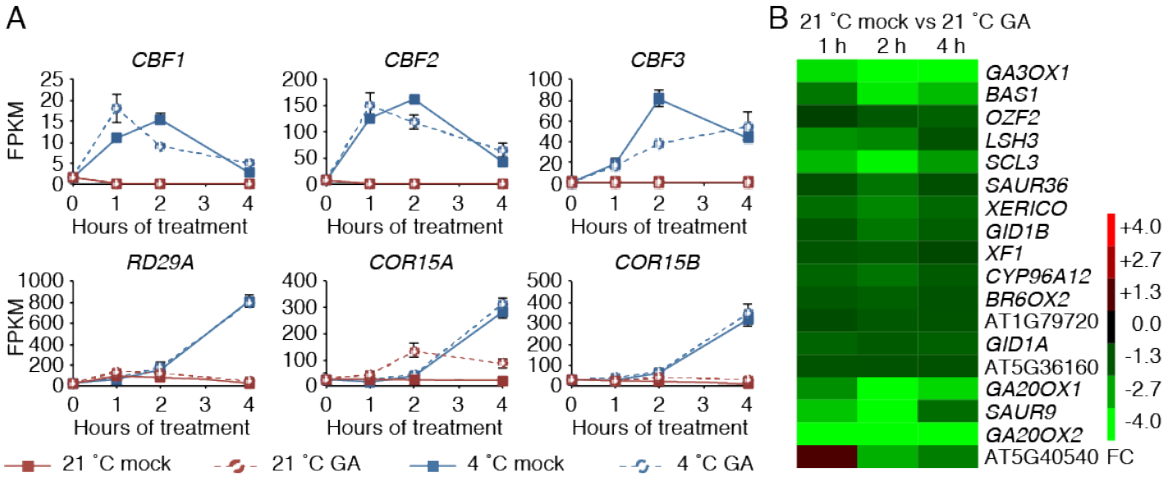


**Figure 16: Transcription changes of cold stress and GA marker genes in the transcriptomics experiment.**

(A) Transcript behaviour of cold stress marker genes in the transcriptomics experiment in response to 100 µM $GA_3$ at 21 °C and 4 °C. (B) Heat map of the fold changes in expression of GA marker genes in response to GA 21 °C treatment (21 °C mock vs 21 °C 100 µM $GA_3$). FPKM (Fragments per kilobase of exon model per million mapped reads). False discovery rate corrected) p-value < 0.01 (Claeys et al., 2014; Cluster 3.0, TreeView).

The impact of temperature and GA treatments was also evaluated based on the transcript behaviour of genes known to be regulated by the two responses. Expression upregulation of the established cold stress marker genes *CBF1*, *CBF2*, *CBF3*, *RD29A* and *COR15A/B* showed that the seedlings reacted to cold stress as expected (Fig. 16A) (Gilmour et al., 2004; Eremina et al., 2016). Moreover, the previous qRT-PCR results for *CBF1* matched the RNA-seq analysis results (Fig. 15D and 16A). The GA treatments at 21 °C repressed the expression of 18 out of 20 previously identified GA-regulated genes (Fig. 16B) (Claeys et al., 2014). Along these lines, the seedlings perceived the exogenously applied GA and this led to RGA degradation and the anticipated transcription changes (Fig. 15C and 16B).

The DEGs after GA treatments at 21 °C (21 °C + mock vs 21 °C + GA; GA 21 °C), at 4 °C (4 °C + mock vs 4 °C + GA; GA 4 °C) as well as after cold stress (21 °C + mock vs 4 °C + mock; cold stress) were identified (FC > 1.5, FDR corrected p-value < 0.01; Fig. 17A, 17B, 17C and 17D). In total 676 and 816 genes were differentially expressed after GA application at 21 °C and 4 °C, respectively (Fig. 17D). Only 23 (1 h), 46 (2 h) and 23 (4 h) genes were GA-regulated in both temperatures at the same time (Fig. 17A, 17B, 17C). The number of GA-controlled genes in both 21 °C- and 4 °C-treated plants increased to 165 when the individual time point results were combined (Fig. 17D). Hierarchical clustering analysis of the 165 DEGs showed that the majority of these genes as similarly up- or downregulated. In addition, the 2 and 4 hours-samples were grouped together according to temperature, as some of those genes behaved differently in response to GA in the two temperature regimes. (Fig. 17E). A further 511 (GA 21 °C) and 651 (GA 4 °C) DEGs were GA-regulated in either 21 °C or 4 °C (Fig. 17D). Thus, GA affected gene expression in a temperature-dependent manner.

Cold stress changed the transcription of a total of 7343 genes in the experiment, which is in line with previous studies that found similar numbers of DEGs (Fig. 17D) (Jia et al., 2016; Zhao et al., 2016; Calixto et al., 2018). These included 3264, 3602 and 4800 DEGs after 1, 2 and 4 hours of cold stress respectively (Fig. 17A, 17B and 17C). Among those, only 183 (5.6 %; 1 h), 165 (4.5 %; 2 h) and 187 (3.9 %; 4h)

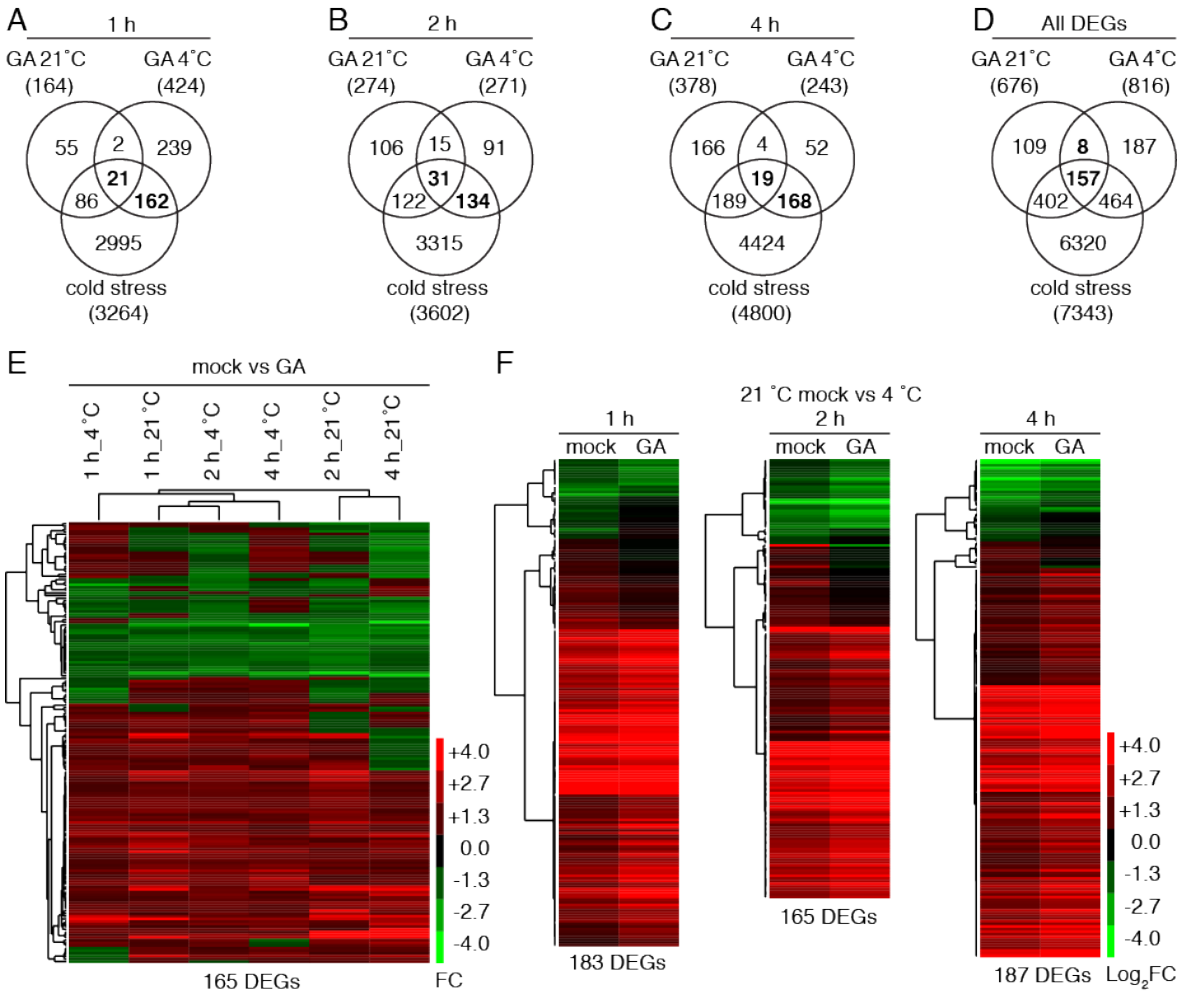


**Figure 17: Gibberellin treatment modifies cold stress transcription with largely unique targets compared to its effect in ambient temperature.**

(A), (B) and (C) Venn diagrams of the differentially expressed genes (DEGs) after cold stress (21 °C mock vs 4 °C mock), GA 21 °C (21 °C mock vs 21 °C 100 µM $GA_3$) and GA 4 °C (4 °C mock vs 4°C 100 µM $GA_3$) treatments for 1, 2 and 4 hours, respectively. Numbers of DEGs in response to cold stress and to GA at 4 °C are annotated with bold. (D) Venn diagram of the total number of differentially expressed genes after 1, 2 and 4 hours of treatments. The common DEGs after GA treatment at both 21 °C and 4 °C are annotated with bold. (E) Hierarchical clustering of the 165 DEGs (annotated with bold tones) in Venn diagram (D) and arrays according to the fold changes in expression in response to 100 µM $GA_3$ compared to the mock treatment in 21 °C and 4 °C after 1, 2 and 4 hours of treatments. (Cluster 3.0, correlation uncentered, average linkage, TreeView). (F) Hierarchical clustering of the log2-transformed fold changes in expression of 183, 165 and 187 DEGs (annotated with bold tones) in Venn diagrams (A), (B) and (C) in response to mock 4 °C as well as 100 µM $GA_3$ 4 °C treatments, compared to the mock 21 °C treatments. (Cluster 3.0, correlation uncentered, complete linkage, TreeView). Fold change ≥ 1.5; false discovery rate corrected p-value < 0.01.

were also differentially expressed after GA treatments at 4 °C (Fig. 17F). Hierarchical clustering analysis of the cold and GA 4 °C regulated genes revealed

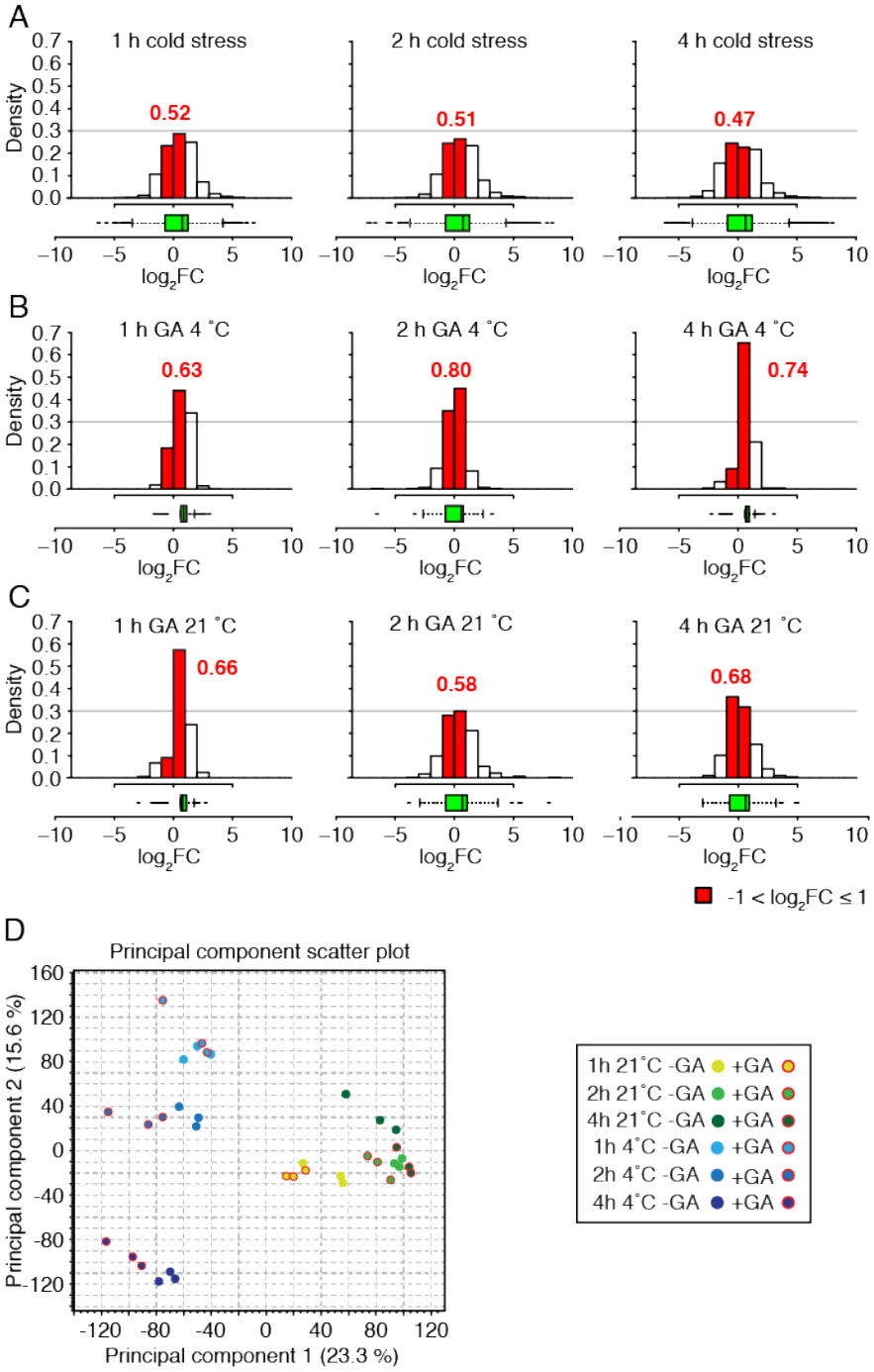


**Figure 18: Fold changes in mRNA abundance after GA treatments are milder compared to cold stress.**

(A), (B) and (C) Density histograms and boxplots of the log2 fold-changes in mRNA abundance of differentially expressed genes after 1, 2 and 4 hours of cold stress (21 °C mock vs 4 °C mock), GA 4 °C (4 °C mock vs 4 °C 100 µM $GA_3$) and GA 21 °C (21 °C mock vs 21 °C 100 µM $GA_3$) treatments respectively. Probability densities for $log_2$ transformed fold-changes ($log_2FC$) between -1 and 1 are shown in red. (D) Principal component analysis for the transcriptomics analysis (PCA for RNA-seq tool; CLC Genomics Workbench 10.1.1).

that GA affected gene expression in a positive or antagonistic way in relation to cold stress (Fig. 17F). A moderate effect the GA compared to cold treatments was also observed in the FCs of the respective DEGs. About half of the cold-regulated genes after 1 h (52 %), 2 h (51 %) and 4 h (47 %) of treatment had FC < 2 in expression (Fig. 18A). This number increased dramatically in the GA treatments. More specifically, 63 %, 80 % and 74 % of GA 21 °C DEGs and 66 %, 58 % and 68 % of GA 4 °C DEGs had FC < 2 in expression (Fig. 18B and 18C). Furthermore, in principal component analysis, the 4 °C-treated samples were separated from the 21 °C-treated in the first component (23.3 %), and the 1 h, 2 h and 4 h of cold stress in the second (15.6 %) (Fig. 18D). In summary, the GA 4 °C DEGs represented a small fraction of cold-regulated genes and resulted in relatively smaller FCs. Cold stress had a stronger impact on gene transcription, which was partially modulated by GA (Fig. 17 and 18).

### 3.2.3. DELLAs interact with a broad set of structurally distinct transcription factors to regulate cold transcription

GA-promoted DELLA degradation results in gene expression changes because of the interruption of the DELLA-transcription factor interactions in multiple pathways (Schwechheimer, 2014; Daviere and Achard, 2016). For the identification of such interactions in cold stress, N-terminally truncated versions of RGA and GAI were tested for interactions with 1956 transcription factors from a previously cloned collection of transcription-related genes (Pruneda-Paz et al., 2014). RGA and GAI interacted with 244 and 243 transcription factors respectively, and a majority of 86.6 % (226) transcription factors interacted with both DELLAs (Fig. 19A, 19B and 19C; Appendix II). The high number of common interactions is in line with the high sequence similarity and the functional redundancy of the two DELLA proteins (Gallego-Bartolome et al., 2010). A total of 261 putative DELLA-interactors belonged to 51 transcription factor-families characterized by different conserved domains (Appendix II) (Pruneda-Paz et al., 2014). 50 out of these 261 interactions were previously reported whereas 211 were new (Fig. 19B) (Van De Velde et al.,

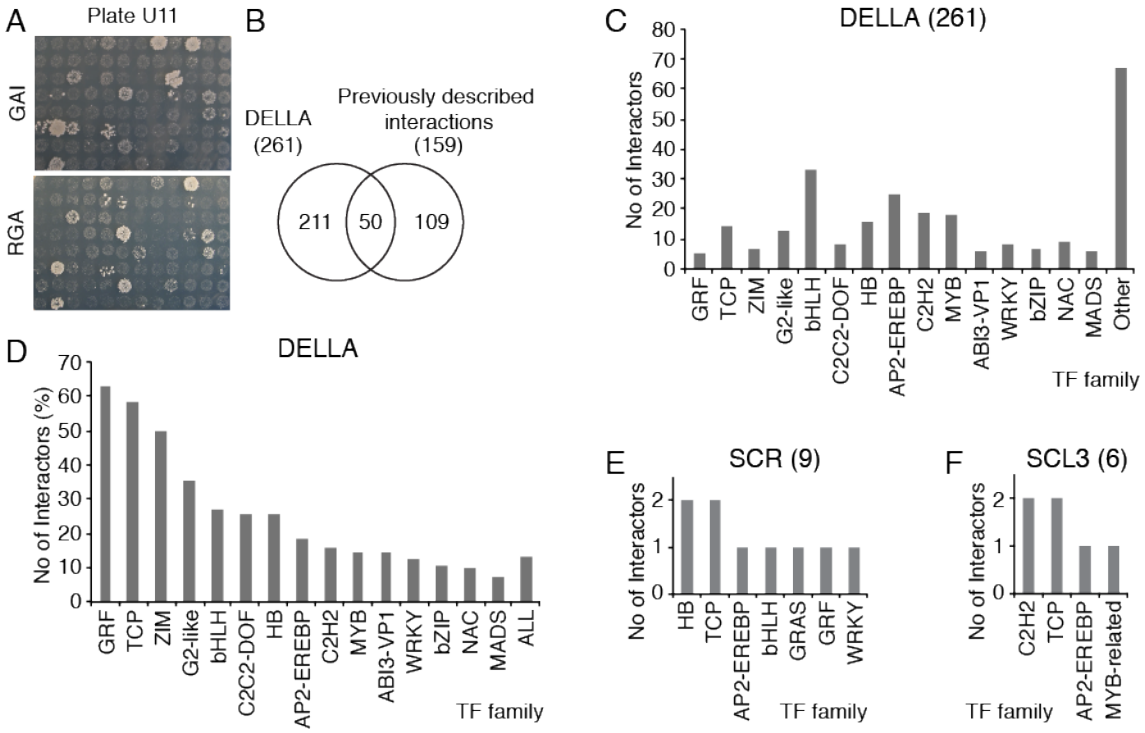


**Figure 19: Yeast two-hybrid interactome of the GRAS proteins RGA, GAI, SCR and SCL3 against the UCSD collection of transcription factors (Pruneda-Paz 2014, cell reports).**

(A) Representative yeast -Leu-Trp-His plates for GAI and RGA baits from the screen. (B) Venn diagram of DELLA-identified interactions compared to previously described interactions (Appendix II) (Van De Velde et al., 2017)). (C) RGA and GAI (DELLA) absolute number of interacting transcription factors (TFs) in yeast belonging to the specified TF-families. (D) Relative number of RGA- and GAI-interacting (DELLA) (%) TFs of the total number of family members present in the collection. TF-families with more than 5 DELLA interactions are included in (C) and (D). (E) and (F) Absolute number of SCR and SCL3 detected interactions by TF-family.

2017). These included 13 interactions that were previously shown to be biologically relevant and relate with specific phenotypes, such as with the BRASSINAZOLE RESISTANT1 (BZR1), JASMONATE ZIM DOMAIN1 (JAZ1) and INDETERMINATE (IDD) transcription factors (Appendix II) (Hou et al., 2010; Bai et al., 2012; Oh et al., 2012; Van De Velde et al., 2017). In addition, 109 previously reported interactions, which included 65 interactions with probes that were present in the transcription factor collection, were not detected (Appendix II) (Van De Velde et al., 2017). Relatively, most interactions compared to the total number of transcription factor-family members that were screened, were observed for the GRF (63 %), TCP (58 %) and ZIM domain (50 %) proteins (Fig. 19D). In order to investigate the specificity of the identified interactions, the GRAS-domain transcription factors SCR and SCL3

were also tested. These proteins lack the GID1-binding N-terminal domains DELLA and TVHVNP, which are deleted in the two DELLAs screened herein, and share with them the GRAS domain (Pysh et al., 1999; Ueguchi-Tanaka et al., 2007; Murase et al., 2008). Strikingly, only nine and six interactions were detected for SCR and SCL3, respectively (Fig. 19E and 19F). These interactions were also present in the DELLA screen results, apart from that with APETALA2 (Appendix II). The combined number of previously and newly discovered DELLA interactions was much higher (370) compared to the number of interactions of the non-DELLAs SCR and SCL3 (Appendix II, Fig. 19).

Next, 17 cold and GA 4 °C DEGs (RNA-seq) that interacted with DELLAs were identified (Fig. 17F and 20A). As several previously studied DELLA-interactor encoding genes were feedback-regulated by GA, these proteins could be mediators of the effect of GA on cold stress-imposed transcription changes (Fig. 20A, 20B and 20D)(Yoshida et al., 2014). These included three out of nine *GRF* genes, which were significantly activated after cold stress but not in the presence of GA (Fig. 20B). Furthermore, the effect of the GA treatments on *GRF* expression at 21 °C was smaller (Fig. 20B and 20C). Similar expression patterns were observed for *GRF6*, *GRF7* and *GRF9,* however, these changes were not significant (FC < 1.5 and/or FDR p-value > 0.01) (Fig. 20C). In addition, six DELLA interactors namely *MYC2* (AT1G32640), *JAZ7* (AT2G34600), *ERF13* (AT2G44840), *ERF6* (AT4G17490), *ABR1* (AT5G64750), and *SIP4* (AT2G30360) were cold stress-upregulated and GA further activated their expression but only at 4 °C (Fig. 20D). The transcript behaviour of *SPL2* (AT5G43270), an integrase-type DNA-binding protein (AT1G77200) and *AIF1* (AT3G05800) was similar to that of the GRFs (Fig. 20B and 20D). Finally, the transcription factors, *HBI1* (AT2G18300), *ZFP8* (AT2G41940), *SCL3* (AT1G50420) and *BOI* (AT4G19700) and *BRG2* (AT1G79110) responded to GA at both 21 °C and 4 °C (Fig. 20D). In conclusion, several GA 4 °C and cold stress DEGs interacted with DELLAs and thus qualified as candidate genes that regulated transcription changes downstream of GA in cold stress response. These included three GRFs and the previously studied DELLA interactions with MYC2, SPL2,

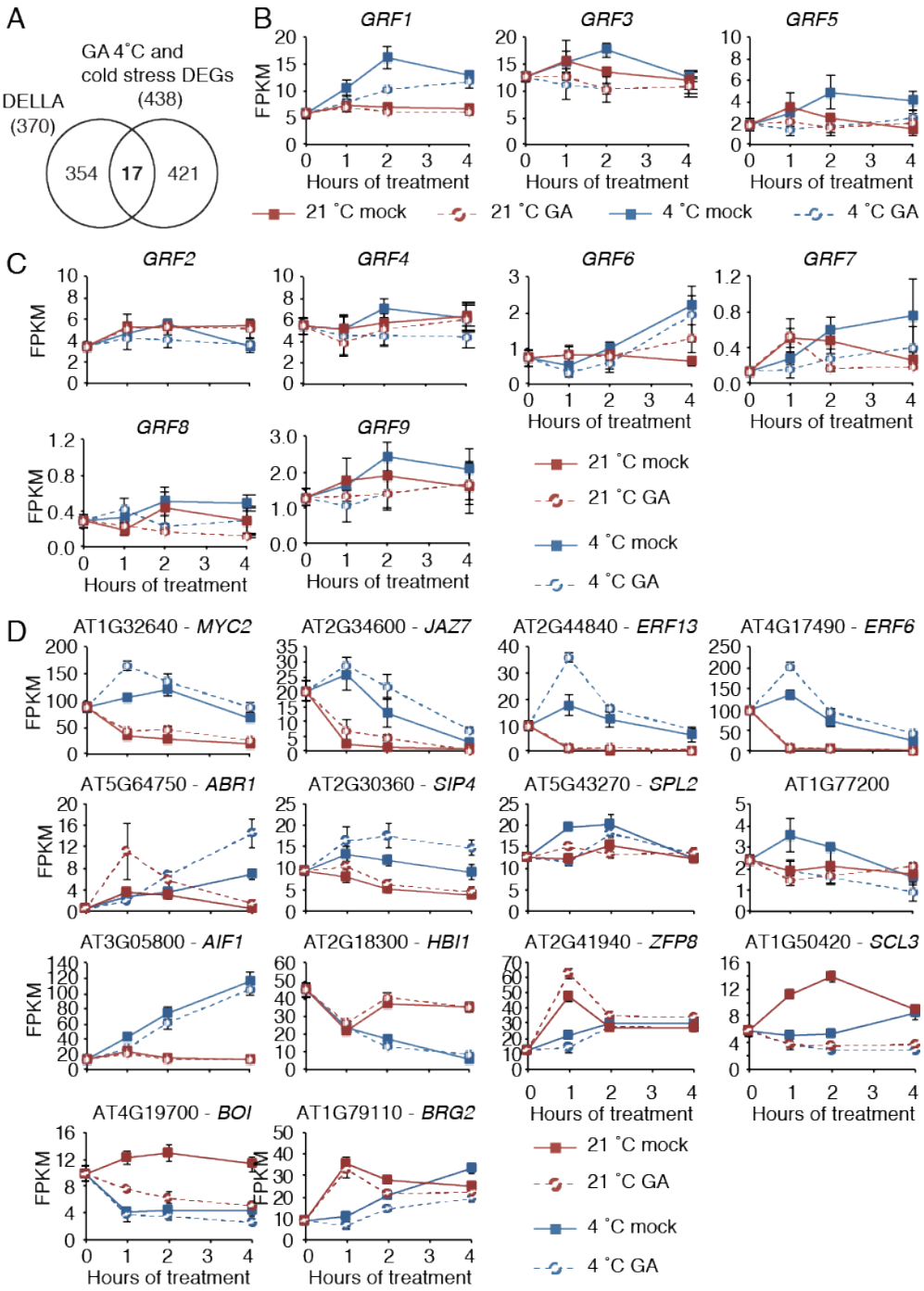


**Figure 20: Transcript behaviour of putative DELLA interactors in the transcriptomics experiment.**

(A) Venn diagram of all DELLA reported interactions (from Fig. 5A) compared to all GA controlled genes in cold stress after 1, 2 and 4 hours of treatments (from Fig. 3E). (B) Changes in the mRNA abundance of *GRF1*, *GRF3* and *GRF5* identified in (A). (B) Transcript behaviour of the six additional GRF family members in the experiment. (D) Transcript behaviour of the remaining 14 DELLA-interacting proteins from (A). FPKM, Fragments per kilobase of exon model per million mapped reads.

SCL3, BOI and BGR2 (Appendix II, Fig. 20B and 20D) (Zhang et al., 2011; Hong et al., 2012; Yu et al., 2012; Park et al., 2013; Van De Velde et al., 2017).

As five out of eight GRFs interacted with DELLAs in the yeast two-hybrid screen, and as *GRF1*, *GRF3* and *GRF5* were cold stress-activated in a GA-dependant manner, this transcription factor family was very prominent in this analysis (Fig. 19 and 20). Therefore, the following experiments sought to confirm the DELLA-GRF protein interactions. A yeast two-hybrid test between the N-terminally truncated DELLAs (RGA and GAI) and eight out of nine GRFs (GRF1-GRF7 and GRF9) was carried out as before. The DELLA interactions with GRF1, GRF3, GRF5, GRF7 and GRF9 were confirmed, and the additional interactions with GRF2 and GRF4 were observed (Fig. 21A). GRF8 was not included in this analysis as cDNA isolation from seedlings or seeds was not successful. This was because the gene annotation at the TAIR database for *GRF8* was incorrect as it was later kindly pointed out by Prof. Jeong Hoe Kim. The interactions of RGA and GAI with GRF3 and GRF5 were confirmed in *Nicotiana benthamiana* cells with Bimolecular fluorescence complementation. A miRNA396-resistant version of GRF3 (rGRF3) that includes silent mutations in the miRNA396-binding site, and GRF5, which does not have a miRNA396-binding site, were chosen to achieve GRF overexpression (Fig. 21B and 21C) (Hewezi et al., 2012). YFP signal was observed in the nucleus of the cells that expressed GRF5 or GRF3 in combination with the DELLAs. The GRF INTERACTING FACTOR 1 (GIF1) and the RING E3 ubiquitin ligase XERICO were included as positive and negative controls, respectively (Kim and Kende, 2004; Ko et al., 2006). GIF1 interacted with the two GRFs and, surprisingly, also with the two DELLAs (Fig. 21B and 21C). Signal for DELLA-GIF1 interactions was observed in the nucleus and cytoplasm. DELLA dimerization was also observed in agreement with previous reports (Fig. 21C) (Itoh et al., 2002; Li et al., 2016). Signal was not observed in any combination that included XERICO and GRFs or GIF1 or the N-terminally truncated DELLAs, but weak nuclear signal was rarely observed in cells that expressed XERICO with the full length RGA (Fig. 21B and 21C). Altogether, the transcript behaviour of the *GRF* genes in the RNA-seq experiment and the

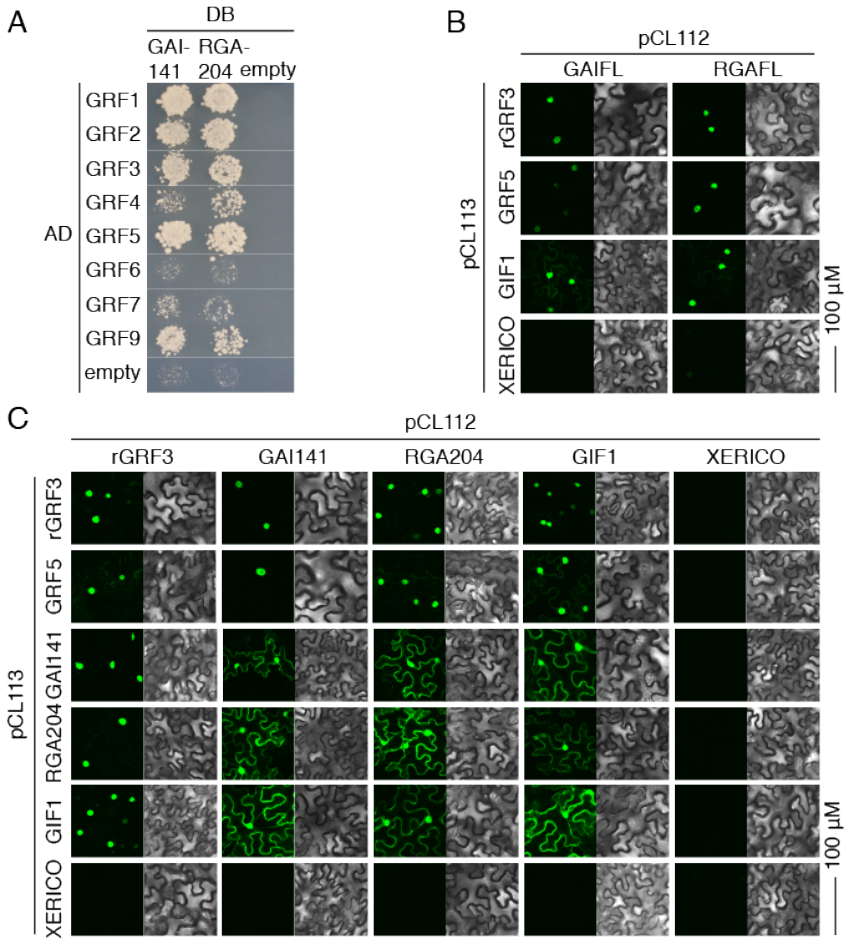


**Figure 21: GRF protein -family members interact with DELLAs in yeast and in planta.**

(A) GRF1, GRF2, GRF3, GRF4, GRF7 and GRF9 yeast two-hybrid interactions with truncated GAI and RGA. Representative photos of BiFC interactions between GRF3, GRF5 and GIF1 and the full length (B) or the truncated versions (C) of GAI and RGA, in transiently transformed N. benthamiana leaves. The experiment was repeated three times.

confirmed DELLA-GRF interactions, suggested their involvement in the regulation of cold and GA responses.

### 3.2.4. GRFs are DELLA targets for the control leaf and root growth

DELLA proteins as well as GRFs are involved in the control of cell proliferation and growth (Kim et al., 2003; Horiguchi et al., 2005; Achard et al., 2009; Ubeda-Tomas et al., 2009; Rodriguez et al., 2010; Rodriguez et al., 2015; Ercoli et al., 2018). Therefore, the role the DELLA-GRF interactions in the regulation of leaf and root growth in cold stress was examined. The response of the wild type, a *GRF5* overexpressing line (35S:GRF5) and *miRNA396b* overexpressing line

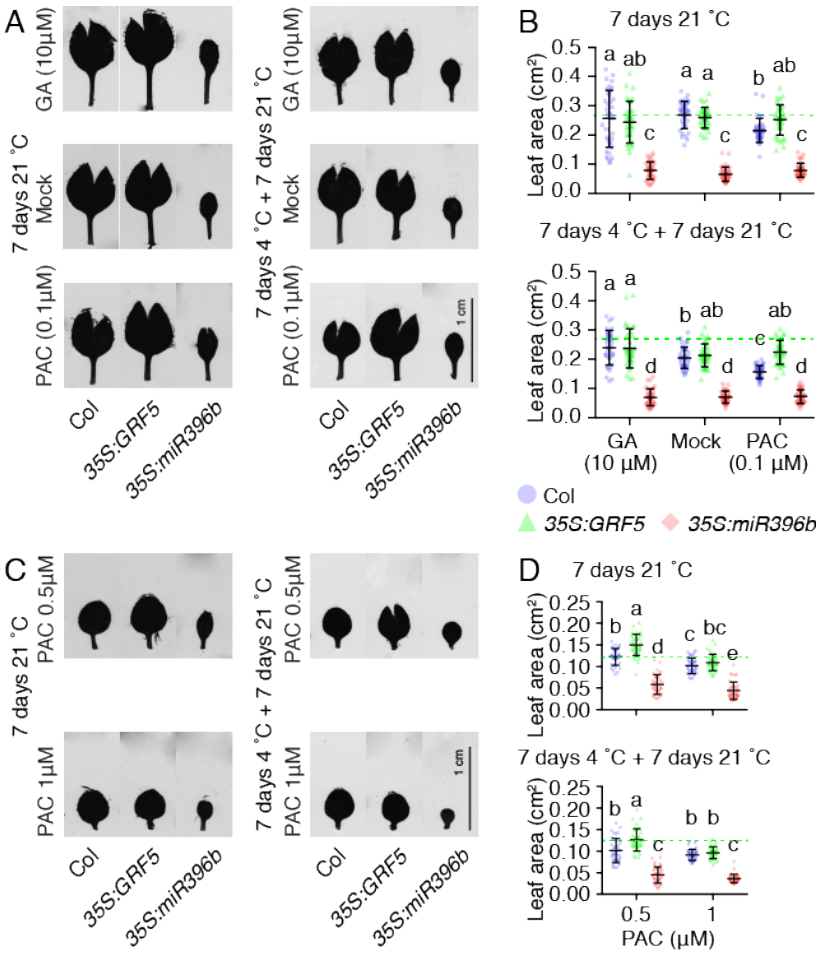


**Figure 22: Leaf growth recovery of GRF5 and miR396b overexpressors treated with GA or the GA biosynthesis inhibitor PAC after 4 °C induced growth inhibition and at 21 °C.**

(A) Representative leaf photos of seedlings grown for six days, and subsequently transferred on plates supplied with mock or 10 µM GA3 or 0.1 µM PAC for seven days at 21 °C, or 7 days at 4 °C followed by 7 days at 21 °C. (B) Quantification of leaf area from (A). (C) Representative leaf photos of seedlings grown as in (A) on plates supplied with 0.5 µM or 1 µM PAC (D) Quantification of leaf area from (C). N=36 Same letters indicate no significant differences between genotypes or treatments (Tukey HSD, $p < 0.05$). The experiment was repeated three times with similar results.

(35S:miRNA396b), which post-transcriptionally downregulates seven out of nine GRFs and thus has reduced *GRF* levels and smaller leaves, to various GA and PAC levels was assessed (Horiguchi et al., 2005; Rodriguez et al., 2010). Seeds were germinated on ½ MS 0.8 % agar plates at 21 °C for six days. Afterwards, they were transferred to medium supplied with $GA_3$ (10 µM), the GA biosynthesis inhibitor PAC (0.1 µM, 0.5 µM, 1.0 µM) or the respective mock solution and were grown for seven days at 21 °C or 4 °C. As no seedling growth was observed after growth for seven

days at 4 °C (data not shown), the seedlings were transferred to 21 °C for an additional seven days and their growth recovery after cold stress was examined. The GA treatment did not promote leaf area growth in any of the genotypes in this experiment (Fig. 22A and 22B). PAC treatments inhibited the leaf growth of the wild type and the 35S:GRF5 overexpressing line but in a differential manner. More specifically, the lowest applied PAC concentration (0.1 µM) repressed leaf growth of the wild type but not of 35S:GRF5 at 21 °C (7 days 21 °C) and more profoundly after cold stress (7 days 4 °C + 7 days 21 °C) (Fig. 22A and 22B). A higher PAC concentration (0.5 µM) resulted in a stronger inhibition of wild type leaf growth compared to 35S:GRF5 and in the highest PAC amount (1 µM) the two genotypes had the same leaf size (Fig. 22C and 22D). Thus, *GRF5* overexpressing seedlings were in a dosage-dependent manner less sensitive to PAC-imposed leaf growth inhibition compared to the wild type. In addition, the leaf size of 35S:miRNA396b expressing seedlings was mostly not affected by GA or PAC treatments and only a small reduction was observed in the 1 µM PAC-treated seedlings at 21 °C (Fig. 22). In summary, high GRF5 protein content outcompeted the growth inhibitory effect of DELLAs after the PAC treatment and the low GRF levels in 35S:miRNA396b phenotypically mimicked the PAC-treated wild type seedlings. Therefore, DELLAs supressed leaf growth in a GRF-dependent manner.

Leaf size is determined by cell division and elongation, in which both GRFs and GA were shown to play a role (Gonzalez and Inze, 2015). To understand whether the differential leaf growth of wild type, 35S:GRF5 and 35S:miRNA396b in PAC is due altered cell size or/and numbers the latter were quantified. Seedlings were grown on ½ MS 0.8 % agar plates at 21 °C for four days and an additional seven days in medium containing 0.1 µM or 0.5 µM or 1 µM PAC. Cell sizes and numbers were counted in 400 µm x 400 µm images from the middle of the first two true leaves. Cell size was reduced proportionally only after 0.5 µM and 1 µM PAC in all three genotypes but no significant differences were observed between the wild type and the GRF5 overexpressing seedlings (Fig. 23A and 23B). The leaf cells of *miR396b* overexpressing seedlings were bigger compared to the other two genotypes as it

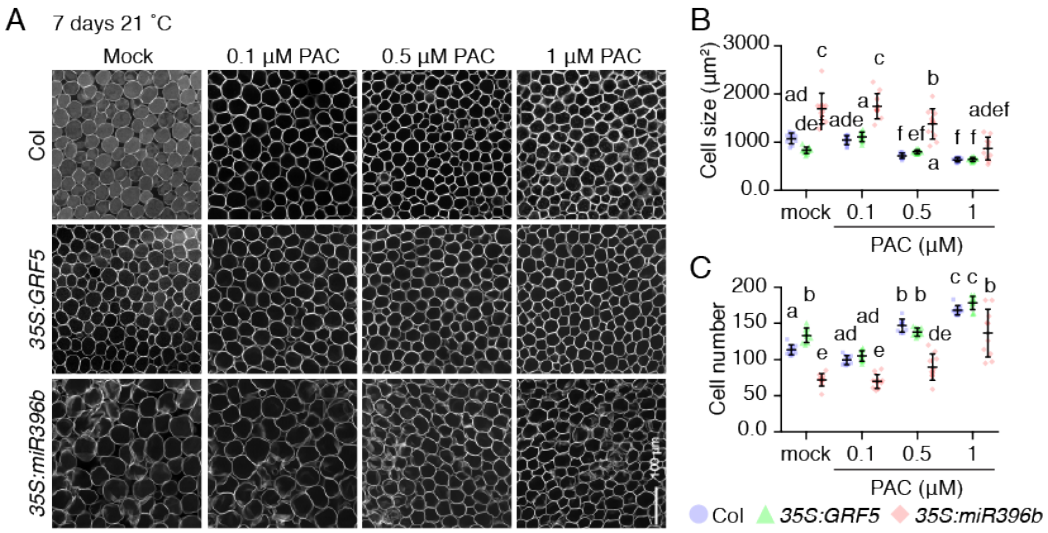


**Figure 23. The effect of the GA biosynthesis inhibitor PAC on cell elongation in WT, GRF5 and miR396b overexpressors.**

(A) Representative first leaf photos of the palisade cell layer bellow the epidermis, in the middle along the leaf axis, for the specified genotypes and treatments. The seedlings were grown for five days, and subsequently transferred on plates with the mentioned treatments for seven days. Quantification of cell size (B) and cell number (C) in a 400 x 400 µm leaf area as described above N=10 photos.

was previously shown, and this was only normalised in the 1 µM PAC treatment (Fig. 23A and 23B) (Horiguchi et al., 2005; Ferjani et al., 2007; Rodriguez et al., 2010). On the other side, cell number per area was decreased in 35S:miR396b but it was not significantly different between the wild type and 35S:GRF5 in the different PAC concentrations (Fig. 23A and 23C). Furthermore, increased cell number was observed in the mock-treated 35S:GRF5 compared to the wild type suggesting that the cells in the same region were not fully elongated (Fig. 23C). Since cell size and numbers were similar between the wild type and the 35S:GRF5 in the different PAC treatments, the observed differences in leaf size were attributed to increased cell proliferation in the 35S:GRF5 overexpressing line (Fig. 23).

Since the *GRF5* overexpressing seedlings were partially insensitive to PAC, the effects of the transgene in the *ga1* mutant background and the DELLA levels in different *GRF* genotypes were investigated next (Fig. 24). *ga1* was crossed with 35S:GRF5 and two transgenic lines homozygous for *ga1* were phenotypically analysed. Wild type, *ga1* and *ga1* 35S:GRF5 seeds were treated with 100 µM $GA_3$

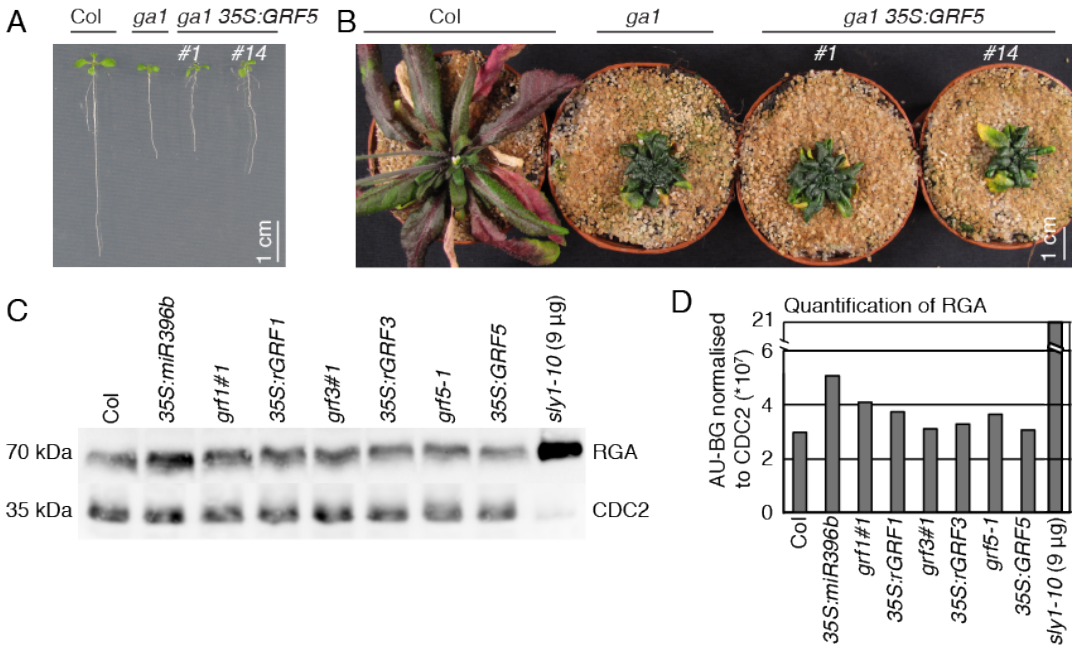


**Figure 24. GRF overexpression neither rescues the GA deficiency-induced developmental and growth defects, nor does it affect RGA levels.**

(A) Representative photos of nine-days-old seedlings of WT, GA-deficient mutant *ga1* and *ga1 35S:GRF5*. (B) Representative photos of six-weeks-old plants of specified genotypes. (C) RGA western blot from total protein of shoot extracts of nine-days-old seedlings and (D) signal quantification (LAS) for the indicated genotypes. *sly1-10* was used as control. The experiment was repeated twice with similar results.

for 5 days during the stratification at 4 °C to promote germination. Subsequently, $GA_3$ was removed through multiple washing steps with water. However, nine-days-old as well as six-weeks-old *ga1 35S:GRF5* seedlings phenotypically resembled the single *ga1* mutant (Fig. 24A and 24B). Thus, increased GRF5 levels alone did not alleviate growth in this background. Furthermore, the RGA protein content of shoot extracts of the 35S:miR396b line, the single *grf1*, *grf3* and *grf5-1* mutants and the respective overexpressors was quantified after immunoblot analysis (Fig. 24C and 24D). The RGA content was similar to the wild type in all backgrounds, with the exception of the 35S:miR396b line, which showed increased RGA levels (Fig. 24C and 24D). In summary, *GRF* overexpression did not promote growth of the *ga1* mutant nor affected RGA levels but interestingly, downregulation of multiple GRFs in the 35S:miR396b line led to RGA protein upregulation indicating the existence of feedback regulation of DELLA levels by the GRFs.

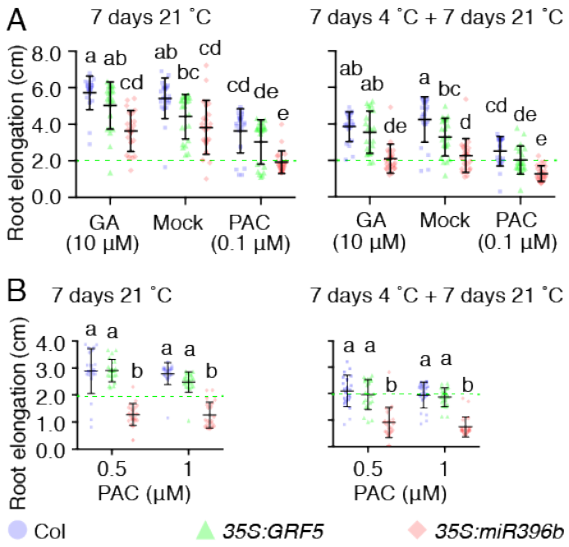


**Figure 25: Root growth recovery of GRF5 and miR396b overexpressors treated with GA or the GA biosynthesis inhibitor PAC after 4 °C induced growth inhibition and at 21 °C.**

(A) Root elongation quantification of seedlings grown for six days, and subsequently transferred on plates supplied with mock or 10 µM GA3 or 0.1 µM PAC for seven days at 21 °C, or 7 days at 4 °C followed by 7 days at 21 °C. (B) Root elongation quantification of seedlings grown as in (A) on plates supplied with 0.5 µM or 1 µM PAC. N=21. Same letters indicate no significant differences between genotypes or treatments (Tukey HSD, $p < 0.05$).

Next, the effects of GA and PAC on root growth after 7 days at 21 °C and 7 days 4 °C + 7 days 21 °C were examined. Overall, the root elongation of the 4 °C-treated seedlings was reduced and GA (10 µM) did not rescue root elongation in these conditions (Fig. 25A). In addition, the root growth of the wild type and 35S:GRF5 expressing seedlings grown in PAC was inhibited to a similar degree (Fig. 25A and 25B). Interestingly, the root elongation of the 35S:miR396b line was diminished in the 4 °C-stressed seedlings and even more strongly in the presence of PAC (Fig. 25A and 25B). Thus, cold stress and PAC treatments suppressed root elongation in all the genotypes examined, while the 35S:miR396b root growth was profoundly inhibited in the presence of PAC.

To understand why root growth of 35S:miR396b in PAC was abolished, this phenotype was more closely examined. The wild type and the miR396b overexpression line were grown in ½ MS 0.8 % agar plates for five days and then for an additional eight days on medium containing either 5 µM PAC or 5 µM PAC + 10 µM GA or the respective mock treatment (Fig. 26A). Only 23 % of PAC-treated 35S:miR396b roots were macroscopically similar to wild type. In the remaining 77 % of the seedlings, root growth was disturbed (17 %) or completely abolished (60 %) with tumour-like growth and bloated cells (Fig. 26A). GA rescued these defects in the presence of PAC indicating that the high DELLA levels in combination with the low GRF-expression in 35S:miR396b line resulted in the meristem collapse (Fig.

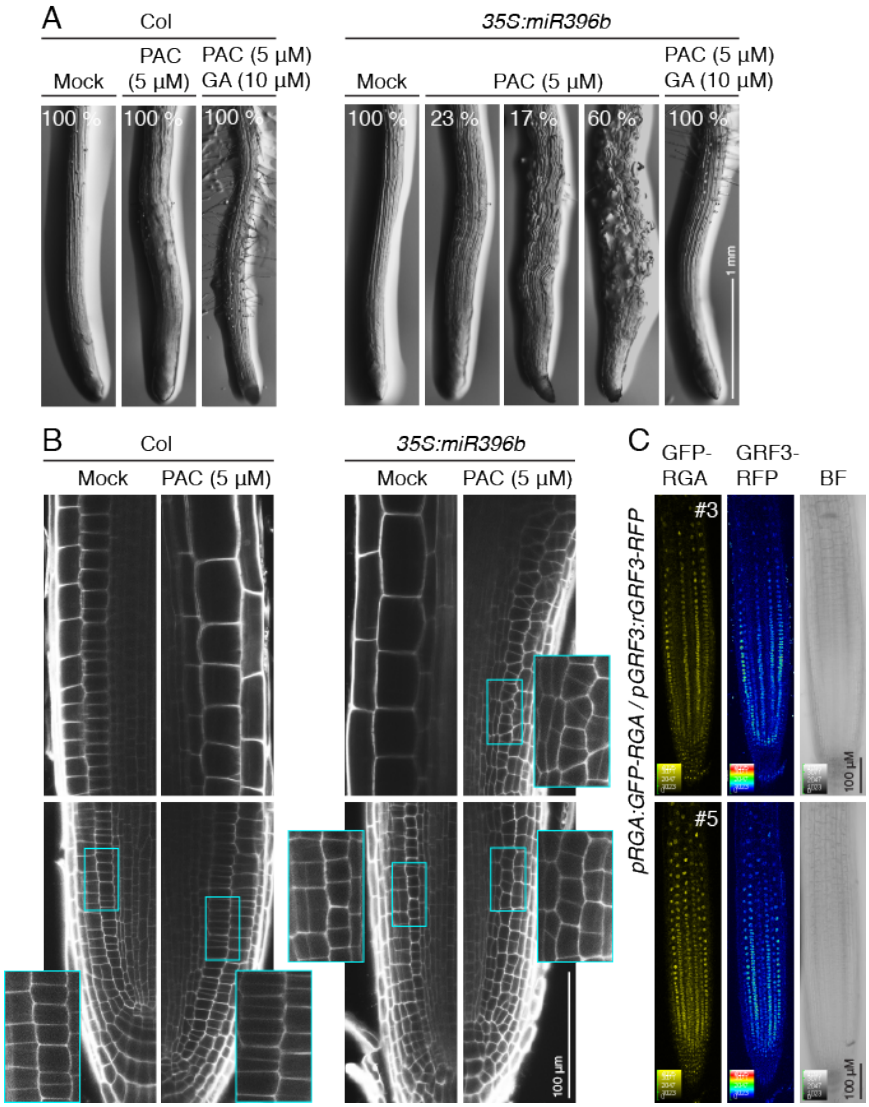


**Figure 26. 35S:miR396b roots are hypersensitive to the GA biosynthesis inhibitor PAC.**

(A) Representative photos of 13-days-old Col and *35S:miR396b* roots after growth for eight days on mock or 5 µM PAC or 5 µM PAC + 10 µM $GA_3$. Included are the percentages of seedlings with the respective phenotypes for each treatment. (B) Representative photos of ten-days-old Col and *35S:miR396b* roots after growth for five days on mock or 5 µM PAC. In boxes are details of the epidermis/cortex cell layers (box length 100 µm). (C) Confocal images of the roots of two independent *pRGA:GFP-RGA pGRF3:rGRF3-RFP* expressing lines.

26A). Microscopically, defects in the determination of cell division planes were observed, which disturbed the root meristem structure and ultimately led to its collapse (Fig. 26B). Furthermore, plants expressing *pRGA:GFP-RGA* together with p*GRF3:rGRF3-RFP* showed that the expression domain of RGA overlaps with that of rGRF3 in the root proliferation zone (Fig. 26C). Thus, the reduced GRF-protein

content of the 35S:miR396b line in combination with high DELLA levels resulted in the disturbance of root growth.

### 3.2.5. *GRF5*- and GA- dependent transcription changes in cold stress

To identify the transcription targets of the DELLA-GRF interactions in cold stress and confirm their role in the regulation of cold and GA DEGs genes, an RNA-seq experiment was performed as detailed before (Fig. 15A). Since the GA-dependent *GRF* cold stress activation was observed after 2 h of treatments, the latest time point (4 h) was chosen for this analysis to allow sufficient time for GRF translation. Briefly, the wild type and *35S:GRF5* seedlings were treated for four hours with 100 µM $GA_3$ at 4 °C or mock at 4 °C or mock at 21 °C. Total mRNA was sequenced and the DEGs were identified. The thresholds for determining the DEGs of FC>1.5 and FDR

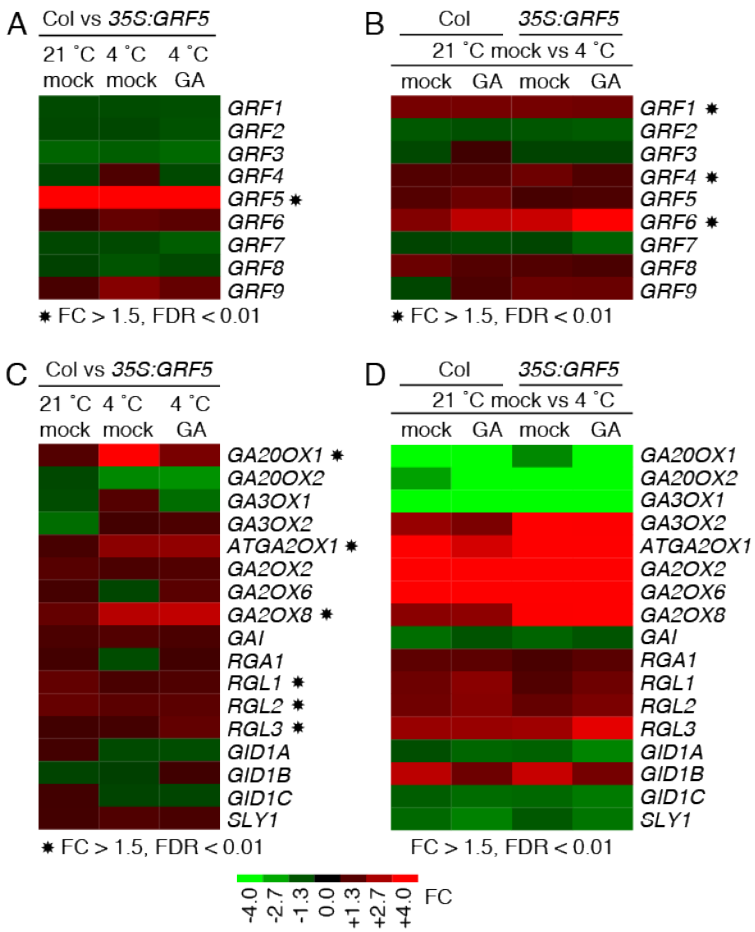


**Figure 27. Transcript behavior of GA pathway and GRF genes in the wild type and GRF5 overexpressor after 4 h of GA and cold stress treatment.**

(A) Heatmap of the fold changes in expression of the nine *GRF* genes in *GRF5* overexpressor compared to the wild type. (B) Heatmap of the fold changes in expression of the nine *GRF* genes in response to the treatments in Col and *35S:GRF5*. (C) Heatmap of the fold changes in expression of GA pathway genes in *GRF5* overexpressor compared to the wild type. (D) Heatmap of the fold changes in expression of GA pathway genes in response the treatments in Col and *35S:GRF5*. False discovery rate corrected p-value < 0.01; Cluster 3.0, TreeView). Data from RNA-seq.

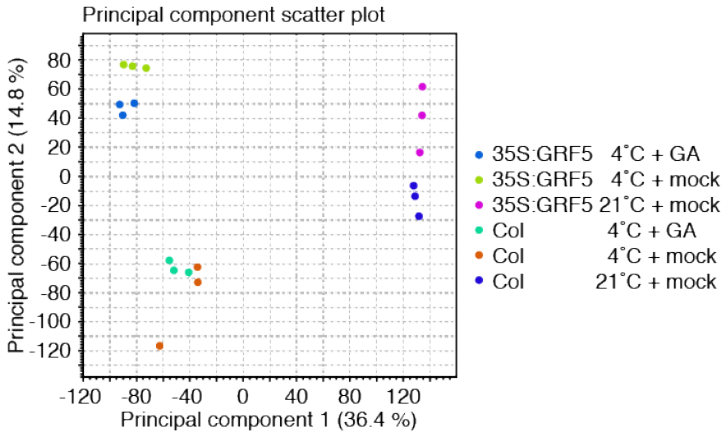


**Figure 28. Principal component analysis of the gene expression data of each sequenced sample.**

PCA for RNA-seq tool; CLC Genomics Workbench 10.1.1.

corrected p-value < 0.01 were implemented as in the initial experiment. *GRF5* expression was highly increased with FC>100 in all three experimental conditions while the transcript levels of the other *GRFs* were the same in 35S:GRF5 line compared to the wild type (Fig. 27A). Furthermore, *GRF1* and *GRF6* were upregulated in response to the 4 h 4 °C treatment but not to $GA_3$ in both genotypes, similarly to the initial RNA-seq experiment (Fig. 27B). Additionally, *GRF4* mRNA levels were increased in response to 4 h 4 °C treatment only in the *35S:GRF5* expressing seedlings (Fig. 27B). Thus, overall the *GRF* gene expression in response to cold and GA was similar to that of the first RNA-seq experiment (Fig. 27B, 20B and 20C). Moreover, GA metabolism and signaling gene expression was influenced by *GRF5* overexpression. *GA20ox1*, *GA2ox1*, *GA2ox8* and *RGL1*, *RGL2* and *RGL3* were upregulated in 35S:GRF5 compared to the wild type in one or more conditions (Fig. 27C). However, the cold-imposed transcript regulation of the GA pathway genes was much stronger compared to the genotype effect (Fig. 27D). The identified GA pathway DEGs were the same as in the initial RNA-seq experiment apart from GAI, which was detected following the statistical criteria, only in the second experiment. Furthermore, the transcript behaviour of the latter was strikingly similar between the two experiments supporting the reproducibility of the results (Fig. 15E and 27D). Overall, cold stress affected GA pathway gene expression that may lead to a reduction of GA levels and consequently DELLA accumulation.

A subsequent principal component analysis of the RNA-seq samples showed a strong influence of the temperature (PC1, 36.4 %) and the genotype for the cold-

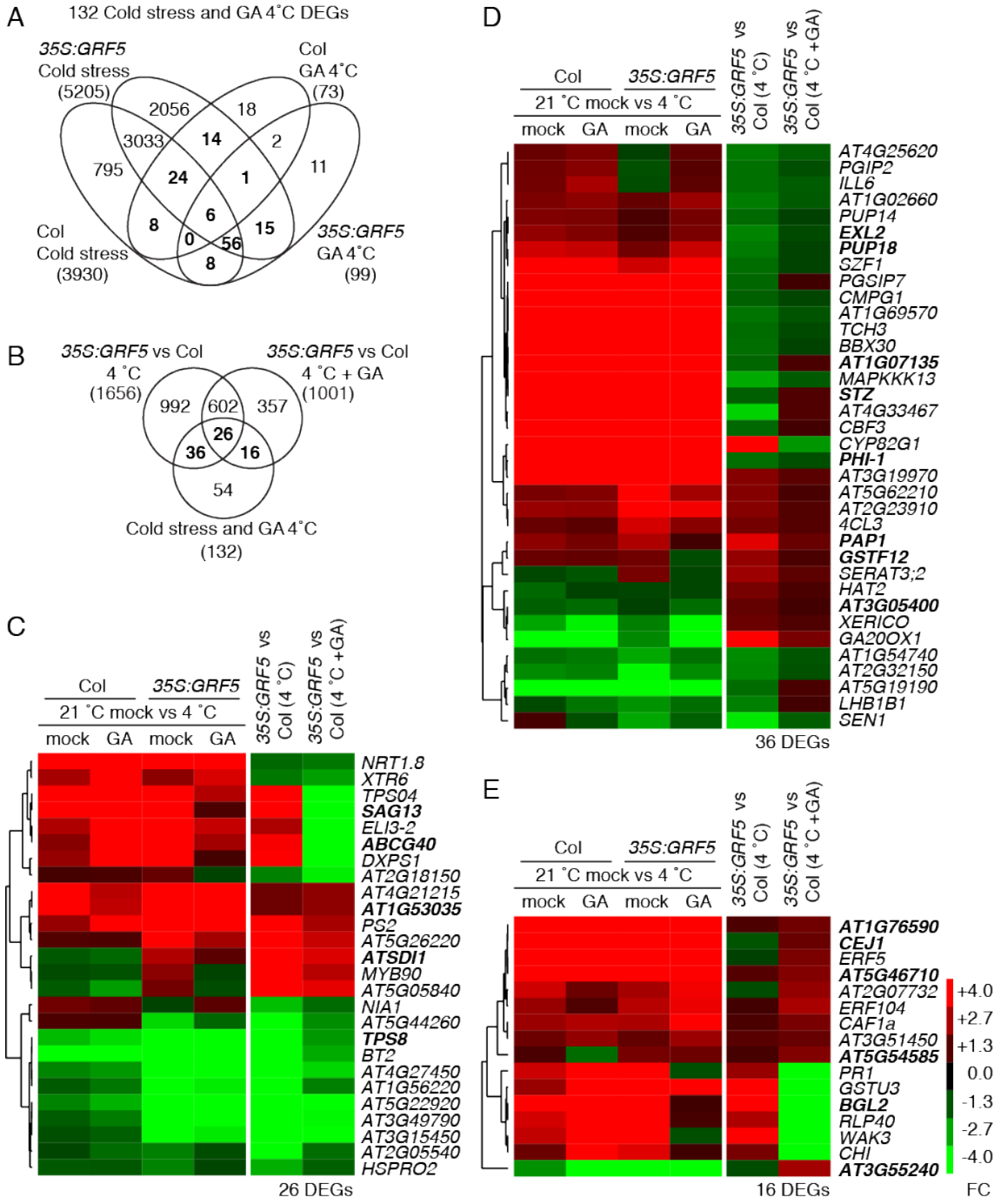


**Figure 29. RNA-seq experiment for the identification of DELLA and GRF –dependent transcriptional changes after cold stress and GA treatment.**

(A) Venn diagram of the differentially expressed genes (DEGs) after 4 hours of cold stress (21 °C mock vs 4 °C mock) and GA 4 °C (4 °C mock vs 4 °C 100 µM $GA_3$) treatments in Col-0 and *GRF5* overexpressor. The 132 DEGs that respond to cold stress and GA 4 °C are annotated with bold. (B) Venn diagram of the 132 cold stress and GA 4 °C DEGs from (A) and the misregulated genes in *GRF5* overexpressor compared to Col-0 after 4 hours 4 °C mock and 4 °C 100 µM $GA_3$ treatments. In bold, are the DEGs that are misregulated in the *GRF5* overexpressor in a cold stress and GA 4 °C dependent manner. (C), (D) and (E) hierarchical clustering of the fold changes in expression of the 26, 36 and 16 DEGs from Venn diagram (B). Genes annotated with bold are CBF regulated (Cluster 3.0, correlation uncentered, complete linkage, TreeView).

treated samples (PC2, 14.8 %) (Fig. 28). In addition, the samples were not strongly separated according to the GA treatment similarly to the previous RNA-seq experiment (Fig. 18D and 28). In conclusion, the major factor influencing gene expression in both RNA-seq experiments was cold stress, while the GA treatment had a smaller impact.

In light of the DELLA-GRF protein-protein interactions, it was anticipated that the GA- and cold stress-controlled gene expression depends on GRF protein abundance. In response to cold stress, 3319 genes were differentially expressed in both the wild type and *35S:GRF5* line whereas 811 and 2086 were only differentially expressed in either one, respectively (Fig. 29A). Furthermore, only nine genes were DE in response to GA at 4 °C in both genotypes, while 64 and 90 DEGs were only detected in either one or the other genotype. In total, 132 genes were DE in response to cold stress and GA treatment at 4 °C in the wild type and *35S:GRF5,* and the majority of them was expressed in a genotype-specific way (Fig. 29A). Thus, *GRF5* overexpression affected strongly the cold stress transcription responses as well as the GA- and DELLA-dependent transcription changes.

To further explore the effect of *GRF5* overexpression on the 132 cold-stress and GA DEGs, the latter where categorized according to their transcript behaviour in the *35S:GRF5* line compared to the wild type. In total, between the transgenic line and the wild type 1656 and 1001 genes were DE after 4 h of 4 °C and 4 h of 4 °C + GA (100 µM) treatments, respectively (Fig. 29B). Thus, the number of miss-regulated genes in *35S:GRF5* after cold stress was reduced by 39.5 % in the presence of GA. From the 132 cold stress and GA DEGs, 26 genes were mis-regulated in the overexpressor both in the presence and absence of GA at 4 °C (Fig. 29C). Moreover, the expression of 36 genes was normalized to the wild type levels after the 4 °C + GA treatment (Fig. 29D). Finally, 16 genes were DE in *35S:GRF5* compared to the wild type only after the 4 °C + GA treatment (Fig. 29E). Thus, the GA-promoted transcription regulation in cold stress depends on intracellular GRF5 levels.

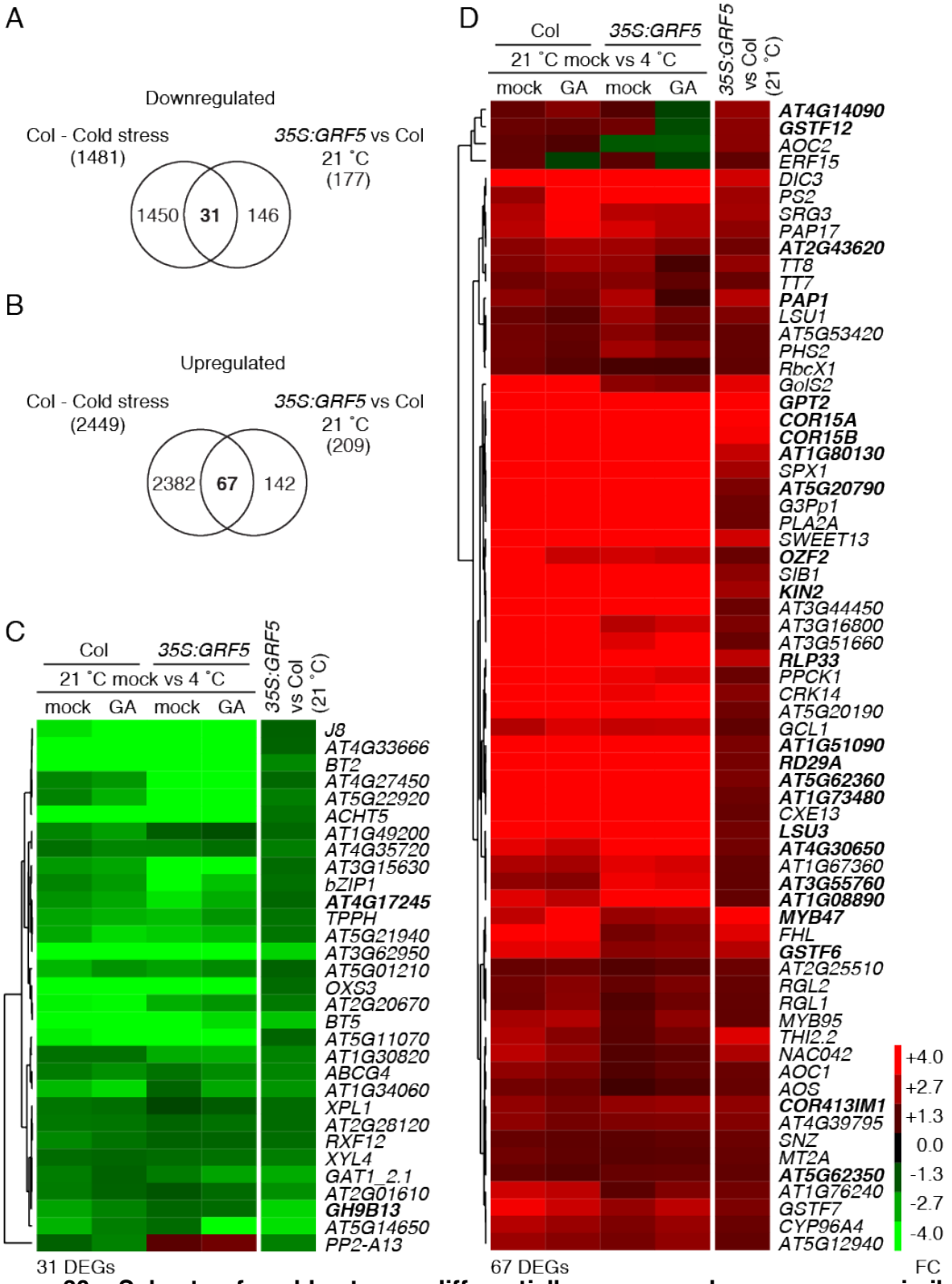


**Figure 30. Subset of cold stress differentially expressed genes are similarly missregulated in the GRF5 overexpressor at 21 °C.**

(A) and (B) Venn diagrams of the down- and upregulated differentially expressed genes (DEGs) respectively, in Col-0 after 4 hours of cold stress (21 °C mock vs 4 °C mock) and in *GRF5* overexpressor compared to Col-0 after 4 hours 21 °C mock treatment. (C) Hierarchical clustering of the fold changes in expression of the 31 downregulated DEGs (from B), in response to 4 hours 4 °C mock and 4 °C 100 µM $GA_3$ treatment compared to the 21 °C mock treatment as well as the fold changes in expression in *GRF5* overexpressor compared to Col-0 after 4 hours of 21 °C mock treatment. (D) Hierarchical clustering as in (C) of the fold changes in expression of 67 upregulated DEGs (from A). Genes annotated with bold are also targets of the CBF regulon (Cluster 3.0, correlation uncentered, complete linkage, TreeView).

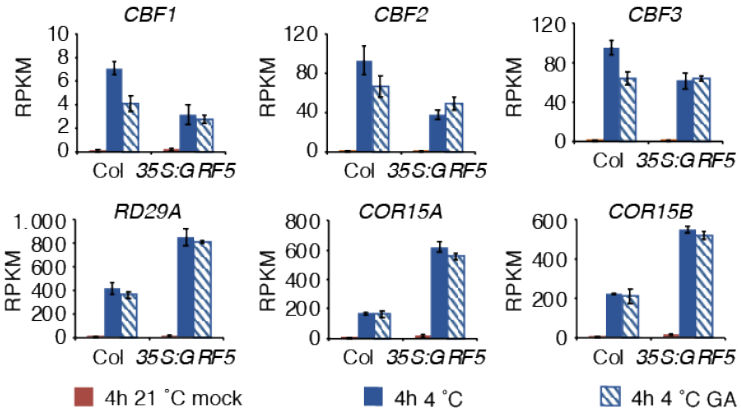


**Figure 31. mRNA levels of cold stress marker genes in the wild type and GRF5 overexpressor after GA and cold stress treatment.**

Transcript behavior of and cold stress marker genes in the transcriptomics experiment in response to 4 hours mock 21 °C, mock 4 °C and 100 µM $GA_3$ 4 °C treatments. RPKM, Reads per kilobase of exon model per million mapped reads.

As *GRF5* was upregulated after cold stress, it was hypothesized that transgene expression in the *35S:GRF5* line would in turn affect stress-promoted gene expression. Indeed, the expression of 25.3 % (98 out of 386 DEGs) of the DEGs in *GRF5* overexpressing seedlings, compared to the wild type at 21 °C, changed in a similar manner after cold stress in the wild type (Fig. 30A and 30B). More specifically, after 4 h of cold stress, 1481 and 2449 genes were down- and upregulated in the wild type, respectively (Fig. 30A and 30B). From those, the expression of 31 and 67 DEGs was also down- and upregulated in 35S:GRF5 compared to the wild type at ambient temperature (Fig. 30C and 30D). Notably, 26 of them, including the established cold stress marker genes *COR15A*, *COR15B*, *RD29A* and *KIN2*, were also previously shown to be CBF regulated (Fig. 30C, 30D and 31) (Park et al., 2015; Jia et al., 2016; Zhao et al., 2016). A closer look into the expression pattern of those CBF-targeted genes, revealed that they were not only upregulated by GRF5 at 21 °C, but additionally, that their induction after cold stress was much stronger in this genotype (Fig. 31). Thus, increased GRF5 levels affected the expression of core cold stress responsive genes in ambient temperature in the absence of other known regulators such as the CBFs, indicating that those genes might be direct GRF5 targets. Contrarily, the cold-promoted *CBF* upregulation was reduced in 35S:GRF5 compared to the wild type for all three *CBF* genes (Fig. 31). Furthermore, the *CBF* gene upregulation after cold stress was reduced in the wild type in the presence of GA, something that did not occur in the GRF5 overexpressor

(Fig. 31). Therefore, the increased GRF5 levels in the overexpressor might have affected *CBF* gene expression directly or indirectly due to protein-protein interactions with the DELLAs. In conclusion, both the responses to cold as well as to GA relied on the GRF5 intracellular content, which is controlled by DELLA proteins at the RNA-transcription and protein level through protein-protein interactions.

# 4. Discussion

## 4.1. GA and SL treatments affect gene expression and plant morphology in *Arabidopsis thaliana* in an additive manner

The hormones GA and SL are involved in the regulation of plant growth and response to phosphate limitation, and they share similarities in their signaling perception mechanisms (Jiang et al., 2007; Kapulnik and Koltai, 2016; Marzec, 2017). GA and SLs are bound to the *a/b* hydrolase family receptors GID1 and D14, respectively, and this binding promotes the proteasomal degradation of specific target proteins. The DELLA- and members of the SMXL-family proteins are degraded in the presence and act downstream of GA and SL, respectively (Schwechheimer, 2014; Marzec, 2016). The role of GA and DELLA proteins in the regulation of transcription has been extensively studied, while increasing evidence suggest their involvement in protein trafficking and auxin transport as well (Willige et al., 2011; Locascio et al., 2013; Lofke et al., 2013; Yoshida et al., 2014; Van De Velde et al., 2017; Salanenka et al., 2018; Shanmugabalaji et al., 2018). SLs control plant architecture and growth through the regulation of auxin transport and gene transcription (Waldie et al., 2014; Bennett et al., 2016; Wang et al., 2020). A recent report showed that the SL-targeted SMXLs act as transcription factors (Wang et al., 2020). Although, it was reported that GA and SL act independently to control phenotypic responses, the direct interaction of the two signaling pathways at the molecular level had also been suggested (de Saint Germain et al., 2013; Nakamura et al., 2013; Marzec, 2017).

Here, the combined effect of the two hormones in the control of plant growth and molecular responses was examined. Phenotypic analysis of single and double GA and SL biosynthesis mutants revealed that GA is required for the expression of the increased branching and reduced plant height phenotypes of SL-deficient-mutants, indicating that GA acts upstream in the regulation of those processes (Fig. 7). The same phenotypes were expressed and regulated in an additive manner by the two hormones in the *ga1 max* mutants, when growth was partially rescued after GA

treatments (Fig7). In a study that was conducted in pea, where the double mutant of the SL-deficient mutant *rms1* (*max4*) and the GA biosynthesis mutant *le-1* (*PsGA3ox1*) were analysed, evidence for additive effects of the two hormones on the same phenotypes was also presented (de Saint Germain et al., 2013). Therefore, the effect of SL in the inhibition of branch outgrowth and promotion of shoot elongation, is independent from GA when the latter is at a critically low level to allow meristem activation and growth. At the molecular level, this could mean that GA-specific targets are needed for meristem activation, or that in the absence of GA, as it is the case in the *ga1* mutant, DELLAs supress SL responses by binding to D14 as it was previously suggested (Nakamura et al., 2013).

In order to investigate whether the suggested DELLA-D14 interaction could affect DELLA stability, RGA (DELLA) levels were quantified in different GA- and SL-deficient mutant genotypes and after GA and GR24 treatments. The RGA seedling protein levels where only affected by changes in GA but not in SL levels, in line with previous observations in Arabidopsis roots and shoots where the GFP-RGA protein levels were monitored (Fig. 8) (de Saint Germain et al., 2013; Bennett et al., 2016). Since DELLA stability is not affected by the presence of SL, it is unlikely that DELLA proteins are SL targeted through their direct interaction with D14 as it was previously suggested (Nakamura et al., 2013). Furthermore, no difference in root growth was observed between the *ga1* and *ga1 max1* mutants under low phosphate conditions, which promote SL biosynthesis (Fig. 7E) (Kohlen et al., 2011). This indicates that even if the DELLA-D14 binding occurs in the presence of SL, it does not affect the DELLA-imposed growth inhibition in this genetic background. It could thus be argued that the suggested DELLA-D14 interaction does not influence DELLA-mediated responses. Another possibility could be that the DELLA-D14 interaction interferes with the proteasomal degradation of the SMXL proteins affecting in this way SL signaling. In the case of KAR-mediated signaling, although GA is required for the KAR-promoted activation of seed germination, the KAI2 downstream transcription changes of a severe GA-deficient mutant were similar to that of the wild-type. It was suggested that DELLA proteins do not block or affect transcription

changes in response to KAR (Nelson et al., 2010). Thus, analysis of the transcriptional responses downstream of GA and SL was performed for the investigation of the plausibility of such interactions.

The utilization of the GA and SL biosynthesis deficient mutant *ga1 max1* allowed the analyses of the global changes in transcript abundance after hormone treatments, without the changes in mRNA levels that would occur due to the developmental differences of the single GA and SL biosynthesis mutants. In a two-hour time-course experiment, the 210 genes that were identified as being differentially expressed after GA treatment, included many known GA-regulated transcripts (Fig. 9B) (Appendix I) (Claeys et al., 2014). After SL treatment, application of *rac*-GR24 resulted in the expression changes of a total of 73 genes (Fig. 9B). These included genes that were previously shown to be SL-regulated such as *MAX3* and *MAX4*, abut also many new transcription targets (Fig. 9 and 12) (Mashiguchi et al., 2009). Although *rac*-GR24 can activate D14 and KAI2 downstream signaling, gene expression changes are expected to have occurred mainly through D14, as KAI2 signaling is active in the *ga1 max1* mutant (Scaffidi et al., 2014). Thus, the observed transcription changes after the single $GA_3$ and GR24 treatments were in line with previous observations, supporting the validity of the experiment.

When the transcription changes after the $GA_3$ and GR24 treatments were compared, only seven genes were identified as being differentially expressed in both cases, suggesting, that the two hormones have mostly different target gene sets (Fig. 9C). Surprisingly though, the concurrent application of both substances led to the identification of 386 DEGs, 261 of which were differentially expressed only in this condition (Fig. 9). The fold changes in expression for the majority of the 261 DEGs were mathematically predicted to be close to the experimental fold changes that occurred after the single treatments ($|FC_{Calculated} - FC_{Experimental}| > 0.5$) (Fig. 10). Thus, the enhanced gene expression changes after the combined treatment for the majority of the DEGs that were exclusively detected in this condition, can be explained as the result of the additive effects of each of the two hormones on their

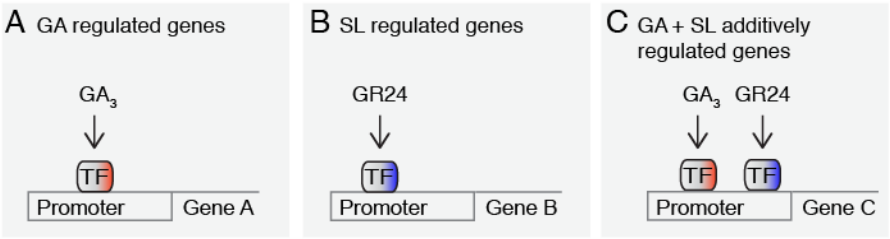


**Figure 32. Simplified diagram summarizing the main groups of GA and SL regulated genes.**

Transcription activation or suppression of the GA- (A) and SL- regulated (B) genes is the result of the action of transcription factor(s) that are exclusively controlled by one or the other hormone and bind the promoters of non-overlapping gene targets. (C) Genes that are regulated in an additive way by GA and SL are common targets of GA- and SL-controlled transcription factors or the additive effect of the two hormones on the same transcription factor(s).

mRNA transcription rates. In addition, a synergistic effect of the two hormones on gene expression could be proposed for a small subset of those genes, as the predicted fold changes were not similar to the experimental ones from the combined treatment according to the arbitrary threshold that was set (Fig. 10, Table 3). The robust reproducibility of these results in all three time points suggests that this was rather unlikely to have occurred due to variation in gene expression between biological replicates. Nevertheless, a higher number of biological replicates in the current study could have facilitated the identification of more DEGs and added more power to the analyses (Lamarre et al., 2018). In summary, GA and GR24, have both separate and also common transcription targets, which they regulate mostly in an independent manner.

The differentially expressed genes can be thus categorised into three main groups. The first two categories include genes that are exclusively regulated by one or the other hormone (Fig. 32A and 32B). The third group includes a substantial number of genes that are controlled by both hormones in an additive manner (Fig. 32C). At the molecular level, the additive regulation of gene expression could be the result of GA- and SL-controlled transcription factors that bind to different *cis* or *trans* elements of those genes (Fig. 32). According to a GO analysis, the group of additively regulated genes was enriched in genes involved in responses to other hormones such as ethylene and salicylic acid (Appendix I). Thus, some of the common GA and GR24 transcription targets might be targeted by multiple

hormones. Analyses of genomic binding sites of 27 different transcription factors in *Arabidopsis* showed that the majority of the genes are targeted by at least two transcription factors, while genes that are regulated by multiple transcription factors are more likely to be rather broadly than specifically expressed (Heyndrickx et al., 2014). The transcriptomics analyses presented here supports the existence of common transcription targets of GA and SL and possibly other hormones.

Since the control of gene expression of GA and SL metabolism and signaling genes could be another point of hormone signaling interference, this aspect was closely examined. GR24 alone did not have an effect on the expression of GA pathway genes, which changed only in response to the treatments that contained $GA_3$, the latter being in line with the introduced model for GA feedback regulation (Fig. 11) (Middleton et al., 2012; Yoshida et al., 2014). On the other hand, $GA_3$ supressed the expression of the SL biosynthesis genes *MAX4* and *LBO1* suggesting that GA negatively impacts SL hormone levels (Fig. 12). In rice, GA was shown to reduce SL biosynthesis through the downregulation of mRNA abundance of the respective biosynthetic genes (Ito et al., 2017). Therefore, downregulation of SL levels by GA might also be occurring in *Arabidopsis*.

Interestingly, in the presence of both hormones, the GA catabolism gene *GA2ox*, the SL signaling gene *SMXL8* and the SMXL6-targeted gene *BRC1* were synergistically activated (Fig. 10) (Wang et al., 2020). This implies the existence of shared *cis* or *trans* regulatory factors by the two pathways that control GA catabolism and SL signaling. For example, one possibility could be that both the release of a transcription suppressor from the gene promoter in presence of SL, and the binding of a transcription activator in the presence of GA, are required for an increase in their mRNA levels. The exact mechanism behind this type of regulation, as well as timing and developmental context requires further investigation. In the case of phosphate deficiency for example, the DELLA proteins are stabilised while SL levels are increased indicating that at least in specific cell types of the root, either SL- or GA-downstream signaling would predominantly affect transcription (Jiang et al., 2007; Kohlen et al., 2011). In summary, the observed changes in transcript

abundance of GA and SL metabolism and signaling genes suggest a direct effect of GA on SL biosynthesis, while the aforementioned GA catabolism and SL signaling genes were regulated in a synergistic manner.

Finally, several genes that belong to the families of characterized GA (NPF, SWEET) and SL (ABC) hormone transporters were identified as being differentially expressed after the treatments that contained the respective hormones (Kretzschmar et al., 2012; Saito et al., 2015; Sasse et al., 2015; Kanno et al., 2016; Tal et al., 2016). In the case of GA, *NPF2.13*, *NPF5.2* and *NPF5.8* showed similar transcript behaviour to that of the know GA transporter *NPF3.1*, suggesting that they might be involved in GA transport in seedlings (Fig. 13A and 13B). This is further supported by hormone transport experiments yeast, for *NPF2.13* and *NPF5.2*, which were able to transport both $GA_1$ and $GA_3$ (Chiba et al., 2015). Furthermore, several genes of the ABC family of transporters were transcriptionally activated by GR24 (Fig. 13C). As the only know SL transporter to date from petunia belongs to the same family and is transcriptionally regulated by SL, those transporters qualify as candidates of SL transport in Arabidopsis (Kretzschmar et al., 2012; Sasse et al., 2015). Thus, from this analysis putative GA and SL hormone transporters were identified and their role in active hormone transport could be examined in the future.

In conclusion, the analyses of the transcription responses of the *ga1 max1* mutant to GA and SL, provided us with evidence suggesting signaling convergence of the two hormones at the level of transcription regulation of common target genes. Further research is needed to understand the physiological context where the observed molecular signaling takes place and how it affects developmental decisions and responses to external stimuli.

### 4.2. GA transcription response and targets in low temperature stress.

GAs are modulated in the response to cold stress both after a short-term exposure as well as an evolutionary adaptation to cold temperatures (Achard et al., 2008; Luo et al., 2015; Zhou et al., 2017). The stabilization of DELLA proteins is observed

within the first hours of cold exposure in *Arabidopsis* and increased DELLA levels are associated with reduced growth and freezing stress resistance (Achard et al., 2008). Although the seedling growth of DELLA mutants is less inhibited compared to wild-type during cold-warm temperature fluctuations or at 12 °C, continuous plant exposure at 4 °C completely inhibits seedling growth regardless of the DELLA status (Fig. 14) (Achard et al., 2008; Zhou et al., 2017). This might be the result of the strong effect that temperature has on enzymatic activity in combination with the action of other signaling pathways that are activated in cold stress, including other hormones, which might be acting in epistatic way (Miura and Furumoto, 2013; Penfield and MacGregor, 2014). As no seedling phenotype is linked to the rapid DELLA stabilization that is observed at 4 °C, it is tempting to hypothesize that DELLAs might act as a switch for a fast growth response when the temperature is increased. Analyses of the effect that GA has on transcription in the context of cold stress, and identification the molecular targets that act downstream of the DELLA proteins can help increasing our understanding of the role of GA in the plant's response to cold stress and facilitate the development of stress-resistant plants. Here, mRNA-seq and DELLA-transcription factor interactomics analyses were combined that led to the identification of the GRF transcription factors as downstream DELLA targets in cold stress.

### 4.2.1. GA signaling regulation of cold stress-induced transcription changes

In order to understand the role of GA signaling and DELLA stabilization in cold stress response, the gene expression changes after seedling exposure to $GA_3$ and 4 °C stress were analyzed. First, an increase in the protein amount of the DELLA protein RGA, was observed after 2 h of seedling exposure to 4 °C, similarly to previously reported observations (Fig. 15B and 15C) (Achard et al., 2008). Furthermore, the expression of selected marker genes, such as cold-induced *CBF1*, changed as early as 1 h of cold and GA treatments suggesting a fast influence of DELLA stabilization in gene expression regulation in cold stress (Fig. 15D). Consequently, for the identification of direct DELLA targets, the early time points of 1, 2 and 4 hours of

treatments were chosen for the monitoring of the global of changes in mRNA abundance with RNA-seq (Fig. 17). The observed transcript behavior of previously established cold and GA regulated genes in the RNA-seq analyses, supports the credibility of the experiment, as it is in line with previous publications (Fig. 16) (Thomashow, 2010; Claeys et al., 2014; Eremina et al., 2016).

The expression of several GA metabolism and signaling genes changed after cold stress in a robust way, indicating a strict transcription regulation of GA and DELLA levels. More specifically, GA biosynthesis genes (*GA20oxs*, *GA3ox1*) were downregulated and GA catabolism genes (*GA2oxs*) were upregulated, suggesting that cold stress signaling promotes a reduction in bioactive GAs (Fig. 15E) (Achard et al., 2008; Zhou et al., 2017). Furthermore, four DELLA protein-encoding genes (*RGA*, *RGL1*, *RGL2*, *RGL3*) were upregulated while components of the GA receptor complex (*GID1*, *SLY1*) were downregulated (Fig. 15E). Thus, an increase in DELLA protein synthesis and a reduction in GA-receptor complexes could be additionally contributing to the observed increase in DELLA nuclear levels (Fig. 15). Although similar observations were made by others, those studies identified and focused on a smaller number of GA pathway cold stress-regulated genes which were mostly not expressed in the same way or were not detected in this RNA-seq experiment (Achard et al., 2008; Zhou et al., 2017). The transcriptional regulation of GA metabolism and signaling genes has also been reported in response to other abiotic stresses as well as GA treatments (Colebrook et al., 2014). The evident changes in transcript abundance of multiple genes of GA metabolism and signaling support the involvement and regulation of the hormone in cold stress response.

The effect of GA on transcription was strongly influenced by the temperature regime. GA treatments at 21 °C and 4 °C altered the expression of 676 and 816 genes, respectively, from which only 165 were regulated in both temperatures (Fig. 17E). Distinct effects of GA treatments on transcription in different tissues or conditions were previously shown (Cao et al., 2006). Differential regulation and binding of transcription factors by DELLA proteins in different conditions and tissues is likely causative for the divergent responses to GA.

Cold stress had a stronger effect on transcription in terms of number of regulated genes and fold changes in expression compared to the GA treatments (Fig. 17D and 18). In total 7346 DEGs were identified as cold regulated, while about 5 % of those genes were also GA regulated at each individual time point (Fig. 17A to 17F). Thus, GA affected a small subset of cold stress-regulated genes. Contrarily, about 76 % of the GA regulated genes at 4 °C were also cold stress regulated, suggesting the strong involvement of GA signaling and GA-regulated genes in the response to cold stress. Furthermore, the GA treatments mostly enhanced or suppressed but did not abolish the cold-promoted gene expression changes for a vast majority of those genes, suggesting that the latter are controlled by multiple TFs (Fig. 17F). These results fit with previous observations that several TFs are cold stress-induced in parallel with the CBFs and that they share common target genes (Park et al., 2015). Overexpression of some of those first wave TFs resulted in dwarf phenotypes but without altered expression of cold stress-upregulated GA catabolism enzyme-encoding genes (Fig. 15E) (Park et al., 2015). These results suggest that different TFs control growth in cold temperatures by partially overlapping and also independent signaling pathways and could thus explain the changes in gene expression observed here after GA treatments, as well as the fact that GA alone did not alleviate the growth inhibition at 4 °C (Fig. 14 and 17F) (Park et al., 2015).

### 4.2.2. DELLA possibly interact with numerous transcription factors to regulate gene expression in cold

For the discovery of novel candidate DELLA interactors that regulate the response to cold stress, a yeast-two-hybrid screen was performed. In total, 261 *Arabidopsis thaliana* transcription factors were identified as putative DELLA interactors for both RGA and GAI, 86% from which interacted with both DELLAs, in line with previous evidence of functional redundancy of the Arabidopsis DELLA proteins (Fig. 19A, 19B, 19C and 19D) (Appendix II) (Gallego-Bartolome et al., 2010). These transcription factors belonged in 51 different protein families, evident for their high structural variability (Appendix II). Previously reported DELLA interactions, including

many with proven roles in the regulation of biological processes, also included proteins from diverse transcription factor families (Appendix II) (Marin-de la Rosa et al., 2014; Pruneda-Paz et al., 2014; Van De Velde et al., 2017). This study contributes 211 new putative DELLA-controlled transcription factors in addition to the 159 that were previously described (Appendix II) (Claeys et al., 2014; Marin-de la Rosa et al., 2014; Van De Velde et al., 2017). As many of the biologically validated DELLA interactions were initially shown in yeast two-hybrid experiments, it is likely that many of the newly identified interactions also have biological functions and will be the focus of future studies (Appendix II) (Yoshida et al., 2014; Van De Velde et al., 2017).

In contrast to the yeast two-hybrid screen results for the two DELLAs, only 9 and 6 interacting partners were found for each of the other two GRAS proteins SCR and SCL3, respectively (Fig. 19E and 19F). The latter, also belonged to different transcription factor families, and all but one interacted with the DELLAs, suggesting that shared motifs between the four proteins probably mediate these common interactions (Fig. 33). All four tested proteins have the GRAS domain and additional motifs but the percentage of identical bases between the two truncated DELLAs is much higher (88 %) compared to the sequence identities that they share with SCR (22 %) and SCL3 (28 %) (Fig. 33, Geneious 7.1.9, https://www.geneious.com). Thus, DELLAs, but not the other two GRAS proteins, have a unique sequence identity that gives them higher binding affinities for a variety proteins, including possibly more than 15 % of the Arabidopsis transcription factors and also other proteins such as the PFDs and (Fig. 19) (Locascio et al., 2013; Pruneda-Paz et al., 2014). Several motifs as well as post-translational mortifications that affect some of the DELLA interactions have been already identified but further research is needed to find the DELLA-specific sequences, protein properties and mechanisms that enable their interaction with this remarkable number of different proteins (de Lucas et al., 2008; Hou et al., 2010; Bai et al., 2012; Zentella et al., 2016; Zentella et al., 2017). In addition, such a comparative analyses can be repeated with different protein-protein interaction detection methods to achieve a reduction in false

positives, resulting from assay artifacts, as well as false negative results (Braun et al., 2013). Nevertheless, the findings of the yeast two-hybrid experiment are in line with the ever-growing literature of validated DELLA-transcription factor interactions (Schwechheimer, 2014; Van De Velde et al., 2017).

From all DELLA interactors, 17 were also DELLA- and cold stress-regulated at the transcription level and thus qualified as candidate DELLA targets in cold stress response. Those included the previously described DELLA interactions with MYC2, SPL2, SCL3, BOI and BRG2 as well as additional interactions first reported in this study (Fig. 20B and 20D) (Zhang et al., 2011; Hong et al., 2012; Yu et al., 2012; Park et al., 2013). The latter included the DELLA interaction with the jasmonate signaling protein JAZ7, which was also regulated by GA and cold at the transcription level (Fig. 20D). DELLA interactions with other JAZ proteins were previously described and suggested to play a role in the DELLA-dependent *CBF* gene activation (Hou et al., 2010; Yang et al., 2012; Qi et al., 2014; Zhou et al., 2017). Thus, it is likely that the DELLA-JAZ7 interaction could affect *CBF* gene expression although the role of this and the other identified DELLA-targeted genes in cold stress response should be further investigated in future studies. Given the dynamic and variable changes in transcription after GA treatments, and the numerous GA-regulated DELLA interactors, it is expected that DELLAs control the response to cold stress through the binding of multiple transcription factors.

The most prominent transcription factor family in the interactomics data-set was that of the GRFs. Seven out of the nine family members interacted with the DELLAs in yeast, while the genes encoding three of them, *GRF1*, *GRF3* and *GRF5* were cold stress and GA 4 °C regulated (Fig. 19D and 20B). The GRF3 and GRF5 interactions with the two DELLAs were confirmed *in planta* with BiFC (Fig. 21). Further attempts to verify these interactions in stably-transformed plants with epitope-tagged GRFs were unsuccessful, probably due to the low protein expression of the tagged-GRFs in combination with unspecific antibody binding (data not shown). Remarkably though, while the work for this thesis was ongoing, the interaction between SLR1,

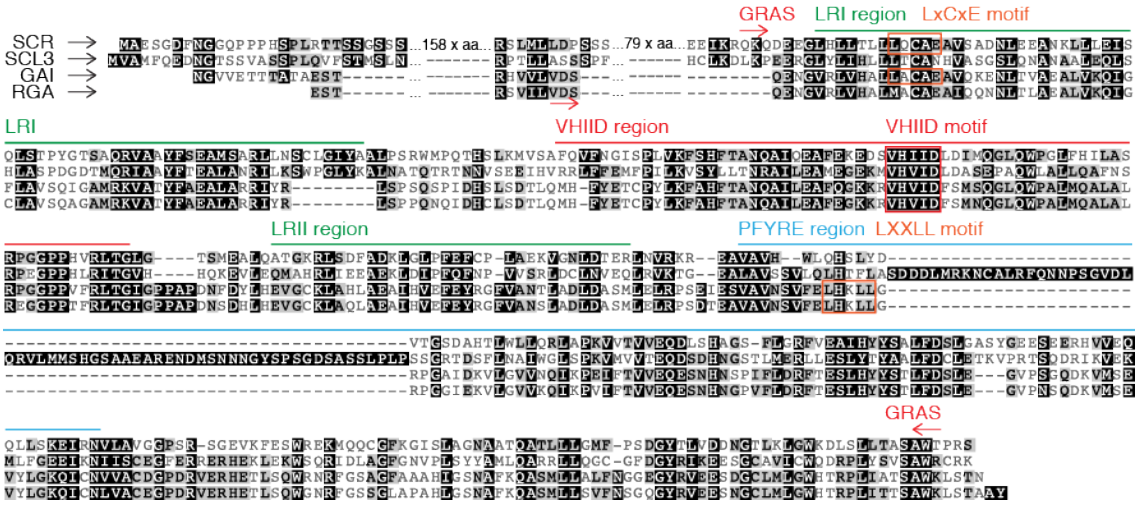


**Figure 33. Alignment and domain structure of the GRAS proteins that served as baits in the yeast two-hybrid experiment.**

Multiple sequence alignment of the protein sequences of SCR, SCL3 and N-terminally truncated GAI and RGA truncated versions that were used as baits in the yeast two-hybrid screen. Annotated are the regions and motifs identified with PROSITE (MUSCLE, Geneious 7.1.9, https://www.geneious.com).

the DELLA protein of rice, and GRF4 was shown with BiFC, co-immunoprecipitation and fluorescence resonance energy transfer experiments in a study about nitrogen use efficiency in rice (Li et al., 2018). This discovery is in line the findings presented here and suggests that DELLA-GRF interactions are conserved in monocots and dicots (Li et al., 2018). The role of the GRF-DELLA interactions in Arabidopsis is discussed in the following paragraphs.

### 4.2.3. GRFs are DELLA targets for the control growth and gene expression

The first described GRF transcription factor was identified as a GA-regulated gene and this work presents evidence through a comprehensive analysis of the involvement of members of this family from Arabidopsis in GA signaling and cold stress (van der Knaap et al., 2000).

The nine *Arabidopsis thaliana* GRF transcription factors have been involved in various developmental processes and responses including the control of cell proliferation, meristem homeostasis, osmotic and UV-B radiation stress (Hoe Kim and Tsukaya, 2015; Omidbakhshfard et al., 2015). The GRF proteins interact the

members of the GIF family of transcription cofactors, with three members in Arabidopsis named GIF1, GIF2 and GIF3, and together promote cell proliferation and leaf growth as well as the maintenance of the root meristem (Kim and Kende, 2004; Horiguchi et al., 2005; Lee et al., 2009; Debernardi et al., 2014). In addition, the miR396 post-transcriptionally downregulates seven out of nine *Arabidopsis thaliana* GRFs and miR396 overexpressing transgenic lines have low GRF content compared to the wild type (Liu et al., 2009; Rodriguez et al., 2010; Wang et al., 2010; Beltramino et al., 2018). Cell proliferation in the leaves is activated by the GRFs expressed in the leaf base, while *miR396* expression at the tip downregulates the GRFs and promotes cell elongation (Liu et al., 2009; Rodriguez et al., 2010; Beltramino et al., 2018). As the leaves get older, *miR396* expression is extended towards the leaf base to reduce GRF activity and the cells elongate (Beltramino et al., 2018). Plants that overexpress GRF5, which is not bound by *miR396*, or silent mutations of *miR396*-resistant versions of other GRFs have bigger leaves while *miR396* overexpressing plants have smaller leaves (Kim et al., 2003; Horiguchi et al., 2005; Rodriguez et al., 2010; Beltramino et al., 2018). Therefore, GRFs are subjects to different levels of regulation including transcriptional regulation by GA, posttranscriptional regulation through the miR396 as well DELLA regulation at the protein level and proteasomal degradation (Fig. 20 and 21) (Omidbakhshfard et al., 2015).

Manipulation of DELLA levels distinctly affected the shoot and root growth of plants with different GRF levels, signifying thus the role of the GRF-DELLA interactions in the control of the latter (Fig. 22 and 25). GA or PAC treatments had almost no impact on leaf growth of *35S:miR396b* expressing seedlings, therefore, *GRF* expression is necessary for the promotion of leaf growth by GA (Fig. 22). Similar results were reported for rice where it was shown that the leaf elongation of *miR396* overexpressing lines was partially insensitive to GA treatments (Tang et al., 2018). Besides, PAC-treated *GRF5* overexpressing seedlings were partially resistant to the DELLA-imposed inhibition of leaf growth, in a dosage-dependent manner, and more strongly when they were additionally exposed to cold stress (Fig. 22). The latter

suggests that the DELLA-GRF5 binding interferes with the GRF5 activation of cell-proliferation in leaves (Horiguchi et al., 2005). Furthermore, the root growth of *35S:miR396b* expressing seedlings in PAC- and cold stress was strongly arrested, and strikingly, their root meristem function was severely disturbed when they were in PAC containing medium (Fig. 25 and 26). Interestingly, a similar root phenotype defect was reported for root endodermis and cortex specific promoter-driven GAI expression, while higher numbers of cell divisions with the wrong orientation were shown in *miR396b* overexpressing seedlings compared to the wild type (Ubeda-Tomas et al., 2009; Rodriguez et al., 2015). As DELLA and GRF protein expression in the root proliferation zone overlap, it can be anticipated that the proteins interact in this tissue (Fig. 26C). Therefore, a DELLA-GRF balance is required for the coordination of cell proliferation and elongation in the root meristem zone. In summary, the effect of DELLA stabilization on leaf and root growth was dependent on the GRF protein abundance, which supports the hypothesis that the GRF transcription factors are DELLA targets regulated transcriptionally as well as through the DELLA-GRF protein interactions.

The role of the DELLA-GRF5 interaction in the control of cold stress- and GA-promoted gene expression was further investigated with RNA-seq analyses of the wild type and the GRF5 overexpressor. In line with the first RNA-seq experiment, the impact of cold stress on gene expression was stronger as opposed to that of GA for both genotypes, while the observed changes in transcript abundance of GA pathway genes in response to cold stress were almost identical between the two experiments, confirming the reproducibility of the results (Fig. 15E, 27D and 28). GRF5 activated the expression of the GA metabolism genes and DELLA genes, *GA20ox1*, *GA2ox1*, *GA2ox8*, *RGL1*, *RGL2* and *RGL3* (Fig. 27C). These results are in line with previous reports, although, there a different gene was shown to be GRF-controlled (Hewezi et al., 2012; Fina et al., 2017). The GRF-regulation of GA and DELLA levels is further supported by the observation that miR396b overexpressing seedlings have higher DELLA content compared to the wild-type (Fig. 24). Thus, GRF5 and possibly other GRFs transcriptionally regulate GA pathway genes.

In agreement with the hypothesis that GRFs are DELLA targets in cold stress, *GRF5* overexpression strongly affected gene expression changes in response to GA and cold stress treatments (Fig. 29). The identity of the regulated genes was largely different between 35S:GRF5 and the wild type as only 9 out 132 genes were differentially expressed in both (Fig. 29A). Therefore, the DELLA-controlled GRF5 abundance determined the GA response in cold stress. Interestingly, the CBF3 transcription factor was among the putative DELLA-GRF5 target genes in cold stress response (Fig. 29D and 31). In the wild type its expression was cold stress activated while GA partially suppressed *CBF* activation in line with a previous report (Fig. 31) (Zhou et al., 2017). *CBF1* and *CBF2* had also similar expression patterns as *CBF3* but the observed changes were not significant according to the applied statistical criteria (Fig. 31). In contrast to the wild-type, *CBF* gene expression was not as strongly activated after cold stress nor GA-regulated in the *GRF5* overexpressor (Fig. 31). The latter could be the result of the direct *CBF* suppression by GRF5 through promoter binding in combination with an additional cold induced transcription factor, as the CBFs were not activated in the 35S:GRF5 line at ambient temperature. Another explanation could be that the regulation of different transcription factors by DELLAs, such as the JAZ proteins, was abolished in this genotype due to the decreased number of free from GRF DELLA molecules (Fig. 20D) (Zhou et al., 2017). Furthermore, a quarter of the DEGs between the *GRF5* overexpressing line and the wild-type at ambient temperature, were also regulated in the same manner after cold stress in the wild type, suggesting that GRF5 directly controls the expression of those genes (Fig. 30). The latter included 26 genes of the CBF regulon which were regulated by GRF5 in the absence of CBF expression at 21 °C (Fig. 30) (Park et al., 2015; Jia et al., 2016; Zhao et al., 2016). For example, *RD29A*, *COR15A* and *COR15b* were upregulated in the *GRF5* overexpressor compared to the wild-type at ambient temperature, as well as after cold stress but they were not GA-regulated (Fig. 31). These results are in line with previous reports that showed cold stress induction of CBF regulon genes in *cbf* triple mutants (Jia et al., 2016; Zhao et al., 2016). Therefore, GRF5 controls the expression of both GA-dependent and independent cold stress differentially expressed genes.

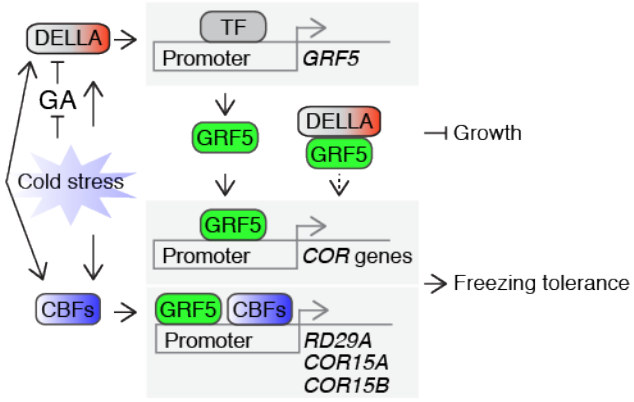


**Figure 34. Schematic representation of GA and GRF5 signaling in cold stress.**

Cold stress promotes DELLA stabilization through the downregulation of GA levels and the upregulation of *DELLA* gene expression, in both a CBF-dependent and independent manner. DELLAs consequently promote the *GRF5* upregulation, which activates the expression of cold regulated genes (*COR*), including CBF target genes to promote freezing tolerance. The DELLA-GRF5 complex formation plays a growth inhibitory role possibly thought by the sequestration of GRF5 from gene promoters that activate cell proliferation and the promotion of expression of *COR* genes.

In summary, the cold stress transcriptional response in Arabidopsis is controlled by GRF5 and possibly the GRF1 and GRF3 transcription factors, which are a subject to GA and DELLA regulation (Fig. 34). Thus, an additional role of these transcription factors in an abiotic stress response is uncovered as part of this work on top of their already described functions in ambient temperature-grown plants (Debernardi et al., 2014; Hoe Kim and Tsukaya, 2015; Omidbakhshfard et al., 2015; Rodriguez et al., 2015; Li et al., 2018). As a DELLA-GRF interaction was also reported in rice to play a role in nitrogen use efficiency, it is likely that these interactions are conserved in different plant species and play crucial roles in the regulation of growth, yield and abiotic stress resistance (Duan et al., 2015; Gao et al., 2015; Li et al., 2018; Xue et al., 2020). Further elucidation and characterization of the molecular signaling mechanisms that act downstream of GA and DELLA proteins and their interactors, is crucial for the future development of cold stress resistant and high yielding crops.

# Bibliography


**Abdrakhamanova A, Wang QY, Khokhlova L, Nick P** (2003) Is microtubule disassembly a trigger for cold acclimation? Plant Cell Physiol **44:** 676-686

**Achard P, Cheng H, De Grauwe L, Decat J, Schoutteten H, Moritz T, Van Der Straeten D, Peng J, Harberd NP** (2006) Integration of plant responses to environmentally activated phytohormonal signals. Science **311:** 91-94

**Achard P, Gong F, Cheminant S, Alioua M, Hedden P, Genschik P** (2008) The cold-inducible CBF1 factor-dependent signaling pathway modulates the accumulation of the growth-repressing DELLA proteins via its effect on gibberellin metabolism. Plant Cell **20:** 2117-2129

**Achard P, Gusti A, Cheminant S, Alioua M, Dhondt S, Coppens F, Beemster GT, Genschik P** (2009) Gibberellin signaling controls cell proliferation rate in Arabidopsis. Curr Biol **19:** 1188-1193

**Agusti J, Herold S, Schwarz M, Sanchez P, Ljung K, Dun EA, Brewer PB, Beveridge CA, Sieberer T, Sehra EM, Greb T** (2012) Correction for Agusti et al., Strigolactone signaling is required for auxin-dependent stimulation of secondary growth in plants. Proc Natl Acad Sci U S A **109:** 14277-14277

**Akiyama K, Matsuzaki K, Hayashi H** (2005) Plant sesquiterpenes induce hyphal branching in arbuscular mycorrhizal fungi. Nature **435:** 824-827

**Al-Babili S, Bouwmeester HJ** (2015) Strigolactones, a Novel Carotenoid-Derived Plant Hormone. Annu Rev Plant Biol

**Altmann M, Altmann S, Falter C, Falter-Braun P** (2018) High-Quality Yeast-2-Hybrid Interaction Network Mapping. Curr Protoc Plant Biol **3:** e20067

**Ariizumi T, Lawrence PK, Steber CM** (2011) The role of two f-box proteins, SLEEPY1 and SNEEZY, in Arabidopsis gibberellin signaling. Plant Physiol **155:** 765-775

**Arite T, Umehara M, Ishikawa S, Hanada A, Maekawa M, Yamaguchi S, Kyozuka J** (2009) d14, a strigolactone-insensitive mutant of rice, shows an accelerated outgrowth of tillers. Plant Cell Physiol **50:** 1416-1424

**Bai MY, Shang JX, Oh E, Fan M, Bai Y, Zentella R, Sun TP, Wang ZY** (2012) Brassinosteroid, gibberellin and phytochrome impinge on a common transcription module in Arabidopsis. Nat Cell Biol **14:** 810-817

**Bauer J, Chen K, Hiltbunner A, Wehrli E, Eugster M, Schnell D, Kessler F** (2000) The major protein import receptor of plastids is essential for chloroplast biogenesis. Nature **403:** 203-207

**Baxter B** (2014) Plant acclimation and adaptation to cold environments. *In* KA Franklin, PA Wigge, eds, Temperature and Plant Development, pp 19-48

**Beltramino M, Ercoli MF, Debernardi JM, Goldy C, Rojas AML, Nota F, Alvarez ME, Vercruyssen L, Inze D, Palatnik JF, Rodriguez RE** (2018) Robust increase of leaf size by Arabidopsis thaliana GRF3-like transcription factors under different growth conditions. Sci Rep **8:** 13447

**Bennett T, Liang Y, Seale M, Ward S, Muller D, Leyser O** (2016) Strigolactone regulates shoot development through a core signalling pathway. Biol Open **5:** 1806-1820

**Bennett T, Sieberer T, Willett B, Booker J, Luschnig C, Leyser O** (2006) The Arabidopsis MAX pathway controls shoot branching by regulating auxin transport. Curr Biol **16:** 553-563

**Binenbaum J, Weinstain R, Shani E** (2018) Gibberellin Localization and Transport in Plants. Trends Plant Sci **23:** 410-421

**Booker J, Auldridge M, Wills S, McCarty D, Klee H, Leyser O** (2004) MAX3/CCD7 is a carotenoid cleavage dioxygenase required for the synthesis of a novel plant signaling molecule. Curr Biol **14:** 1232-1238

**Booker J, Sieberer T, Wright W, Williamson L, Willett B, Stirnberg P, Turnbull C, Srinivasan M, Goddard P, Leyser O** (2005) MAX1 encodes a cytochrome P450 family member that acts downstream of MAX3/4 to produce a carotenoid-derived branch-inhibiting hormone. Dev Cell **8:** 443-449

**Bos JI, Armstrong MR, Gilroy EM, Boevink PC, Hein I, Taylor RM, Zhendong T, Engelhardt S, Vetukuri RR, Harrower B, Dixelius C, Bryan G, Sadanandom A, Whisson SC, Kamoun S, Birch PR** (2010) Phytophthora infestans effector AVR3a is essential for virulence and manipulates plant immunity by stabilizing host E3 ligase CMPG1. Proc Natl Acad Sci U S A **107:** 9909-9914

**Braun P, Aubourg S, Van Leene J, De Jaeger G, Lurin C** (2013) Plant protein interactomes. Annu Rev Plant Biol **64:** 161-187

**Brewer PB, Dun EA, Gui R, Mason M, Beveridge CA** (2015) Strigolactone inhibition of branching independent of polar auxin transport. Plant Physiol

**Brewer PB, Koltai H, Beveridge CA** (2013) Diverse roles of strigolactones in plant development. Mol Plant **6:** 18-28

**Brewer PB, Yoneyama K, Filardo F, Meyers E, Scaffidi A, Frickey T, Akiyama K, Seto Y, Dun EA, Cremer JE, Kerr SC, Waters MT, Flematti GR, Mason MG, Weiller G, Shinjiro Yamaguchig, Nomura T, Smith SM, Yoneyama K, Beveridge CA** (2016) LATERAL BRANCHING OXIDOREDUCTASE acts in the final stages of strigolactone biosynthesis in Arabidopsis. Proceedings of the National Academy of Sciences **113:** 6301–6306

**Calixto CPG, Guo W, James AB, Tzioutziou NA, Entizne JC, Panter PE, Knight H, Nimmo HG, Zhang R, Brown JWS** (2018) Rapid and Dynamic Alternative Splicing Impacts the Arabidopsis Cold Response Transcriptome. Plant Cell **30:** 1424-1444

**Camut L, Daviere JM, Achard P** (2017) Dynamic Regulation of DELLA Protein Activity: SPINDLY and SECRET AGENT Unmasked! Mol Plant **10:** 785-787

**Cao D, Cheng H, Wu W, Soo HM, Peng J** (2006) Gibberellin mobilizes distinct DELLA-dependent transcriptomes to regulate seed germination and floral development in Arabidopsis. Plant Physiol **142:** 509-525

**Causier B, Ashworth M, Guo W, Davies B** (2012) The TOPLESS interactome: a framework for gene repression in Arabidopsis. Plant Physiol **158:** 423-438

**Chiba Y, Shimizu T, Miyakawa S, Kanno Y, Koshiba T, Kamiya Y, Seo M** (2015) Identification of Arabidopsis thaliana NRT1/PTR FAMILY (NPF) proteins capable of transporting plant hormones. J Plant Res **128:** 679-686

**Claeys H, De Bodt S, Inze D** (2014) Gibberellins and DELLAs: central nodes in growth regulatory networks. Trends Plant Sci **19:** 231-239

**Colebrook EH, Thomas SG, Phillips AL, Hedden P** (2014) The role of gibberellin signalling in plant responses to abiotic stress. The Journal of Experimental Biology **217:** 67-75

**Conn CE, Nelson DC** (2015) Evidence that KARRIKIN-INSENSITIVE2 (KAI2) Receptors may Perceive an Unknown Signal that is not Karrikin or Strigolactone. Front Plant Sci **6:** 1219

**Consortium AIM** (2011) Evidence for network evolution in an Arabidopsis interactome map. Science **333:** 601-607

**Conti L, Nelis S, Zhang C, Woodcock A, Swarup R, Galbiati M, Tonelli C, Napier R, Hedden P, Bennett M, Sadanandom A** (2014) Small Ubiquitin-like Modifier protein SUMO enables plants to control growth independently of the phytohormone gibberellin. Dev Cell **28:** 102-110

**Crawford S, Shinohara N, Sieberer T, Williamson L, George G, Hepworth J, Muller D, Domagalska MA, Leyser O** (2010) Strigolactones enhance competition between shoot branches by dampening auxin transport. Development **137:** 2905-2913

**Dai C, Xue HW** (2010) Rice early flowering1, a CKI, phosphorylates DELLA protein SLR1 to negatively regulate gibberellin signalling. EMBO J **29:** 1916-1927

**Daviere JM, Achard P** (2016) A Pivotal Role of DELLAs in Regulating Multiple Hormone Signals. Mol Plant **9:** 10-20

**de Hoon MJ, Imoto S, Nolan J, Miyano S** (2004) Open source clustering software. Bioinformatics **20:** 1453-1454

**de Lucas M, Daviere JM, Rodriguez-Falcon M, Pontin M, Iglesias-Pedraz JM, Lorrain S, Fankhauser C, Blazquez MA, Titarenko E, Prat S** (2008) A molecular framework for light and gibberellin control of cell elongation. Nature **451:** 480-484

**de Saint Germain A, Clave G, Badet-Denisot MA, Pillot JP, Cornu D, Le Caer JP, Burger M, Pelissier F, Retailleau P, Turnbull C, Bonhomme S, Chory J, Rameau C, Boyer FD** (2016) An histidine covalent receptor and butenolide complex mediates strigolactone perception. Nat Chem Biol **12:** 787-794

**de Saint Germain A, Ligerot Y, Dun EA, Pillot JP, Ross JJ, Beveridge CA, Rameau C** (2013) Strigolactones stimulate internode elongation independently of gibberellins. Plant Physiol **163:** 1012-1025

**Debernardi JM, Mecchia MA, Vercruyssen L, Smaczniak C, Kaufmann K, Inze D, Rodriguez RE, Palatnik JF** (2014) Post-transcriptional control of GRF transcription factors by microRNA miR396 and GIF co-activator affects leaf size and longevity. Plant Journal **79:** 413-426

**Dill A, Thomas SG, Hu J, Steber CM, Sun TP** (2004) The Arabidopsis F-box protein SLEEPY1 targets gibberellin signaling repressors for gibberellin-induced degradation. Plant Cell **16:** 1392-1405

**Du J, Jiang H, Sun X, Li Y, Liu Y, Sun M, Fan Z, Cao Q, Feng L, Shang J, Shu K, Liu J, Yang F, Liu W, Yong T, Wang X, Yuan S, Yu L, Liu C, Yang W** (2018) Auxin and Gibberellins Are Required for the Receptor-Like Kinase

ERECTA Regulated Hypocotyl Elongation in Shade Avoidance in Arabidopsis. Front Plant Sci **9:** 124

**Duan P, Ni S, Wang J, Zhang B, Xu R, Wang Y, Chen H, Zhu X, Li Y** (2015) Regulation of OsGRF4 by OsmiR396 controls grain size and yield in rice. Nature Plants **2**

**Ercoli MF, Ferela A, Debernardi JM, Perrone AP, Rodriguez RE, Palatnik JF** (2018) GIF Transcriptional Coregulators Control Root Meristem Homeostasis. Plant Cell **30:** 347-359

**Eremina M, Unterholzner SJ, Rathnayake AI, Castellanos M, Khan M, Kugler KG, May ST, Mayer KF, Rozhon W, Poppenberger B** (2016) Brassinosteroids participate in the control of basal and acquired freezing tolerance of plants. Proc Natl Acad Sci U S A **113:** E5982-E5991

**Feng S, Martinez C, Gusmaroli G, Wang Y, Zhou J, Wang F, Chen L, Yu L, Iglesias-Pedraz JM, Kircher S, Schafer E, Fu X, Fan LM, Deng XW** (2008) Coordinated regulation of Arabidopsis thaliana development by light and gibberellins. Nature **451:** 475-479

**Ferjani A, Horiguchi G, Yano S, Tsukaya H** (2007) Analysis of leaf development in fugu mutants of Arabidopsis reveals three compensation modes that modulate cell expansion in determinate organs. Plant Physiol **144:** 988-999

**Fina J, Casadevall R, AbdElgawad H, Prinsen E, Markakis MN, Beemster GTS, Casati P** (2017) UV-B Inhibits Leaf Growth through Changes in Growth Regulating Factors and Gibberellin Levels. Plant Physiol **174:** 1110-1126

**Floss DS, Levy JG, Levesque-Tremblay V, Pumplin N, Harrison MJ** (2013) DELLA proteins regulate arbuscule formation in arbuscular mycorrhizal symbiosis. Proc Natl Acad Sci U S A **110:** E5025-5034

**Fonouni-Farde C, Diet A, Frugier F** (2016) Root Development and Endosymbioses: DELLAs Lead the Orchestra. Trends in Plant Science **21:** 898-900

**Fu X, Richards DE, Ait-Ali T, Hynes LW, Ougham H, Peng J, Harberd NP** (2002) Gibberellin-mediated proteasome-dependent degradation of the barley DELLA protein SLN1 repressor. Plant Cell **14:** 3191-3200

**Fu X, Richards DE, Fleck B, Xie D, Burton N, Harberd NP** (2004) The Arabidopsis mutant sleepy1gar2-1 protein promotes plant growth by increasing the affinity of the SCFSLY1 E3 ubiquitin ligase for DELLA protein substrates. Plant Cell **16:** 1406-1418

**Fukazawa J, Teramura H, Murakoshi S, Nasuno K, Nishida N, Ito T, Yoshida M, Kamiya Y, Yamaguchi S, Takahashi Y** (2014) DELLAs function as coactivators of GAI-ASSOCIATED FACTOR1 in regulation of gibberellin homeostasis and signaling in Arabidopsis. Plant Cell **26:** 2920-2938

**Gallego-Bartolome J, Minguet EG, Marin JA, Prat S, Blazquez MA, Alabadi D** (2010) Transcriptional diversification and functional conservation between DELLA proteins in Arabidopsis. Mol Biol Evol **27:** 1247-1256

**Galvao VC, Horrer D, Kuttner F, Schmid M** (2012) Spatial control of flowering by DELLA proteins in Arabidopsis thaliana. Development **139:** 4072-4082

**Gao F, Wang K, Liu Y, Chen Y, Chen P, Shi Z, Luo J, Jiang D, Fan F, Zhu Y, Li S** (2015) Blocking miR396 increases rice yield by shaping inflorescence architecture. Nature Plants **2**

**Gilmour SJ, Fowler SG, Thomashow MF** (2004) Arabidopsis transcriptional activators CBF1, CBF2, and CBF3 have matching functional activities. Plant Mol Biol **54:** 767-781

**Gomez-Roldan V, Fermas S, Brewer PB, Puech-Pages V, Dun EA, Pillot JP, Letisse F, Matusova R, Danoun S, Portais JC, Bouwmeester H, Becard G, Beveridge CA, Rameau C, Rochange SF** (2008) Strigolactone inhibition of shoot branching. Nature **455:** 189-194

**Gonzalez N, Inze D** (2015) Molecular systems governing leaf growth: from genes to networks. J Exp Bot **66:** 1045-1054

**Griffiths J, Murase K, Rieu I, Zentella R, Zhang ZL, Powers SJ, Gong F, Phillips AL, Hedden P, Sun TP, Thomas SG** (2006) Genetic characterization and functional analysis of the GID1 gibberellin receptors in Arabidopsis. Plant Cell **18:** 3399-3414

**Hamiaux C, Drummond RS, Janssen BJ, Ledger SE, Cooney JM, Newcomb RD, Snowden KC** (2012) DAD2 is an alpha/beta hydrolase likely to be involved in the perception of the plant branching hormone, strigolactone. Curr Biol **22:** 2032-2036

**Hayward A, Stirnberg P, Beveridge C, Leyser O** (2009) Interactions between auxin and strigolactone in shoot branching control. Plant Physiol **151:** 400-412

**Hedden P** (2003) The genes of the Green Revolution. Trends Genet **19:** 5-9

**Hedden P, Sponsel V** (2015) A Century of Gibberellin Research. J Plant Growth Regul **34:** 740-760

**Hedden P, Thomas SG** (2012) Gibberellin biosynthesis and its regulation. Biochem J **444:** 11-25

**Hewezi T, Maier TR, Nettleton D, Baum TJ** (2012) The Arabidopsis microRNA396-GRF1/GRF3 regulatory module acts as a developmental regulator in the reprogramming of root cells during cyst nematode infection. Plant Physiology **159:** 321-335

**Heyndrickx KS, Van de Velde J, Wang C, Weigel D, Vandepoele K** (2014) A functional and evolutionary perspective on transcription factor binding in Arabidopsis thaliana. Plant Cell **26:** 3894-3910

**Hirano K, Nakajima M, Asano K, Nishiyama T, Sakakibara H, Kojima M, Katoh E, Xiang H, Tanahashi T, Hasebe M, Banks JA, Ashikari M, Kitano H, Ueguchi-Tanaka M, Matsuoka M** (2007) The GID1-mediated gibberellin perception mechanism is conserved in the Lycophyte Selaginella moellendorffii but not in the Bryophyte Physcomitrella patens. Plant Cell **19:** 3058-3079

**Hoe Kim J, Tsukaya H** (2015) Regulation of plant growth and development by the GROWTH-REGULATING FACTOR and GRF-INTERACTING FACTOR duo. Journal of Experimental Botany **66:** 6093-6107

**Hong GJ, Xue XY, Mao YB, Wang LJ, Chen XY** (2012) Arabidopsis MYC2 interacts with DELLA proteins in regulating sesquiterpene synthase gene expression. Plant Cell **24:** 2635-2648

**Horiguchi G, Kim GT, Tsukaya H** (2005) The transcription factor AtGRF5 and the transcription coactivator AN3 regulate cell proliferation in leaf primordia of Arabidopsis thaliana. Plant Journal **43:** 68-78

**Hou X, Lee LY, Xia K, Yan Y, Yu H** (2010) DELLAs modulate jasmonate signaling via competitive binding to JAZs. Dev Cell **19:** 884-894

**Hu Y, Jiang L, Wang F, Yu D** (2013) Jasmonate regulates the inducer of cbf expression-C-repeat binding factor/DRE binding factor1 cascade and freezing tolerance in Arabidopsis. Plant Cell **25:** 2907-2924

**Huang RF, Lloyd CW** (1999) Gibberellic acid stabilises microtubules in maize suspension cells to cold and stimulates acetylation of α-tubulin 1. FEBS Letters **443:** 317-320

**Hussain A, Cao D, Cheng H, Wen Z, Peng J** (2005) Identification of the conserved serine/threonine residues important for gibberellin-sensitivity of Arabidopsis RGL2 protein. Plant J **44:** 88-99

**Hwang JU, Song WY, Hong D, Ko D, Yamaoka Y, Jang S, Yim S, Lee E, Khare D, Kim K, Palmgren M, Yoon HS, Martinoia E, Lee Y** (2016) Plant ABC Transporters Enable Many Unique Aspects of a Terrestrial Plant's Lifestyle. Mol Plant **9:** 338-355

**Ito S, Yamagami D, Umehara M, Hanada A, Yoshida S, Sasaki Y, Yajima S, Kyozuka J, Ueguchi-Tanaka M, Matsuoka M, Shirasu K, Yamaguchi S, Asami T** (2017) Regulation of Strigolactone Biosynthesis by Gibberellin Signaling. Plant Physiol **174:** 1250-1259

**Itoh H, Ueguchi-Tanaka M, Sato Y, Ashikari M, Matsuoka M** (2002) The gibberellin signaling pathway is regulated by the appearance and disappearance of SLENDER RICE1 in nuclei. Plant Cell **14:** 57-70

**Jha UC, Bohra A, Jha R** (2017) Breeding approaches and genomics technologies to increase crop yield under low-temperature stress. Plant Cell Rep **36:** 1-35

**Jia Y, Ding Y, Shi Y, Zhang X, Gong Z, Yang S** (2016) The cbfs triple mutants reveal the essential functions of CBFs in cold acclimation and allow the definition of CBF regulons in Arabidopsis. New Phytol **212:** 345-353

**Jiang C, Gao X, Liao L, Harberd NP, Fu X** (2007) Phosphate starvation root architecture and anthocyanin accumulation responses are modulated by the gibberellin-DELLA signaling pathway in Arabidopsis. Plant Physiol **145:** 1460-1470

**Jiang L, Liu X, Xiong G, Liu H, Chen F, Wang L, Meng X, Liu G, Yu H, Yuan Y, Yi W, Zhao L, Ma H, He Y, Wu Z, Melcher K, Qian Q, Xu HE, Wang Y, Li J** (2013) DWARF 53 acts as a repressor of strigolactone signalling in rice. Nature **504:** 401-405

**Kanno Y, Oikawa T, Chiba Y, Ishimaru Y, Shimizu T, Sano N, Koshiba T, Kamiya Y, Ueda M, Seo M** (2016) AtSWEET13 and AtSWEET14 regulate gibberellin-mediated physiological processes. Nat Commun **7:** 13245

**Kapulnik Y, Koltai H** (2016) Fine-tuning by strigolactones of root response to low phosphate. J Integr Plant Biol **58:** 203-212

**Kim JH, Choi D, Kende H** (2003) The AtGRF family of putative transcription factors is involved in leaf and cotyledon growth in Arabidopsis. Plant J **36:** 94-104

**Kim JH, Kende H** (2004) A transcriptional coactivator, AtGIF1, is involved in regulating leaf growth and morphology in Arabidopsis. Proc Natl Acad Sci U S A **101:** 13374-13379

**Ko JH, Yang SH, Han KH** (2006) Upregulation of an Arabidopsis RING-H2 gene, XERICO, confers drought tolerance through increased abscisic acid biosynthesis. Plant J **47:** 343-355

**Kohlen W, Charnikhova T, Liu Q, Bours R, Domagalska MA, Beguerie S, Verstappen F, Leyser O, Bouwmeester H, Ruyter-Spira C** (2011) Strigolactones are transported through the xylem and play a key role in shoot architectural response to phosphate deficiency in nonarbuscular mycorrhizal host Arabidopsis. Plant Physiol **155:** 974-987

**Kretzschmar T, Kohlen W, Sasse J, Borghi L, Schlegel M, Bachelier JB, Reinhardt D, Bours R, Bouwmeester HJ, Martinoia E** (2012) A petunia ABC protein controls strigolactone-dependent symbiotic signalling and branching. Nature **483:** 341-344

**Kumar M, Pandya-Kumar N, Dam A, Haor H, Mayzlish-Gati E, Belausov E, Wininger S, Abu-Abied M, McErlean CS, Bromhead LJ, Prandi C, Kapulnik Y, Koltai H** (2015) Arabidopsis response to low-phosphate conditions includes active changes in actin filaments and PIN2 polarization and is dependent on strigolactone signalling. J Exp Bot **66:** 1499-1510

**Kumar SV, Lucyshyn D, Jaeger KE, Alos E, Alvey E, Harberd NP, Wigge PA** (2012) Transcription factor PIF4 controls the thermosensory activation of flowering. Nature **484:** 242-245

**Lamarre S, Frasse P, Zouine M, Labourdette D, Sainderichin E, Hu G, Le Berre-Anton V, Bouzayen M, Maza E** (2018) Optimization of an RNA-Seq Differential Gene Expression Analysis Depending on Biological Replicate Number and Library Size. Front Plant Sci **9:** 108

**Lee BH, Ko JH, Lee S, Lee Y, Pak JH, Kim JH** (2009) The Arabidopsis GRF-INTERACTING FACTOR gene family performs an overlapping function in determining organ size as well as multiple developmental properties. Plant Physiology **151:** 655-668

**Li A, Zhou M, Wei D, Chen H, You C, Lin J** (2017) Transcriptome Profiling Reveals the Negative Regulation of Multiple Plant Hormone Signaling Pathways Elicited by Overexpression of C-Repeat Binding Factors. Front Plant Sci **8:** 1647

**Li R, Zhang J, Li J, Zhou G, Wang Q, Bian W, Erb M, Lou Y** (2015) Prioritizing plant defence over growth through WRKY regulation facilitates infestation by non-target herbivores. Elife **4:** e04805

**Li S, Tian Y, Wu K, Ye Y, Yu J, Zhang J, Liu Q, Hu M, Li H, Tong Y, Harberd NP, Fu X** (2018) Modulating plant growth-metabolism coordination for sustainable agriculture. Nature **560:** 595-600

**Li S, Zhao Y, Zhao Z, Wu X, Sun L, Liu Q, Wu Y** (2016) Crystal Structure of the GRAS Domain of SCARECROW-LIKE7 in Oryza sativa. Plant Cell **28:** 1025-1034

**Liang Y, Ward S, Li P, Bennett T, Leyser O** (2016) SMAX1-LIKE7 Signals from the Nucleus to Regulate Shoot Development in Arabidopsis via Partially EAR Motif-Independent Mechanisms. Plant Cell **28:** 1581-1601

**Lim S, Park J, Lee N, Jeong J, Toh S, Watanabe A, Kim J, Kang H, Kim DH, Kawakami N, Choi G** (2013) ABA-insensitive3, ABA-insensitive5, and DELLAs Interact to activate the expression of SOMNUS and other high-temperature-inducible genes in imbibed seeds in Arabidopsis. Plant Cell **25:** 4863-4878

**Lin H, Wang R, Qian Q, Yan M, Meng X, Fu Z, Yan C, Jiang B, Su Z, Li J, Wang Y** (2009) DWARF27, an iron-containing protein required for the biosynthesis of strigolactones, regulates rice tiller bud outgrowth. Plant Cell **21:** 1512-1525

**Liu D, Song Y, Chen Z, Yu D** (2009) Ectopic expression of miR396 suppresses GRF target gene expression and alters leaf growth in Arabidopsis. Physiologia Plantarum **136:** 223-236

**Livne S, Lor VS, Nir I, Eliaz N, Aharoni A, Olszewski NE, Eshed Y, Weiss D** (2015) Uncovering DELLA-Independent Gibberellin Responses by Characterizing New Tomato procera Mutants. Plant Cell **27:** 1579-1594

**Lo SF, Yang SY, Chen KT, Hsing YI, Zeevaart JA, Chen LJ, Yu SM** (2008) A novel class of gibberellin 2-oxidases control semidwarfism, tillering, and root development in rice. Plant Cell **20:** 2603-2618

**Locascio A, Blazquez MA, Alabadi D** (2013) Dynamic regulation of cortical microtubule organization through prefoldin-DELLA interaction. Curr Biol **23:** 804-809

**Lofke C, Zwiewka M, Heilmann I, Van Montagu MC, Teichmann T, Friml J** (2013) Asymmetric gibberellin signaling regulates vacuolar trafficking of PIN auxin transporters during root gravitropism. Proc Natl Acad Sci U S A **110:** 3627-3632

**Luo L, Li W, Miura K, Ashikari M, Kyozuka J** (2012) Control of Tiller Growth of Rice by OsSPL14 and Strigolactones, Which Work in Two Independent Pathways. Plant Cell Physiology **53:** 1793–1801

**Luo Y, Dong X, Yu T, Shi X, Li Z, Yang W, Widmer A, Karrenberg S** (2015) A Single Nucleotide Deletion in Gibberellin20-oxidase1 Causes Alpine Dwarfism in Arabidopsis. Plant Physiol **168:** 930-937

**MacMillan J, Suter PJ** (1958) The occurrence of gibberellin A1 in higher plants: Isolation from the seed of runner bean (Phaseolus multiflorus). Naturwissenschaften **45:** 46

**Marin-de la Rosa N, Pfeiffer A, Hill K, Locascio A, Bhalerao RP, Miskolczi P, Gronlund AL, Wanchoo-Kohli A, Thomas SG, Bennett MJ, Lohmann JU, Blazquez MA, Alabadi D** (2015) Genome Wide Binding Site Analysis Reveals Transcriptional Coactivation of Cytokinin-Responsive Genes by DELLA Proteins. PLoS Genet **11:** e1005337

**Marin-de la Rosa N, Sotillo B, Miskolczi P, Gibbs DJ, Vicente J, Carbonero P, Onate-Sanchez L, Holdsworth MJ, Bhalerao R, Alabadi D, Blazquez MA** (2014) Large-scale identification of gibberellin-related transcription factors defines group VII ETHYLENE RESPONSE FACTORS as functional DELLA partners. Plant Physiol **166:** 1022-1032

**Marzec M** (2016) Perception and Signaling of Strigolactones. Front Plant Sci **7:** 1260

**Marzec M** (2017) Strigolactones and Gibberellins: A New Couple in the Phytohormone World? Trends Plant Sci **22:** 813-815

**Mashiguchi K, Sasaki E, Shimada Y, Nagae M, Ueno K, Nakano T, Yoneyama K, Suzuki Y, Asami T** (2009) Feedback-regulation of strigolactone biosynthetic genes and strigolactone-regulated genes in Arabidopsis. Biosci Biotechnol Biochem **73:** 2460-2465

**Mayzlish-Gati E, De-Cuyper C, Goormachtig S, Beeckman T, Vuylsteke M, Brewer PB, Beveridge CA, Yermiyahu U, Kaplan Y, Enzer Y, Wininger S, Resnick N, Cohen M, Kapulnik Y, Koltai H** (2012) Strigolactones are involved in root response to low phosphate conditions in Arabidopsis. Plant Physiol **160:** 1329-1341

**Mayzlish-Gati E, LekKala SP, Resnick N, Wininger S, Bhattacharya C, Lemcoff JH, Kapulnik Y, Koltai H** (2010) Strigolactones are positive regulators of light-harvesting genes in tomato. J Exp Bot **61:** 3129-3136

**Middleton AM, Ubeda-Tomas S, Griffiths J, Holman T, Hedden P, Thomas SG, Phillips AL, Holdsworth MJ, Bennett MJ, King JR, Owen MR** (2012) Mathematical modeling elucidates the role of transcriptional feedback in gibberellin signaling. Proc Natl Acad Sci U S A **109:** 7571-7576

**Miura K, Furumoto T** (2013) Cold signaling and cold response in plants. Int J Mol Sci **14:** 5312-5337

**Morffy N, Faure L, Nelson DC** (2016) Smoke and Hormone Mirrors: Action and Evolution of Karrikin and Strigolactone Signaling. Trends Genet **32:** 176-188

**Murase K, Hirano Y, Sun TP, Hakoshima T** (2008) Gibberellin-induced DELLA recognition by the gibberellin receptor GID1. Nature **456:** 459-463

**Nakajima M, Shimada A, Takashi Y, Kim YC, Park SH, Ueguchi-Tanaka M, Suzuki H, Katoh E, Iuchi S, Kobayashi M, Maeda T, Matsuoka M, Yamaguchi I** (2006) Identification and characterization of Arabidopsis gibberellin receptors. Plant J **46:** 880-889

**Nakamura H, Xue YL, Miyakawa T, Hou F, Qin HM, Fukui K, Shi X, Ito E, Ito S, Park SH, Miyauchi Y, Asano A, Totsuka N, Ueda T, Tanokura M, Asami T** (2013) Molecular mechanism of strigolactone perception by DWARF14. Nat Commun **4:** 2613

**Nelson DC, Flematti GR, Riseborough JA, Ghisalberti EL, Dixon KW, Smith SM** (2010) Karrikins enhance light responses during germination and seedling development in Arabidopsis thaliana. Proc Natl Acad Sci U S A **107:** 7095-7100

**Nelson DC, Scaffidi A, Dun EA, Waters MT, Flematti GR, Dixon KW, Beveridge CA, Ghisalberti EL, Smith SM** (2011) F-box protein MAX2 has dual roles in karrikin and strigolactone signaling in Arabidopsis thaliana. Proceedings of the National Academy of Sciences of the United States of America **108:** 8897-8902

**Oh E, Zhu JY, Wang ZY** (2012) Interaction between BZR1 and PIF4 integrates brassinosteroid and environmental responses. Nat Cell Biol **14:** 802-809

**Omidbakhshfard MA, Proost S, Fujikura U, Mueller-Roeber B** (2015) Growth-Regulating Factors (GRFs): A Small Transcription Factor Family with Important Functions in Plant Biology. Molecular Plant **8:** 998-1010

**Park J, Nguyen KT, Park E, Jeon JS, Choi G** (2013) DELLA proteins and their interacting RING Finger proteins repress gibberellin responses by binding to the promoters of a subset of gibberellin-responsive genes in Arabidopsis. Plant Cell **25:** 927-943

**Park S, Lee CM, Doherty CJ, Gilmour SJ, Kim Y, Thomashow MF** (2015) Regulation of the Arabidopsis CBF regulon by a complex low-temperature regulatory network. Plant J **82:** 193-207

**Penfield S** (2008) Temperature perception and signal transduction in plants. New Phytol **179:** 615-628

**Penfield S, MacGregor D** (2014) Temperature sensing in plants, Ed K.a. Franklin and P.a. Wigge

**Peng J, Carol P, Richards DE, King KE, Cowling RJ, Murphy GP, Harberd NP** (1997) The Arabidopsis GAI gene defines a signaling pathway that negatively regulates gibberellin responses Genes & Development **11:** 3194-3205

**Perea-Resa C, Rodriguez-Milla MA, Iniesto E, Rubio V, Salinas J** (2017) Prefoldins Negatively Regulate Cold Acclimation in Arabidopsis thaliana by Promoting Nuclear Proteasome-Mediated HY5 Degradation. Mol Plant **10:** 791-804

**Pinthus MJ, Gale MD, Appleford NE, Lenton JR** (1989) Effect of Temperature on Gibberellin (GA) Responsiveness and on Endogenous GA(1) Content of Tall and Dwarf Wheat Genotypes. Plant Physiol **90:** 854-859

**Pruneda-Paz JL, Breton G, Nagel DH, Kang SE, Bonaldi K, Doherty CJ, Ravelo S, Galli M, Ecker JR, Kay SA** (2014) A genome-scale resource for the functional characterization of Arabidopsis transcription factors. Cell Rep **8:** 622-632

**Pysh LD, Wysocka-Diller JW, Camilleri C, Bouchez D, Benfey PN** (1999) The GRAS gene family in Arabidopsis: sequence characterization and basic expression analysis of the SCARECROW-LIKE genes. Plant J **18:** 111-119

**Qi T, Huang H, Wu D, Yan J, Qi Y, Song S, Xie D** (2014) Arabidopsis DELLA and JAZ proteins bind the WD-repeat/bHLH/MYB complex to modulate gibberellin and jasmonate signaling synergy. Plant Cell **26:** 1118-1133

**Rademacher EH, Offringa R** (2012) Evolutionary Adaptations of Plant AGC Kinases: From Light Signaling to Cell Polarity Regulation. Front Plant Sci **3:** 250

**Regnault T, Daviere JM, Wild M, Sakvarelidze-Achard L, Heintz D, Carrera Bergua E, Lopez Diaz I, Gong F, Hedden P, Achard P** (2015) The gibberellin precursor GA12 acts as a long-distance growth signal in Arabidopsis. Nat Plants **1:** 15073

**Rieu I, Ruiz-Rivero O, Fernandez-Garcia N, Griffiths J, Powers SJ, Gong F, Linhartova T, Eriksson S, Nilsson O, Thomas SG, Phillips AL, Hedden P** (2008) The gibberellin biosynthetic genes AtGA20ox1 and AtGA20ox2 act, partially redundantly, to promote growth and development throughout the Arabidopsis life cycle. Plant J **53:** 488-504

**Rizza A, Jones AM** (2018) The makings of a gradient: spatiotemporal distribution of gibberellins in plant development. Curr Opin Plant Biol **47:** 9-15

**Rizza A, Walia A, Lanquar V, Frommer WB, Jones AM** (2017) In vivo gibberellin gradients visualized in rapidly elongating tissues. Nat Plants **3:** 803-813

**Rodriguez RE, Ercoli MF, Debernardi JM, Breakfield NW, Mecchia MA, Sabatini M, Cools T, De Veylder L, Benfey PN, Palatnik JF** (2015) MicroRNA miR396 Regulates the Switch between Stem Cells and Transit-Amplifying Cells in Arabidopsis Roots. The Plant Cell **27:** 3354-3366

**Rodriguez RE, Mecchia MA, Debernardi JM, Schommer C, Weigel D, Palatnik JF** (2010) Control of cell proliferation in Arabidopsis thaliana by microRNA miR396. Development **137:** 103-112

**Saito H, Oikawa T, Hamamoto S, Ishimaru Y, Kanamori-Sato M, Sasaki-Sekimoto Y, Utsumi T, Chen J, Kanno Y, Masuda S, Kamiya Y, Seo M, Uozumi N, Ueda M, Ohta H** (2015) The jasmonate-responsive GTR1 transporter is required for gibberellin-mediated stamen development in Arabidopsis. Nat Commun **6:** 6095

**Salanenka Y, Verstraeten I, Lofke C, Tabata K, Naramoto S, Glanc M, Friml J** (2018) Gibberellin DELLA signaling targets the retromer complex to redirect protein trafficking to the plasma membrane. Proc Natl Acad Sci U S A **115:** 3716-3721

**Saldanha AJ** (2004) Java Treeview--extensible visualization of microarray data. Bioinformatics **20:** 3246-3248

**Sasse J, Simon S, Gubeli C, Liu GW, Cheng X, Friml J, Bouwmeester H, Martinoia E, Borghi L** (2015) Asymmetric localizations of the ABC transporter PaPDR1 trace paths of directional strigolactone transport. Curr Biol **25:** 647-655

**Scaffidi A, Waters MT, Sun YK, Skelton BW, Dixon KW, Ghisalberti EL, Flematti GR, Smith SM** (2014) Strigolactone Hormones and Their Stereoisomers Signal through Two Related Receptor Proteins to Induce Different Physiological Responses in Arabidopsis. Plant Physiol **165:** 1221-1232

**Schwechheimer C** (2014) Gibberellin - Mechanism of Action. eLS

**Seale M, Bennett T, Leyser O** (2017) BRC1 expression regulates bud activation potential but is not necessary or sufficient for bud growth inhibition in Arabidopsis. Development **144:** 1661-1673

**Serrano-Mislata A, Bencivenga S, Bush M, Schiessl K, Boden S, Sablowski R** (2017) DELLA genes restrict inflorescence meristem function independently of plant height. Nat Plants **3:** 749-754

**Shani E, Weinstain R, Zhang Y, Castillejo C, Kaiserli E, Chory J, Tsien RY, Estelle M** (2013) Gibberellins accumulate in the elongating endodermal cells of Arabidopsis root. Proc Natl Acad Sci U S A **110:** 4834-4839

**Shanmugabalaji V, Chahtane H, Accossato S, Rahire M, Gouzerh G, Lopez-Molina L, Kessler F** (2018) Chloroplast Biogenesis Controlled by DELLA-TOC159 Interaction in Early Plant Development. Curr Biol **28:** 2616-2623 e2615

**Shen H, Luong P, Huq E** (2007) The F-box protein MAX2 functions as a positive regulator of photomorphogenesis in Arabidopsis. Plant Physiol **145:** 1471-1483

**Shimada TL, Shimada T, Hara-Nishimura I** (2010) A rapid and non-destructive screenable marker, FAST, for identifying transformed seeds of Arabidopsis thaliana. Plant J **61:** 519-528

**Shinohara N, Taylor C, Leyser O** (2013) Strigolactone can promote or inhibit shoot branching by triggering rapid depletion of the auxin efflux protein PIN1 from the plasma membrane. PLoS Biol **11:** e1001474

**Silverstone AL, Jung HS, Dill A, Kawaide H, Kamiya Y, Sun TP** (2001) Repressing a repressor: gibberellin-induced rapid reduction of the RGA protein in Arabidopsis. Plant Cell **13:** 1555-1566

**Silverstone AL, Mak PY, Martinez EC, Sun TP** (1997) The new RGA locus encodes a negative regulator of gibberellin response in Arabidopsis thaliana. Genetics **146:** 1087-1099

**Soundappan I, Bennett T, Morffy N, Liang Y, Stanga JP, Abbas A, Leyser O, Nelson DC** (2015) SMAX1-LIKE/D53 Family Members Enable Distinct MAX2-Dependent Responses to Strigolactones and Karrikins in Arabidopsis. Plant Cell **27:** 3143-3159

**Stanga JP, Smith SM, Briggs WR, Nelson DC** (2013) SUPPRESSOR OF MORE AXILLARY GROWTH2 1 controls seed germination and seedling development in Arabidopsis. Plant Physiol **163:** 318-330

**Stirnberg P, van De Sande K, Leyser HM** (2002) MAX1 and MAX2 control shoot lateral branching in Arabidopsis. Development **129:** 1131-1141

**Stoddart JL, Tapster SM, Jones TW** (1978) Temperature dependence of the gibberellin response in lettuce hypocotyls. Planta **141:** 283-288

**Sun TP** (2011) The molecular mechanism and evolution of the GA-GID1-DELLA signaling module in plants. Current Biology **21:** R338-345

**Takeda N, Handa Y, Tsuzuki S, Kojima M, Sakakibara H, Kawaguchi M** (2015) Gibberellins interfere with symbiosis signaling and gene expression and alter colonization by arbuscular mycorrhizal fungi in Lotus japonicus. Plant Physiol **167:** 545-557

**Tal I, Zhang Y, Jorgensen ME, Pisanty O, Barbosa IC, Zourelidou M, Regnault T, Crocoll C, Olsen CE, Weinstain R, Schwechheimer C, Halkier BA, Nour-Eldin HH, Estelle M, Shani E** (2016) The Arabidopsis NPF3 protein is a GA transporter. Nat Commun **7:** 11486

**Tanaka Y, Nakamura S, Kawamukai M, Koizumi N, Nakagawa T** (2011) Development of a series of gateway binary vectors possessing a tunicamycin resistance gene as a marker for the transformation of Arabidopsis thaliana. Biosci Biotechnol Biochem **75:** 804-807

**Tang Y, Liu H, Guo S, Wang B, Li Z, Chong K, Xu Y** (2018) OsmiR396d Affects Gibberellin and Brassinosteroid Signaling to Regulate Plant Architecture in Rice. Plant Physiol **176:** 946-959

**Thomashow MF** (2010) Molecular basis of plant cold acclimation: insights gained from studying the CBF cold response pathway. Plant Physiol **154:** 571-577

**Tian C, Wan P, Sun S, Li J, Chen M** (2004) Genome-wide analysis of the GRAS gene family in rice and Arabidopsis. Plant Mol Biol **54:** 519-532

**Ubeda-Tomas S, Federici F, Casimiro I, Beemster GT, Bhalerao R, Swarup R, Doerner P, Haseloff J, Bennett MJ** (2009) Gibberellin signaling in the endodermis controls Arabidopsis root meristem size. Curr Biol **19:** 1194-1199

**Ueguchi-Tanaka M, Ashikari M, Nakajima M, Itoh H, Katoh E, Kobayashi M, Chow TY, Hsing YI, Kitano H, Yamaguchi I, Matsuoka M** (2005) GIBBERELLIN INSENSITIVE DWARF1 encodes a soluble receptor for gibberellin. Nature **437:** 693-698

**Ueguchi-Tanaka M, Nakajima M, Katoh E, Ohmiya H, Asano K, Saji S, Hongyu X, Ashikari M, Kitano H, Yamaguchi I, Matsuoka M** (2007) Molecular interactions of a soluble gibberellin receptor, GID1, with a rice DELLA protein, SLR1, and gibberellin. Plant Cell **19:** 2140-2155

**Ueguchi-Tanaka M, Nakajima M, Motoyuki A, Matsuoka M** (2007) Gibberellin receptor and its role in gibberellin signaling in plants. Annu Rev Plant Biol **58:** 183-198

**Umehara M, Cao M, Akiyama K, Akatsu T, Seto Y, Hanada A, Li W, Takeda-Kamiya N, Morimoto Y, Yamaguchi S** (2015) Structural Requirements of Strigolactones for Shoot Branching Inhibition in Rice and Arabidopsis. Plant Cell Physiol

**Umehara M, Hanada A, Yoshida S, Akiyama K, Arite T, Takeda-Kamiya N, Magome H, Kamiya Y, Shirasu K, Yoneyama K, Kyozuka J, Yamaguchi S** (2008) Inhibition of shoot branching by new terpenoid plant hormones. Nature **455:** 195-200

**Van De Velde K, Ruelens P, Geuten K, Rohde A, Van Der Straeten D** (2017) Exploiting DELLA Signaling in Cereals. Trends Plant Sci

**van der Knaap E, Kim JH, Kende H** (2000) A novel gibberellin-induced gene from rice and its potential regulatory role in stem growth. Plant Physiology **122:** 695-704

**Villaecija-Aguilar JA, Hamon-Josse M, Carbonnel S, Kretschmar A, Schmidt C, Dawid C, Bennett T, Gutjahr C** (2019) SMAX1/SMXL2 regulate root and root hair development downstream of KAI2-mediated signalling in Arabidopsis. PLoS Genet **15:** e1008327

**Waldie T, McCulloch H, Leyser O** (2014) Strigolactones and the control of plant development: lessons from shoot branching. Plant J **79:** 607-622

**Wang L, Gu X, Xu D, Wang W, Wang H, Zeng M, Chang Z, Huang H, Cui X** (2010) miR396-targeted AtGRF transcription factors are required for coordination of cell division and differentiation during leaf development in Arabidopsis. Journal of Experimental Botany **62:** 761-773

**Wang L, Wang B, Jiang L, Liu X, Li X, Lu Z, Meng X, Wang Y, Smith SM, Li J** (2015) Strigolactone Signaling in Arabidopsis Regulates Shoot Development by Targeting D53-Like SMXL Repressor Proteins for Ubiquitination and Degradation. Plant Cell **27:** 3128-3142

**Wang L, Wang B, Yu H, Guo H, Lin T, Kou L, Wang A, Shao N, Ma H, Xiong G, Li X, Yang J, Chu J, Li J** (2020) Transcriptional regulation of strigolactone signalling in Arabidopsis. Nature **583:** 277-281

**Wang L, Xu Q, Yu H, Ma H, Li X, Yang J, Chu J, Xie Q, Wang Y, Smith SM, Li J, Xiong G, Wang B** (2020) Strigolactone and Karrikin Signaling Pathways Elicit Ubiquitination and Proteolysis of SMXL2 to Regulate Hypocotyl Elongation in Arabidopsis thaliana. Plant Cell

**Wang Y, Zhao J, Lu W, Deng D** (2017) Gibberellin in plant height control: old player, new story. Plant Cell Rep **36:** 391-398

**Waters MT, Brewer PB, Bussell JD, Smith SM, Beveridge CA** (2012) The Arabidopsis ortholog of rice DWARF27 acts upstream of MAX1 in the control of plant development by strigolactones. Plant Physiol **159:** 1073-1085

**Waters MT, Nelson DC, Scaffidi A, Flematti GR, Sun YK, Dixon KW, Smith SM** (2012) Specialisation within the DWARF14 protein family confers distinct responses to karrikins and strigolactones in Arabidopsis. Development **139:** 1285-1295

**Wild M, Daviere JM, Regnault T, Sakvarelidze-Achard L, Carrera E, Lopez Diaz I, Cayrel A, Dubeaux G, Vert G, Achard P** (2016) Tissue-Specific Regulation of Gibberellin Signaling Fine-Tunes Arabidopsis Iron-Deficiency Responses. Dev Cell **37:** 190-200

**Willige BC, Ghosh S, Nill C, Zourelidou M, Dohmann EM, Maier A, Schwechheimer C** (2007) The DELLA domain of GA INSENSITIVE mediates the interaction with the GA INSENSITIVE DWARF1A gibberellin receptor of Arabidopsis. Plant Cell **19:** 1209-1220

**Willige BC, Isono E, Richter R, Zourelidou M, Schwechheimer C** (2011) Gibberellin regulates PIN-FORMED abundance and is required for auxin transport-dependent growth and development in Arabidopsis thaliana. Plant Cell **23:** 2184-2195

**Willige BC, Ogiso-Tanaka E, Zourelidou M, Schwechheimer C** (2012) WAG2 represses apical hook opening downstream from gibberellin and PHYTOCHROME INTERACTING FACTOR 5. Development **139:** 4020-4028

**Xie X, Yoneyama K, Yoneyama K** (2010) The strigolactone story. Annu Rev Phytopathol **48:** 93-117

**Xue H, Zhang Y, Xiao G** (2020) Neo-gibberellin Signaling: Guiding the Next Generation of the Green Revolution. Trends Plant Sci **25:** 520-522

**Yamaguchi S** (2008) Gibberellin metabolism and its regulation. Annu Rev Plant Biol **59:** 225-251

**Yamamoto Y, Hirai T, Yamamoto E, Kawamura M, Sato T, Kitano H, Matsuoka M, Ueguchi-Tanaka M** (2010) A rice gid1 suppressor mutant reveals that gibberellin is not always required for interaction between its receptor, GID1, and DELLA proteins. Plant Cell **22:** 3589-3602

**Yang DL, Yao J, Mei CS, Tong XH, Zeng LJ, Li Q, Xiao LT, Sun TP, Li J, Deng XW, Lee CM, Thomashow MF, Yang Y, He Z, He SY** (2012) Plant hormone jasmonate prioritizes defense over growth by interfering with gibberellin signaling cascade. Proc Natl Acad Sci U S A **109:** E1192-1200

**Yao R, Ming Z, Yan L, Li S, Wang F, Ma S, Yu C, Yang M, Chen L, Chen L, Li Y, Yan C, Miao D, Sun Z, Yan J, Sun Y, Wang L, Chu J, Fan S, He W, Deng H, Nan F, Li J, Rao Z, Lou Z, Xie D** (2016) DWARF14 is a non-canonical hormone receptor for strigolactone. Nature **536:** 469-473

**Yoshida H, Hirano K, Sato T, Mitsuda N, Nomoto M, Maeo K, Koketsu E, Mitani R, Kawamura M, Ishiguro S, Tada Y, Ohme-Takagi M, Matsuoka M, Ueguchi-Tanaka M** (2014) DELLA protein functions as a transcriptional activator through the DNA binding of the indeterminate domain family proteins. Proc Natl Acad Sci U S A **111:** 7861-7866

**Yoshida H, Ueguchi-Tanaka M** (2014) DELLA and SCL3 balance gibberellin feedback regulation by utilizing INDETERMINATE DOMAIN proteins as transcriptional scaffolds. Plant Signal Behav **9:** e29726

**Yoshida H, Ueguchi-Tanaka M, Matsuoka M** (2014) Regulatory Networks Acted Upon by the GID1-DELLA System After Perceiving Gibberellin. Enzymes **35:** 1-25

**Yu S, Galvao VC, Zhang YC, Horrer D, Zhang TQ, Hao YH, Feng YQ, Wang S, Schmid M, Wang JW** (2012) Gibberellin regulates the Arabidopsis floral transition through miR156-targeted SQUAMOSA promoter binding-like transcription factors. Plant Cell **24:** 3320-3332

**Zentella R, Hu J, Hsieh WP, Matsumoto PA, Dawdy A, Barnhill B, Oldenhof H, Hartweck LM, Maitra S, Thomas SG, Cockrell S, Boyce M, Shabanowitz J, Hunt DF, Olszewski NE, Sun TP** (2016) O-GlcNAcylation of master growth repressor DELLA by SECRET AGENT modulates multiple signaling pathways in Arabidopsis. Genes Dev **30:** 164-176

**Zentella R, Sui N, Barnhill B, Hsieh WP, Hu J, Shabanowitz J, Boyce M, Olszewski NE, Zhou P, Hunt DF, Sun TP** (2017) The Arabidopsis O-fucosyltransferase SPINDLY activates nuclear growth repressor DELLA. Nat Chem Biol **13:** 479-485

**Zhang ZL, Ogawa M, Fleet CM, Zentella R, Hu J, Heo JO, Lim J, Kamiya Y, Yamaguchi S, Sun TP** (2011) Scarecrow-like 3 promotes gibberellin signaling by antagonizing master growth repressor DELLA in Arabidopsis. Proc Natl Acad Sci U S A **108:** 2160-2165

**Zhao C, Zhang Z, Xie S, Si T, Li Y, Zhu JK** (2016) Mutational Evidence for the Critical Role of CBF Transcription Factors in Cold Acclimation in Arabidopsis. Plant Physiol **171:** 2744-2759

**Zhao LH, Zhou XE, Yi W, Wu Z, Liu Y, Kang Y, Hou L, de Waal PW, Li S, Jiang Y, Scaffidi A, Flematti GR, Smith SM, Lam VQ, Griffin PR, Wang Y, Li J, Melcher K, Xu HE** (2015) Destabilization of strigolactone receptor DWARF14 by binding of ligand and E3-ligase signaling effector DWARF3. Cell Res **25:** 1219-1236

**Zhou F, Lin Q, Zhu L, Ren Y, Zhou K, Shabek N, Wu F, Mao H, Dong W, Gan L, Ma W, Gao H, Chen J, Yang C, Wang D, Tan J, Zhang X, Guo X, Wang J, Jiang L, Liu X, Chen W, Chu J, Yan C, Ueno K, Ito S, Asami T, Cheng Z, Wang J, Lei C, Zhai H, Wu C, Wang H, Zheng N, Wan J** (2013) D14-SCF(D3)-dependent degradation of D53 regulates strigolactone signalling. Nature **504:** 406-410

**Zhou M, Chen H, Wei D, Ma H, Lin J** (2017) Arabidopsis CBF3 and DELLAs positively regulate each other in response to low temperature. Sci Rep **7:** 39819

# Acknowledgments

First, I would like to thank Prof. Dr. Claus Schwechheimer for the support in many levels throughout my PhD. For the opportunity that he gave me to join his lab and scientific guidance to do this exciting research. For all the amazing collaborations and opportunities to meet top scientists from the field. I also want to thank him for being the speaker of Sonderforschungsbereich 924 (SFB924), a collaboration network, which funded this work as well as the use of the latest next generation sequencing technologies that allowed high resolution in my investigations.

Also, special thanks to Prof. Dr. Caroline Gutjahr for being my mentor for the graduate school, for all the nice discussions, and for being in my exam committee.

Thank you to Prof. Dr. Aphrodite Kapurniotu for taking the time to be the president of the exam committee.

Next, I want to thank additional people that were essential for the work of this thesis. Pascal Falter-Braun for the collaboration on the GA and cold stress project and all his scientific input and technical help. Dr. Carina Klermund for providing the homozygous *ga1 max1-4* and *ga1 max3-9* double mutants, for helping me out with experimental protocols, and for all tips that she gave me in the lab.

Furthermore, I want to thank Dirk Inzé (VIB Ghent, Belgium) for providing 35S:GRF5 transgenic seeds, Javier Palatnik (Instituto de Biología Molecular y Celular de Rosario, Rosario, Argentina) for providing the 35S:miR396b transgenic seeds, Melina Altmann (Technische Universität München, Freising, Germany) for the SCR and SCL3 yeast two-hybrid vectors and Stefan Engelhardt (Technische Universität München, Freising, Germany) for the providing the BiFC vectors pCL112 and pCL113.

Special thanks to Angela Alkofer who executed an important experimental part of the yeast two hybrid screen and provided excellent support for the project.

Thank you to the secretaries of the chair of Plant Systems Biology Petra Wick and Daniela Elephand-Dill for all the technical support.

A big thank you to all my previous colleagues from the chair of Plant Systems Biology for all the scientific help, interesting discussions and good times we had together. Many thanks to previous lab members Uli, Thomas, Manolis, Eva, Benny and Hiro. Special thanks to Ines and Lana for all the help with microscope and cloning and the scientific discussions at the coffee break.

Thank you to Prof. Dr. Erika Isono for all her scientific input and for introducing me to the confocal microscope.

I also want to thank the Young Investigator group of the SFB924 for organizing meetings, courses, scientific sessions and discussions, excursions and nice Bavarian beer-drinking evenings!

Finally, special thank you to my family in Greece and especially my parents Keri and Andreas for supporting my education and choices and bringing me oregano to Germany! Final thank you to all my friends in Germany and elsewhere that were physically or mentally present during this time.

# 5. Appendix

## 5.1. Appendix I

| GO term ID | GO term | p-value (Holm-Bonferroni) |
|---|---|---|
| **GA3 DEGs (210)** | | |
| GO:0009739 | response to gibberellin | 2.97E-14 |
| GO:0009719 | response to endogenous stimulus | 4.16144E-06 |
| GO:0001101 | response to acid chemical | 4.48352E-06 |
| GO:0009725 | response to hormone | 8.55761E-06 |
| GO:0010033 | response to organic substance | 9.07091E-06 |
| GO:0009740 | gibberellic acid mediated signaling pathway | 1.00077E-05 |
| GO:0010476 | gibberellin mediated signaling pathway | 1.14306E-05 |
| GO:0071370 | cellular response to gibberellin stimulus | 1.48276E-05 |
| GO:0033993 | response to lipid | 3.06072E-05 |
| GO:1901700 | response to oxygen-containing compound | 3.60735E-05 |
| GO:0065007 | biological regulation | 0.000958481 |
| GO:0006355 | regulation of transcription, DNA-templated | 0.001794138 |
| GO:1903506 | regulation of nucleic acid-templated transcription | 0.002044645 |
| GO:2001141 | regulation of RNA biosynthetic process | 0.002044645 |
| GO:0051252 | regulation of RNA metabolic process | 0.002839661 |
| GO:0006351 | transcription, DNA-templated | 0.003745224 |
| GO:0009937 | regulation of gibberellic acid mediated signaling pathway | 0.00377791 |
| GO:0097659 | nucleic acid-templated transcription | 0.004647178 |
| GO:0019219 | regulation of nucleobase-containing compound metabolic process | 0.0053784 |
| GO:0032774 | RNA biosynthetic process | 0.005686791 |
| GO:0042221 | response to chemical | 0.008091375 |
| GO:0050789 | regulation of biological process | 0.017577278 |
| GO:0050794 | regulation of cellular process | 0.018447268 |
| GO:0032870 | cellular response to hormone stimulus | 0.019562345 |
| GO:0071495 | cellular response to endogenous stimulus | 0.021571887 |
| GO:0009755 | hormone-mediated signaling pathway | 0.021683409 |
| GO:2000112 | regulation of cellular macromolecule biosynthetic process | 0.023531916 |
| GO:0071229 | cellular response to acid chemical | 0.026392976 |
| GO:0010556 | regulation of macromolecule biosynthetic process | 0.027679024 |
| **GR24 DEGs (73)** | | |
| GO:0042221 | response to chemical | 0.011360743 |
| GO:0050896 | response to stimulus | 0.031378182 |
| **Only GA3 + GR24 DEGs (261)** | | |
| GO:0009719 | response to endogenous stimulus | 1.52E-07 |
| GO:0010033 | response to organic substance | 2.04E-07 |
| GO:0042221 | response to chemical | 5.55E-07 |
| GO:0050896 | response to stimulus | 5.89E-07 |
| GO:0006351 | transcription, DNA-templated | 8.13964E-06 |
| GO:0006355 | regulation of transcription, DNA-templated | 8.73737E-06 |
| GO:0009725 | response to hormone | 8.95313E-06 |
| GO:1903506 | regulation of nucleic acid-templated transcription | 1.0329E-05 |
| GO:2001141 | regulation of RNA biosynthetic process | 1.0329E-05 |
| GO:0010243 | response to organonitrogen compound * | 1.04173E-05 |
| GO:0097659 | nucleic acid-templated transcription | 1.08226E-05 |
| GO:0032774 | RNA biosynthetic process | 1.41432E-05 |
| GO:0051252 | regulation of RNA metabolic process | 1.57308E-05 |
| GO:0019219 | regulation of nucleobase-containing compound metabolic process | 3.57376E-05 |
| GO:1901700 | response to oxygen-containing compound | 8.36059E-05 |
| GO:0031326 | regulation of cellular biosynthetic process * | 0.000107749 |
| GO:0010200 | response to chitin * | 0.000107817 |
| GO:0009889 | regulation of biosynthetic process * | 0.000129751 |
| GO:0009723 | response to ethylene * | 0.000146056 |
| GO:0032870 | cellular response to hormone stimulus | 0.000165645 |
| GO:0071495 | cellular response to endogenous stimulus | 0.000188274 |
| GO:2000112 | regulation of cellular macromolecule biosynthetic process | 0.000239023 |

| | | |
|---|---|---|
| GO:0031323 | regulation of cellular metabolic process * | 0.000246162 |
| GO:0080090 | regulation of primary metabolic process * | 0.000254896 |
| GO:0010556 | regulation of macromolecule biosynthetic process | 0.000294693 |
| GO:0034654 | nucleobase-containing compound biosynthetic process * | 0.000423614 |
| GO:0018130 | heterocycle biosynthetic process * | 0.000562856 |
| GO:1901362 | organic cyclic compound biosynthetic process * | 0.000598727 |
| GO:0051171 | regulation of nitrogen compound metabolic process * | 0.000728878 |
| GO:1901698 | response to nitrogen compound * | 0.000743773 |
| GO:0019222 | regulation of metabolic process * | 0.000885976 |
| GO:0010468 | regulation of gene expression * | 0.001163959 |
| GO:0071310 | cellular response to organic substance * | 0.001170814 |
| GO:0009751 | response to salicylic acid * | 0.001304709 |
| GO:0000160 | phosphorelay signal transduction system * | 0.001391592 |
| GO:0070887 | cellular response to chemical stimulus * | 0.002355248 |
| GO:0060255 | regulation of macromolecule metabolic process * | 0.003770975 |
| GO:0019438 | aromatic compound biosynthetic process * | 0.00490776 |
| GO:0009755 | hormone-mediated signaling pathway | 0.006944708 |
| GO:0071369 | cellular response to ethylene stimulus * | 0.012235306 |
| GO:0065007 | biological regulation | 0.014188383 |
| GO:0001101 | response to acid chemical | 0.021149231 |
| GO:0009873 | ethylene-activated signaling pathway * | 0.025195978 |
| GO:0050789 | regulation of biological process | 0.037532225 |
| GO:0050794 | regulation of cellular process | 0.046869233 |

## 5.2. Appendix II

| Feature ID | Name | Type | Technique | Reference showing interaction | Identified in Y2H screen | Present in UCSD collection |
|---|---|---|---|---|---|---|
| AT1G01030 | NGA3 | ABI3-VP1 | Y2H library | this study | Yes | Yes |
| AT1G01090 | PDH-E1 ALPHA | subunit of pyruvate dehydrogenase complex | Y2H library | Arabidopsis Interactome Mapping Consortium, 2011 | No | No |
| AT1G02340 | HFR1 | bHLH | Y2H library | this study | Yes | Yes |
| AT1G03040 | AT1G03040 | bHLH | Y2H library | this study | Yes | Yes |
| AT1G03150 | AT1G03150 | GNAT | Y2H library | this study | Yes | Yes |
| AT1G03840 | IDD3/MGP | C2H2 Zinc-finger TF | Y2H, BiFC, pull-down | Fukazawa et al., 2014; Yoshida et al., 2014 | Yes | Yes |
| AT1G06040 | BBX24/STO | double B-box type zinc finger protein | Y2H, BiFC, co-IP | Crocco et al., 2015 | No | Yes |
| AT1G06170 | bHLH89 | TF | Y2H library | Marín-de la Rosa et al., 2014 | Yes | Yes |
| AT1G07360 | MAC5A | C3H | Y2H library | this study | Yes | Yes |
| AT1G08010 | GATA11 | C2C2-GATA | Y2H library | this study | Yes | Yes |
| AT1G08970 | NF-YC9 | TF | Y2H (DELLA@AD), pull-down, BiFC, co-IP | Hou et al., 2014; Liu et al., 2016 | No | Yes |
| AT1G09530 | PIF3 | bHLH TF | Y2H library, BiFC, pull-down, co-IP | Feng et al., 2008; Marín-de la Rosa et al., 2014 | No | Yes |
| AT1G09540 | MYB61 | TF | Y2H library | Marín-de la Rosa et al., 2014 | Yes | Yes |
| AT1G10585 | F4I4E1 | | Y2H library | Lumba et al., 2014 | No | Yes |
| AT1G12980 | DRN/ESR1 | TF | Y2H library | Marín-de la Rosa et al., 2014 | Yes | Yes |
| AT1G14030 | LSMT-L | SET / PcG | Y2H library | this study | Yes | Yes |
| AT1G14687 | HB32 | zf-HD | Y2H library | this study | Yes | Yes |
| AT1G14920 | GAI | GRAS | Y2H library | this study | Yes | Yes |
| AT1G17590 | NF-YA8 | CCAAT / CCAAT-HAP2 / CBFB_NFYA | Y2H library | this study | Yes | Yes |
| AT1G18400 | BEE1 | bHLH | Y2H library | this study | Yes | Yes |
| AT1G19180 | JAZ1/TIFY10A | JA ZIM-domain protein | Y2H, BiFC, pull-down, co-IP | Hou et al., 2010 | Yes | Yes |
| AT1G19210 | DREB (A-5)/ERF017 | TF | Y2H library | Marín-de la Rosa et al., 2014 | No | Yes |
| AT1G19350 | BES1 | TF | Y2H (full-length DELLA@AD), BiFC | Bai et al., 2012; Li et al., 2012 | No | Yes |
| AT1G20910 | AT1G20910 | ARID | Y2H library | this study | Yes | Yes |
| AT1G21700 | SWI3C | (SWI)/Sucrose Nonfermenting | BiFC, pull-down | Sarnowska et al., 2013 | Yes | Yes |
| AT1G21970 | LEC1 | CCAAT / CCAAT-HAP3 | Y2H library | this study | Yes | Yes |
| AT1G22070 | TGA3 | bZIP | Y2H library | this study | Yes | Yes |
| AT1G22160 | Q8VY80 | Putative uncharacterized protein | Y2H library | Arabidopsis Interactome Mapping Consortium, 2011 | No | No |
| AT1G22490 | AT1G22490 | bHLH | Y2H library | this study | Yes | Yes |

| | | | | | | |
|---|---|---|---|---|---|---|
| AT1G66140 | ZFP4 | C2H2 | Y2H library | this study | Yes | Yes |
| AT1G66370 | MYB113 | MYB | Y2H library | this study | Yes | Yes |
| AT1G67030 | ZFP6 | C2H2 | Y2H library | this study | Yes | Yes |
| AT1G67260 | TCP1 | class I TCP TF | Y2H library | Marín-de la Rosa et al., 2014 | Yes | Yes |
| AT1G68030 | AT1G68030 | PHD | Y2H library | this study | Yes | Yes |
| AT1G68130 | IDD14 | C2H2 | Y2H library | this study | Yes | Yes |
| AT1G68360 | AT1G68360 | C2H2 | Y2H library | this study | Yes | Yes |
| AT1G68510 | LBD42 | LOB / AS2 | Y2H library | this study | Yes | Yes |
| AT1G68670 | AT1G68670 | G2-like | Y2H library | this study | Yes | Yes |
| AT1G68810 | AT1G68810 | bHLH | Y2H library | this study | Yes | Yes |
| AT1G68920 | bHLH49 | TF | Y2H library | Marín-de la Rosa et al., 2014 | Yes | Yes |
| AT1G69170 | SPL6 | TF | Y2H library | Marín-de la Rosa et al., 2014 | No | Yes |
| AT1G69560 | MYB105 | MYB | Y2H library | this study | Yes | Yes |
| AT1G69570 | AT1G69570 | C2C2-DOF | Y2H library | this study | Yes | Yes |
| AT1G69690 | TCP15 | class I TCP TF | Y2H, Y2H library | Daviere et al., 2014; Marín-de la Rosa et al., 2014 | Yes | Yes |
| AT1G69810 | WRKY36 | Probable WRKY transcription factor 36 | Y2H library | Arabidopsis Interactome Mapping Consortium, 2011 | Yes | Yes |
| AT1G70000 | MYBD | TF | Y2H library | Marín-de la Rosa et al., 2014 | No | Yes |
| AT1G70700 | JAZ9/TIFY7 | JA ZIM-domain protein | Y2H (DELLA@AD), co-IP | Hou et al., 2010; Yang et al., 2012 | Yes | Yes |
| AT1G72010 | TCP22 | class I TCP TF | Y2H | Davière et al., 2014 | No | Yes |
| AT1G72030 | AT1G72030 | GNAT | Y2H library | this study | Yes | Yes |
| AT1G72210 | AT1G72210 | bHLH | Y2H library | this study | Yes | Yes |
| AT1G72570 | AT1G72570 | AP2-EREBP | Y2H library | this study | Yes | Yes |
| AT1G73360 | HDG11 | HB | Y2H library | this study | Yes | Yes |
| AT1G74950 | TIFY10B | ZIM | Y2H library | this study | Yes | Yes |
| AT1G75080 | BZR1 | TF | Y2H (DELLA@AD), BiFC, pull-down, co-IP | Bai et al., 2012; Gallego-Bartolomé et al., 2012; Li et al., 2012 | Yes | Yes |
| AT1G77200 | AT1G77200 | AP2-EREBP | Y2H library | this study | Yes | Yes |
| AT1G79110 | BRG2 | RING domain protein | Y2H (full-length DNA, but GAL4 AD), pull-down | Park et al., 2013 | No | No |
| AT1G80670 | RAE1 | nucleoporin | co-IP (followed by MS/MS) | Tamura et al., 2010 | No | No |
| AT2G01760 | ARR14 | Type-b GARP-ARR | Y2H | Marin-de la Rosa et al., 2015 | No | Yes |
| AT2G02070 | IDD5 | C2H2 Zinc-finger TF | Y2H, BiFC | Fukazawa et al., 2014; Yoshida et al., 2014 | No | Yes |
| AT2G02080 | IDD4 | C2H2 Zinc-finger TF | Y2H, BiFC | Fukazawa et al., 2014; Yoshida et al., 2014 | No | Yes |
| AT2G02450 | LOV1 | NAC | Y2H library | this study | Yes | Yes |
| AT2G02540 | HB21 | zf-HD | Y2H library | this study | Yes | Yes |

| | | | | | | |
|---|---|---|---|---|---|---|
| AT1G23420 | INO | C2C2-YABBY | Y2H library | this study | Yes | Yes |
| AT1G24590 | DRNL | AP2-EREBP | Y2H library | this study | Yes | Yes |
| AT1G26780 | MYB117 | MYB | Y2H library | this study | Yes | Yes |
| AT1G27360 | SPL11 | TF | Y2H (full-length DELLA@AD) | Yu et al., 2012 | No | Yes |
| AT1G27370 | SPL10 | TF | Y2H (full-length DELLA@AD) | Yu et al., 2012 | No | Yes |
| AT1G28160 | AT1G28160 | AP2-EREBP | Y2H library | this study | Yes | Yes |
| AT1G30330 | ARF6 | TF | Y2H, pull-down, co-IP | Oh et al., 2014 | No | No |
| AT1G30490 | PHV | HB | Y2H library | this study | Yes | Yes |
| AT1G30970 | SUF4 | C2H2 | Y2H library | this study | Yes | Yes |
| AT1G31630 | AGL86 | TF | Y2H library | Marín-de la Rosa et al., 2014 | Yes | Yes |
| AT1G32240 | KAN2 | G2-like | Y2H library | this study | Yes | Yes |
| AT1G32640 | MYC2 | bHLH TF | Y2H, co-IP | Hong et al., 2012 | Yes | Yes |
| AT1G35560 | TCP23 | class I TCP TF | Y2H, Y2H library | Davière et al., 2014; Marín-de la Rosa et al., 2014 | No | Yes |
| AT1G43160 | RAP2.6 | AP2-EREBP | Y2H library | this study | Yes | Yes |
| AT1G44830 | AT1G44830 | AP2-EREBP | Y2H library | this study | Yes | Yes |
| AT1G48150 | AT1G48150 | MADS | Y2H library | this study | Yes | Yes |
| AT1G48500 | JAZ4 | JA ZIM-domain protein | Y2H (full-length DELLA@AD) | Yang et al., 2012 | No | Yes |
| AT1G50420 | SCL3 | GRAS TF | Y2H ( full-length DELLA@AD, pull-down, co-IP | Zhang et al., 2011 | No | Yes |
| AT1G51600 | ZML2 | C2C2-GATA / ZIM / CCT | Y2H library | this study | Yes | Yes |
| AT1G53170 | ERF8/EREBP-8 | transcription factor | Y2H library | Lumba et al., 2014 | No | Yes |
| AT1G53230 | TCP3 | class I TCP TF | Y2H library | Marín-de la Rosa et al., 2014 | Yes | Yes |
| AT1G53510 | MPK18 | kinase | Y2H | Arabidopsis Interactome Mapping Consortium, 2011 | No | No |
| AT1G53910 | RAP2.12 | TF | Y2H | Marín-de la Rosa et al., 2014 | No | Yes |
| AT1G54160 | NF-YA5 | HAP2 / | Y2H library | this study | Yes | Yes |
| AT1G54830 | NF-YC3 | TF | Y2H (full-length DELLA@AD), pull-down | Hou et al., 2014; Liu et al., 2016 | No | Yes |
| AT1G56010 | NAC1 | NAC | Y2H library | this study | Yes | Yes |
| AT1G58100 | TCP8 | class I TCP TF | Y2H, Y2H library | Davière et al., 2014; Marín-de la Rosa et al., 2014 | Yes | Yes |
| AT1G60670 | Q94AP2 | Putative uncharacterized protein | Y2H library | Arabidopsis Interactome Mapping Consortium, 2011 | No | No |
| AT1G61660 | AT1G61660 | bHLH | Y2H library | this study | Yes | Yes |
| AT1G62150 | AT1G62150 | mTERF | Y2H library | this study | Yes | Yes |
| AT1G62300 | WRKY6 | WRKY | Y2H library | this study | Yes | Yes |
| AT1G63650 | EGL3 | bHLH TF | Y2H, BiFC, pull-down | Qi et al., 2014 | No | Yes |

| | | | | | | |
|---|---|---|---|---|---|---|
| AT2G11810 | MGD3 | | Y2H library | Lumba et al., 2014 | No | No |
| AT2G13960 | AT2G13960 | MYB-related | Y2H library | this study | Yes | Yes |
| AT2G18160 | bZIP2 | bZIP | Y2H library | this study | Yes | Yes |
| AT2G18300 | HBI1 | bHLH | Y2H library | this study | Yes | Yes |
| AT2G18350 | HB24 | zf-HD | Y2H library | this study | Yes | Yes |
| AT2G20180 | PIL5 | bHLH TF | Y2H | Gallego-Bartolomé et al., 2010 | Yes | Yes |
| AT2G20350 | AT2G20350 | AP2-EREBP | Y2H library | this study | Yes | Yes |
| AT2G20570 | GPRI1 | G2-like | Y2H library | this study | Yes | Yes |
| AT2G20880 | ERF53 | AP2-EREBP | Y2H library | this study | Yes | Yes |
| AT2G22750 | bHLH18 | TF | Y2H library | Marín-de la Rosa et al., 2014 | No | Yes |
| AT2G22800 | HAT9 | HB | Y2H library | this study | Yes | Yes |
| AT2G22840 | GRF1 | GRF | Y2H library | this study | Yes | Yes |
| AT2G23760 | BLH4 | HB | Y2H library | this study | Yes | Yes |
| AT2G25000 | WRKY60 | WRKY | Y2H library | this study | Yes | Yes |
| AT2G25170 | PKL | CHD3 type chromatin | Y2H (full-length DELLA@AD), pull- | Zhang et al., 2014 | No | No |
| AT2G25650 | AT2G25650 | GeBP | Y2H library | this study | Yes | Yes |
| AT2G27050 | EIL1 | TF | Y2H | An et al., 2012 | No | Yes |
| AT2G27230 | LHW | bHLH | Y2H library | this study | Yes | Yes |
| AT2G28160 | FIT | bHLH TF | Y2H, FRET-FLIM, co-IP (tobacco & At) | Wild et al., 2016 | No | Yes |
| AT2G28550 | TOE1 | TF | Y2H library | Marín-de la Rosa et al., 2014 | Yes | Yes |
| AT2G28610 | PRS | HB | Y2H library | this study | Yes | Yes |
| AT2G28810 | AT2G28810 | C2C2-DOF | Y2H library | this study | Yes | Yes |
| AT2G28910 | CXIP4 | TF | Y2H library | Marín-de la Rosa et al., 2014 | Yes | Yes |
| AT2G30340 | LBD13 | LOB / AS2 | Y2H library | this study | Yes | Yes |
| AT2G30360 | CIPK11 | kinase | Y2H library | Lumba et al., 2014 | No | No |
| AT2G30470 | HSI2 | ABI3-VP1 | Y2H library | this study | Yes | Yes |
| AT2G31070 | TCP10 | class I TCP TF | Y2H library | Marín-de la Rosa et al., 2014 | Yes | Yes |
| AT2G31180 | MYB14 | MYB | Y2H library | this study | Yes | Yes |
| AT2G31210 | bHLH91 | TF | Y2H library | Marín-de la Rosa et al., 2014 | Yes | Yes |
| AT2G31380 | STH/BBX25 | TF | Y2H library | Marín-de la Rosa et al., 2014 | No | Yes |
| AT2G32700 | LUH | LUG | Y2H library | this study | Yes | Yes |
| AT2G33070 | NSP2 | TF | BiFC, co-IP | Fonouni-Farde et al., 2016 | No | No |
| AT2G33835 | FES1 | C3H | Y2H library | this study | Yes | Yes |
| AT2G33860 | ETT | ARF | Y2H library | this study | Yes | Yes |
| AT2G33880 | STIMPY/WOX9 | TF | Y2H library | Marín-de la Rosa et al., 2014 | No | Yes |
| AT2G34600 | JAZ7 | ZIM | Y2H library | this study | Yes | Yes |
| AT2G35000 | ATL9 | ND | Y2H library | this study | Yes | Yes |

| | | | | | | |
|---|---|---|---|---|---|---|
| AT2G35940 | BLH1 | HB | Y2H library | this study | Yes | Yes |
| AT2G36270 | ABI5 | TF | co-IP (*in vitro* & *in vivo*) | Lim et al., 2013 | No | Yes |
| AT2G36400 | GRF3 | GRF | Y2H library, BiFC | this study | Yes | Yes |
| AT2G36990 | SIGF | RNApolymerase sigma-subunit F | Y2H library | Arabidopsis Interactome Mapping Consortium, 2011 | No | Yes |
| AT2G37590 | DOF2.4 | C2C2-DOF | Y2H library | this study | Yes | Yes |
| AT2G38300 | AT2G38300 | G2-like | Y2H library | this study | Yes | Yes |
| AT2G40260 | AT2G40260 | G2-like | Y2H library | this study | Yes | Yes |
| AT2G40620 | AT2G40620 | bZIP | Y2H library | this study | Yes | Yes |
| AT2G41370 | BOP2 | TRAF | Y2H library | this study | Yes | Yes |
| AT2G41710 | AT2G41710 | AP2-EREBP | Y2H library | this study | Yes | Yes |
| AT2G41940 | ZFP8 | TF | Y2H library | Marín-de la Rosa et al., 2014 | No | Yes |
| AT2G42200 | SPL9 | TF | Y2H (full-length DELLA@AD), BiFC, co-IP | Yu et al., 2012 | No | Yes |
| AT2G42280 | FBH4 | TF | Y2H library | Marín-de la Rosa et al., 2014 | Yes | Yes |
| AT2G43000 | ANAC042/JUB1 | TF | Y2H library | Marín-de la Rosa et al., 2014 | Yes | Yes |
| AT2G43010 | PIF4 | bHLH TF | Y2H, Y2H library, BiFC, pull-down, co-IP | de Lucas et al., 2008; Marín-de la Rosa et al., 2014 | No | Yes |
| AT2G44840 | ERF13 | AP2-EREBP | Y2H library | this study | Yes | Yes |
| AT2G44910 | HB4 | HB | Y2H library | this study | Yes | Yes |
| AT2G45160 | SCL27 | GRAS TF | Y2H (full-length DELLA@AD), BiFC, co-IP | Ma et al., 2014 | No | Yes |
| AT2G45190 | AFO | C2C2-YABBY | Y2H library | this study | Yes | Yes |
| AT2G45480 | GRF9 | GRF | Y2H library | this study | Yes | Yes |
| AT2G45680 | TCP9 | class I TCP TF | Y2H | Davière et al., 2014 | Yes | Yes |
| AT2G46970 | PIL1 | bHLH | Y2H library | this study | Yes | Yes |
| AT3G01890 | AT3G01890 | SWI/SNF-BAF60b | Y2H library | this study | Yes | Yes |
| AT3G02140 | AFP4/TMAC2 | Ninja-family protein | Y2H library | Lumba et al., 2014 | No | No |
| AT3G02150 | TCP13 | class I TCP TF | Y2H library | Marín-de la Rosa et al., 2014 | Yes | Yes |
| AT3G04030 | MYR2 | G2-like | Y2H library | this study | Yes | Yes |
| AT3G04450 | AT3G04450 | G2-like | Y2H library | this study | Yes | Yes |
| AT3G05625 | Q8GUK5 | Putative uncharacterized protein | Y2H library | Arabidopsis Interactome Mapping Consortium, 2011 | No | No |
| AT3G05690 | NF-YA2 | TF | Y2H, BiFC, but pull-down did not confirm | Hou et al., 2014 | Yes | Yes |
| AT3G05800 | AIF1 | bHLH | Y2H library | this study | Yes | Yes |
| AT3G07740 | ADA2A | MYB-related / SWIRM | Y2H library | this study | Yes | Yes |
| AT3G10480 | ANAC050 | TF | Y2H library | Marín-de la Rosa et al., 2014 | Yes | Yes |
| AT3G11100 | AT3G11100 | TRIHELIX | Y2H library | this study | Yes | Yes |

| | | | | | | |
|---|---|---|---|---|---|---|
| AT3G11440 | MYB65 | MYB | Y2H library | this study | Yes | Yes |
| AT3G12910 | NAC/NAM (MGH6.1) | TF | Y2H library | Marín-de la Rosa et al., 2014 | Yes | Yes |
| AT3G12920 | BRG3 | RING domain protein | Y2H (full-length DNA, but GAL4 AD), pull-down | Park et al., 2013 | No | No |
| AT3G13040 | myb-like HTH | TF | Y2H library | Marín-de la Rosa et al., 2014 | No | Yes |
| AT3G13740 | RNC4/MMM17.15 | | Y2H library | Arabidopsis Interactome Mapping Consortium, 2011 | No | No |
| AT3G13960 | GRF5 | GRF | Y2H library, BiFC | this study | Yes | Yes |
| AT3G15170 | CUC1 | NAC | Y2H library | this study | Yes | Yes |
| AT3G15270 | SPL5 | TF | Y2H library | Marín-de la Rosa et al., 2014 | No | Yes |
| AT3G15510 | AtNAC2/ANAC056 | TF | Y2H library | Marín-de la Rosa et al., 2014 | Yes | Yes |
| AT3G16160 | AT3G16160 | CPP | Y2H library | this study | Yes | Yes |
| AT3G16250 | PNSB3 | | Y2H library | Arabidopsis Interactome Mapping Consortium, 2011 | No | No |
| AT3G16770 | RAP2.3 | TF | Y2H, co-IP | Marin-de la Rosa et al., 2014 | Yes | Yes |
| AT3G16857 | ARR1 | Type-b GARP-ARR | Y2H, BiFC, co-IP | Marin-de la Rosa et al., 2015 | Yes | Yes |
| AT3G17860 | JAZ3/TIFY6B | JA ZIM-domain protein | Y2H (DELLA@AD) | Hou et al., 2010; Yang et al., 2012 | No | Yes |
| AT3G18550 | BRC1 | TCP | Y2H library | this study | Yes | Yes |
| AT3G18650 | AGL103 | MADS | Y2H library | this study | Yes | Yes |
| AT3G20310 | ERF7 | AP2-EREBP | Y2H library | this study | Yes | Yes |
| AT3G20640 | AT3G20640 | ND | Y2H library | this study | Yes | Yes |
| AT3G20770 | EIN3 | TF | Y2H, co-IP | An et al., 2012 | No | Yes |
| AT3G21175 | ZML1 | C2C2-GATA / ZIM / CCT | Y2H library | this study | Yes | Yes |
| AT3G21330 | bHLH87 | TF | Y2H library | Marín-de la Rosa et al., 2014 | Yes | Yes |
| AT3G23130 | SUP | C2H2 | Y2H library | this study | Yes | Yes |
| AT3G24120 | AT3G24120 | G2-like | Y2H library | this study | Yes | Yes |
| AT3G24310 | MYB305 | MYB | Y2H library | this study | Yes | Yes |
| AT3G24650 | ABI3 | TF | co-IP (*in vitro* & *in vivo*) | Lim et al., 2013 | No | Yes |
| AT3G24660 | TMKL1 | kinase | Y2H library | Lalonde et al., 2010 | No | No |
| AT3G25710 | BHLH32 | bHLH | Y2H library | this study | Yes | Yes |
| AT3G25790 | AT3G25790 | G2-like | Y2H library | this study | Yes | Yes |
| AT3G27010 | TCP20 | class I TCP TF | Y2H | Davière et al., 2014 | Yes | Yes |
| AT3G27920 | GL1 | MYB factor | Y2H, BiFC, pull-down | Qi et al., 2014 | No | Yes |
| AT3G28910 | MYB30 | MYB | Y2H library | this study | Yes | Yes |
| AT3G29035 | ANAC059 | TF | Y2H library | Marín-de la Rosa et al., 2014 | Yes | Yes |
| AT3G45150 | TCP16 | class I TCP TF | Y2H library | Marín-de la Rosa et al., 2014 | Yes | Yes |
| AT3G47500 | CDF3 | C2C2-DOF | Y2H library | this study | Yes | Yes |

| | | | | | | |
|---|---|---|---|---|---|---|
| AT3G47620 | TCP14 | class I TCP TF | Y2H, Y2H library, BiFC, co-IP, FRET-FLIM | Daviere et al., 2014; Marín-de la Rosa et al., 2014; Resentini et al., 2015 | No | Yes |
| AT3G48510 | T8P19.20 | Putative uncharacterized protein | Y2H library | Lumba et al., 2014 | No | No |
| AT3G49690 | MYB84 | MYB | Y2H library | this study | Yes | Yes |
| AT3G49760 | bZIP5 | bZIP | Y2H library | this study | Yes | Yes |
| AT3G50330 | HEC2 | bHLH | Y2H library | this study | Yes | Yes |
| AT3G50510 | LBD28 | LOB / AS2 | Y2H library | this study | Yes | Yes |
| AT3G50700 | IDD2/GAF1 | C2H2 Zinc-finger TF | Y2H (full-length + Tup), BiFC, pull-down | Fukazawa et al., 2014 | Yes | Yes |
| AT3G51180 | C3H45 | Zinc-finger TF | Y2H library | Arabidopsis Interactome Mapping Consortium, 2011 | Yes | Yes |
| AT3G51260 | PAD1 | 20S proteasome alpha subunit | Y2H library | Arabidopsis Interactome Mapping Consortium, 2011 | No | No |
| AT3G52250 | AT3G52250 | MYB | Y2H library | this study | Yes | Yes |
| AT3G53310 | AT3G53310 | ABI3-VP1 | Y2H library | this study | Yes | Yes |
| AT3G54220 | SCR | GRAS | Y2H library | this study | Yes | Yes |
| AT3G54390 | AT3G54390 | TRIHELIX | Y2H library | this study | Yes | Yes |
| AT3G54620 | BZIP25 | bZIP | Y2H library | this study | Yes | Yes |
| AT3G54990 | SMZ | AP2-EREBP | Y2H library | this study | Yes | Yes |
| AT3G55730 | MYB109 | MYB | Y2H library | this study | Yes | Yes |
| AT3G56970 | bHLH 38 | bHLH TF | Y2H, FRET-FLIM | Wild et al., 2016 | No | Yes |
| AT3G56980 | bHLH 39 | bHLH TF | Y2H, FRET-FLIM | Wild et al., 2016 | No | Yes |
| AT3G57600 | DREB (A-2)/DREB2F | TF | Y2H library | Marín-de la Rosa et al., 2014 | Yes | Yes |
| AT3G57920 | SPL15 | TF | Y2H (full-length DELLA@AD), co-IP | Hyun et al., 2016 | No | Yes |
| AT3G58070 | GIS | C2H2 | Y2H library | this study | Yes | Yes |
| AT3G60390 | HAT3 | HB | Y2H library | this study | Yes | Yes |
| AT3G60630 | SCL22 | GRAS TF | Y2H (full-length DELLA@AD) | Ma et al., 2014 | No | Yes |
| AT3G61850 | DOF | DOF TF | Y2H (full-length DELLA@AD) | Boccaccini et al., 2014 | No | Yes |
| AT3G62090 | PIL2 | bHLH TF | Y2H | Gallego-Bartolomé et al., 2010 | No | No |
| AT4G00050 | UNE10 | TF | Y2H library | Marín-de la Rosa et al., 2014 | Yes | Yes |
| AT4G00980 | Q8GXX5 | Putative uncharacterized protein | Y2H library | Arabidopsis Interactome Mapping Consortium, 2011 | No | No |
| AT4G01500 | NGA4 | ABI3-VP1 | Y2H library | this study | Yes | Yes |
| AT4G01680 | MYB55 | MYB | Y2H library | this study | Yes | Yes |
| AT4G01720 | WRKY47 | WRKY | Y2H library | this study | Yes | Yes |
| AT4G02590 | UNE12 | bHLH | Y2H library | this study | Yes | Yes |
| AT4G02670 | IDD12 | C2H2 | Y2H library | this study | Yes | Yes |
| AT4G03250 | HDZIP | TF | Y2H library | Marín-de la Rosa et al., 2014 | Yes | Yes |

| | | | | | | |
|---|---|---|---|---|---|---|
| AT4G04450 | WRKY42 | WRKY | Y2H library | this study | Yes | Yes |
| AT4G04770 | ABCI8 | ATPase | Y2H library | Arabidopsis Interactome Mapping Consortium, 2011 | No | No |
| AT4G04885 | PCFS4 | C2H2 | Y2H library | this study | Yes | Yes |
| AT4G04890 | PDF2 | HD-ZIP TF | Y2H (full-length DELLA@BD), BiFC | Rombolá-Caldentey et al., 2014 | No | Yes |
| AT4G05170 | AT4G05170 | bHLH | Y2H library | this study | Yes | Yes |
| AT4G08150 | KNAT1 | HB | Y2H library | this study | Yes | Yes |
| AT4G13640 | UNE16 | G2-like | Y2H library | this study | Yes | Yes |
| AT4G14713 | PPD1 | ZIM | Y2H library | this study | Yes | Yes |
| AT4G14720 | AT4G14720 | ZIM | Y2H library | this study | Yes | Yes |
| AT4G16110 | ARR2 | Type-b GARP-ARR | Y2H | Marin-de la Rosa et al., 2015 | No | No |
| AT4G16750 | DREB (A-4)/ERF039 | TF | Y2H library | Marín-de la Rosa et al., 2014 | No | Yes |
| AT4G16780 | HB-2 | HB | Y2H library | this study | Yes | Yes |
| AT4G17460 | HAT1 | TF | Y2H library | Marín-de la Rosa et al., 2014 | Yes | Yes |
| AT4G17490 | ERF6 | AP2-EREBP | Y2H library | this study | Yes | Yes |
| AT4G17695 | KAN3 | G2-like | Y2H library | this study | Yes | Yes |
| AT4G18170 | WRKY28 | WRKY | Y2H library | this study | Yes | Yes |
| AT4G18390 | TCP2 | class I TCP TF | Y2H library | Marín-de la Rosa et al., 2014 | No | Yes |
| AT4G18430 | RABA1E | | Y2H library | Lumba et al., 2014 | No | No |
| AT4G19700 | BOI | RING domain protein | Y2H (full-lengthDELLA@AD), pull-down, co-IP | Park et al., 2013 | No | No |
| AT4G20150 | Q94AL6 | Putative uncharacterized protein | Y2H library | Arabidopsis Interactome Mapping Consortium, 2011 | No | No |
| AT4G21040 | DOF 4.3 | TF | Y2H library | Marín-de la Rosa et al., 2014 | Yes | Yes |
| AT4G21080 | DOF4.5 | C2C2-DOF | Y2H library | this study | Yes | Yes |
| AT4G21340 | B70 | ND | Y2H library | this study | Yes | Yes |
| AT4G21750 | ML1 | HD-ZIP TF | Y2H (full-length DELLA@BD), BiFC | Rombolá-Caldentey et al., 2014 | No | No |
| AT4G22070 | WRKY31 | WRKY | Y2H library | this study | Yes | Yes |
| AT4G22360 | AT4G22360 | SWI/SNF-BAF60b | Y2H library | this study | Yes | Yes |
| AT4G23050 | F7H19.240 | Putative serine/threonine kinase | Y2H library | Lumba et al., 2014 | No | No |
| AT4G24540 | AGL24 | MADS | Y2H library | this study | Yes | Yes |
| AT4G24960 | HVA22D | | Y2H library | Lumba et al., 2014 | No | No |
| AT4G25410 | AT4G25410 | bHLH | Y2H library | this study | Yes | Yes |
| AT4G27330 | SPL | NOZZLE / NZZ | Y2H library | this study | Yes | Yes |
| AT4G27410 | RD26 | NAC | Y2H library | this study | Yes | Yes |
| AT4G29100 | AT4G29100 | ND | Y2H library | this study | Yes | Yes |
| AT4G30080 | ARF16 | ARF | Y2H library | this study | Yes | Yes |
| AT4G31060 | AT4G31060 | AP2-EREBP | Y2H library | this study | Yes | Yes |
| AT4G32010 | HSL1 | ABI3-VP1 | Y2H library | this study | Yes | Yes |

| | | | | | | |
|---|---|---|---|---|---|---|
| AT4G32570 | TIFY8 | ZIM | Y2H library | this study | Yes | Yes |
| AT4G34000 | ABF3 | bZIP | Y2H library | this study | Yes | Yes |
| AT4G34610 | BLH6 | HB | Y2H library | this study | Yes | Yes |
| AT4G35770 | STR15/SEN1/DIN1 | | Y2H library | Lumba et al., 2014 | No | No |
| AT4G36060 | bHLH11 | TF | Y2H library | Marín-de la Rosa et al., 2014 | No | Yes |
| AT4G36930 | SPT | bHLH TF | Y2H | Gallego-Bartolomé et al., 2010 | Yes | Yes |
| AT4G37130 | TCU1/NUP58 | nucleoporin | Y2H library | Ferrández-Ayela et al., 2013 | No | No |
| AT4G37260 | MYB73 | MYB | Y2H library | this study | Yes | Yes |
| AT4G38180 | FRS5 | FAR1 | Y2H library | this study | Yes | Yes |
| AT5G01820 | CIPK14/SR1 | kinase | Y2H library | Lumba et al., 2014 | No | No |
| AT5G02320 | MYB3R-5 | MYB | Y2H library | this study | Yes | Yes |
| AT5G03150 | IDD10/JKD | C2H2 Zinc-finger TF | Y2H, BiFC, crystal structure | Fukazawa et al., 2014; Yoshida et al., 2014, Hirano et al., 2017 | Yes | Yes |
| AT5G04110 | GYRB3 | MYB-related | Y2H library | this study | Yes | Yes |
| AT5G05790 | AT5G05790 | MYB | Y2H library | this study | Yes | Yes |
| AT5G06070 | RBE | C2H2 | Y2H library | this study | Yes | Yes |
| AT5G06839 | bZIP65/TGA10 | TF | Y2H library | Marín-de la Rosa et al., 2014 | No | Yes |
| AT5G08070 | TCP17 | TCP | Y2H library | this study | Yes | Yes |
| AT5G08130 | BIM1 | bHLH | Y2H library | this study | Yes | Yes |
| AT5G08330 | TCP11 | TCP | Y2H library | this study | Yes | Yes |
| AT5G09460 | AJAX3/bHLH143 | TF | Y2H library | Marín-de la Rosa et al., 2014 | Yes | Yes |
| AT5G09750 | HEC3 | bHLH | Y2H library | this study | Yes | Yes |
| AT5G10030 | OBF4/TGA4 | TF | Y2H library | Marín-de la Rosa et al., 2014 | No | Yes |
| AT5G10140 | FLC | MADS-box TF | Y2H, BiFC, pull-down, co-IP | Li et al., 2016 | No | Yes |
| AT5G10280 | MYB92 | MYB | Y2H library | this study | Yes | Yes |
| AT5G10570 | AT5G10570 | bHLH | Y2H library | this study | Yes | Yes |
| AT5G10970 | AT5G10970 | C2H2 | Y2H library | this study | Yes | Yes |
| AT5G11340 | AT5G11340 | GNAT | Y2H library | this study | Yes | Yes |
| AT5G12190 | Q9FMP4 | splicing factor | Y2H library | Arabidopsis Interactome Mapping Consortium, 2011 | No | No |
| AT5G12840 | NF-YA1 | TF | Y2H, BiFC, co-IP | Hou et al., 2014; Fonouni-Farde et al., 2016 | No | Yes |
| AT5G13220 | JAZ10 | JA ZIM-domain protein | Y2H (full-length DELLA@AD) | Yang et al., 2012 | No | No |
| AT5G13330 | Rap2.6L | AP2-EREBP | Y2H library | this study | Yes | Yes |
| AT5G14170 | CHC1 | SWI/SNF-BAF60b | Y2H library | this study | Yes | Yes |
| AT5G14760 | AO | aspartate oxidase | Y2H library | Lumba et al., 2014 | No | No |
| AT5G15130 | WRKY72 | WRKY | Y2H library | this study | Yes | Yes |
| AT5G15210 | HB30 | zf-HD | Y2H library | this study | Yes | Yes |
| AT5G15840 | CO | B-box Zinc-finger TF | Y2H (full-length DELLA@BD), pull-down, co-IP | Xu et al., 2016 | No | Yes |

| | | | | | | |
|---|---|---|---|---|---|---|
| AT5G16320 | FRL1 | transcriptional regulator | Y2H library | Arabidopsis Interactome Mapping Consortium, 2011 | No | No |
| AT5G17810 | WOX12 | HB | Y2H library | this study | Yes | Yes |
| AT5G18240 | MYR1 | G2-like | Y2H library | this study | Yes | Yes |
| AT5G18450 | AT5G18450 | AP2-EREBP | Y2H library | this study | Yes | Yes |
| AT5G19790 | RAP2.11 | AP2-EREBP | Y2H library | this study | Yes | Yes |
| AT5G20730 | ARF7 | TF | Y2H | Oh et al., 2014 | Yes | Yes |
| AT5G21120 | EIL2 | TF | Y2H library | Marín-de la Rosa et al., 2014 | No | Yes |
| AT5G23000 | MYB37 | MYB | Y2H library | this study | Yes | Yes |
| AT5G23260 | TT16 | MADS | Y2H library | this study | Yes | Yes |
| AT5G23280 | AT5G23280 | TCP | Y2H library | this study | Yes | Yes |
| AT5G23290 | PFD5 | co-chaperone | Y2H, BiFC, co-IP | Locascio et al., 2013 | No | No |
| AT5G25160 | ZFP3 | C2H2 | Y2H library | this study | Yes | Yes |
| AT5G25190 | ESE3 | AP2-EREBP | Y2H library | this study | Yes | Yes |
| AT5G25220 | KNAT3 | HB / KNOX2 | Y2H library | this study | Yes | Yes |
| AT5G25790 | AT5G25790 | CPP | Y2H library | this study | Yes | Yes |
| AT5G26280 | Q93Z83 | | Y2H library | Lumba et al., 2014 | No | No |
| AT5G26650 | AGL36 | MADS | Y2H library | this study | Yes | Yes |
| AT5G26805 | AT5G26805 | REM(B3) | Y2H library | this study | Yes | Yes |
| AT5G27880 | AT5G27880 | C2H2 | Y2H library | this study | Yes | Yes |
| AT5G28770 | BZO2H3 | bZIP | Y2H library | this study | Yes | Yes |
| AT5G29000 | PHL1 | TF | Y2H library | Marín-de la Rosa et al., 2014 | No | Yes |
| AT5G37020 | ARF8 | TF | Y2H | Oh et al., 2014 | No | Yes |
| AT5G38420 | RBCS-2B | Ribulose bisphosphate carboxylase (small chain 2B) family protein | Y2H library | Arabidopsis Interactome Mapping Consortium, 2011 | No | No |
| AT5G39660 | CDF2 | C2C2-DOF | Y2H library | this study | Yes | Yes |
| AT5G39820 | NAC094 | NAC | Y2H library | this study | Yes | Yes |
| AT5G41315 | GL3 | bHLH TF | Y2H, BiFC, pull-down | Qi et al., 2014 | No | Yes |
| AT5G41410 | BEL1 | HB | Y2H library | this study | Yes | Yes |
| AT5G41580 | AT5G41580 | zf-MIZ | Y2H library | this study | Yes | Yes |
| AT5G41920 | AT5G41920 | GRAS | Y2H library | this study | Yes | Yes |
| AT5G43270 | SPL2 | TF | Y2H (full-length DELLA@AD) | Yu et al., 2012 | No | Yes |
| AT5G44160 | NUC | C2H2 | Y2H library | this study | Yes | Yes |
| AT5G44190 | GLK2 | G2-like | Y2H library | this study | Yes | Yes |
| AT5G45100 | BRG1 | RING domain protein | Y2H (full-length DELLA@AD) | Park et al., 2013 | No | No |
| AT5G45980 | WOX8 | HB | Y2H library | this study | Yes | Yes |
| AT5G46915 | AT5G46915 | ABI3-VP1 | Y2H library | this study | Yes | Yes |
| AT5G47640 | NF-YB2 | TF | Y2H (full-length), BiFC, pull-down | Hou et al., 2014 | No | Yes |
| AT5G47790 | AT5G47790 | FHA | Y2H library | this study | Yes | Yes |
| AT5G48150 | PAT1 | GRAS | Y2H library | this study | Yes | Yes |
| AT5G48430 | Q9LV70 | | Y2H library | Lumba et al., 2014 | No | No |
| AT5G49510 | PFD3 | co-chaperone | Y2H | Locascio et al., 2013 | No | No |
| AT5G50010 | AT5G50010 | bHLH | Y2H library | this study | Yes | Yes |

| | | | | | | |
|---|---|---|---|---|---|---|
| AT5G50670 | SPL13B | SBP | Y2H library | this study | Yes | Yes |
| AT5G51780 | AT5G51780 | bHLH | Y2H library | this study | Yes | Yes |
| AT5G51910 | TCP19 | class I TCP TF | Y2H library | Marín-de la Rosa et al., 2014 | Yes | Yes |
| AT5G53660 | GRF7 | GRF | Y2H library | this study | Yes | Yes |
| AT5G53950 | CUC2/ANAC098 | TF | Y2H library | Marín-de la Rosa et al., 2014 | No | Yes |
| AT5G54230 | MYB49 | | Y2H library | Lumba et al., 2014 | No | Yes |
| AT5G54360 | AT5G54360 | C2H2 | Y2H library | this study | Yes | Yes |
| AT5G57180 | CIA2 | Orphans / C2C2-CO-like | Y2H library | this study | Yes | Yes |
| AT5G59220 | SAG113 | | Y2H library | Lumba et al., 2014 | No | No |
| AT5G59800 | MBD7 | ND | Y2H library | this study | Yes | Yes |
| AT5G60120 | TOE2 | TF | Y2H library | Marín-de la Rosa et al., 2014 | Yes | Yes |
| AT5G60970 | TCP5 | class I TCP TF | Y2H library | Marín-de la Rosa et al., 2014 | No | Yes |
| AT5G61270 | PIF7 | bHLH | Y2H library | this study | Yes | Yes |
| AT5G61590 | AT5G61590 | AP2-EREBP | Y2H library | this study | Yes | Yes |
| AT5G61890 | AT5G61890 | AP2-EREBP | Y2H library | this study | Yes | Yes |
| AT5G62260 | AHL6 | TF | Y2H library | Arabidopsis Interactome Mapping Consortium, 2011 | No | No |
| AT5G62430 | CDF1 | C2C2-DOF | Y2H library | this study | Yes | Yes |
| AT5G63470 | NF-YC4 | TF | Y2H (full-length DELLA@AD), pull-down | Liu et al., 2016 | No | Yes |
| AT5G64340 | SAC51 | bHLH | Y2H library | this study | Yes | Yes |
| AT5G64750 | AtABR1 | TF | Y2H library | Marín-de la Rosa et al., 2014 | No | Yes |
| AT5G65790 | MYB68 | TF | Y2H library | Marín-de la Rosa et al., 2014 | No | Yes |
| AT5G66320 | GATA5 | C2C2-GATA | Y2H library | this study | Yes | Yes |
| AT5G66350 | SHI | SRS | Y2H library | this study | Yes | Yes |
| AT5G66730 | IDD1/ENY | C2H2 Zinc-finger TF | Y2H (full-length DELLA@AD), BiFC | Feurtado et al., 2011 | Yes | Yes |
| AT5G67110 | ALC | bHLH TF | Y2H (full-length DELLA@AD), BiFC | Arnaud et al., 2010 | Yes | Yes |
| AT5G67300 | MYBR1 | MYB | Y2H library | this study | Yes | Yes |